



## D3.2: DIGITAL TWIN BASED GEO-MONITORING

Kevin Duffy, InGEO  
Ken Gavin, InGEO

@AshvinH2020   
ASHVIN H2020 Project   
[www.ashvin.eu](http://www.ashvin.eu) 



ASHVIN has received funding from the European Union's Horizon 2020 research and innovation programme under Grant Agreement No 958161. This document reflects only the author's view and the Commission is not responsible for any use that may be made of the information it contains.

<b>Project Title</b>	Assistants for Healthy, Safe, and Productive Virtual Construction Design, Operation & Maintenance using a Digital Twin
<b>Project Acronym</b>	ASHVIN
<b>Grant Agreement No</b>	958161
<b>Instrument</b>	Research & Innovation Action
<b>Topic</b>	LC-EEB-08-2020 - Digital Building Twins
<b>Start Date of Project</b>	1st October 2020
<b>Duration of Project</b>	36 Months

<b>Name of the deliverable</b>	Digital twin based geo-monitoring
<b>Number of the deliverable</b>	D3.2
<b>Related WP number and name</b>	WP 3 Data fusion for real-time construction monitoring
<b>Related task number and name</b>	T3.3 Geo-Monitoring
<b>Deliverable dissemination level</b>	PU
<b>Deliverable due date</b>	30-09-22
<b>Deliverable submission date</b>	30-10-22
<b>Task leader/Main author</b>	Kevin Duffy (InGEO)
<b>Contributing partners</b>	Ken Gavin (InGEO), Rehan Khan (DTT)
<b>Reviewer(s)</b>	Lucian Ungureanu (DIG)

## ABSTRACT

This deliverable presents an overview of how geo-monitoring can be integrated effectively with digital twin development. The requirements and uncertainties associated with the monitoring of geotechnical structures are highlighted, along with an overview of how an effective and efficient digital twin model can be developed. A demonstration case of a quay wall in Rotterdam, the Netherlands, is also presented and shows how digital twins can be used to improve the understanding of the long-term performance of geotechnical structures.

## KEYWORDS

Digital Twin, Geo-Monitoring, Geotechnical, Quay Walls, Asset maintenance,

## REVISIONS

Version	Submission date	Comments	Author
v0.1		First draft of full report	Kevin Duffy (InGEO)
v0.2		Minor corrections	Ken Gavin (InGEO)
v0.3		Review. Minor corrections and adjustment of sections	Lucian Ungureanu (DIG)
v1.0	30/10/22	Final version	Kevin Duffy (InGEO)
.....			

## DISCLAIMER

This document is provided with no warranties whatsoever, including any warranty of merchantability, non-infringement, fitness for any particular purpose, or any other warranty with respect to any information, result, proposal, specification, or sample contained or referred to herein. Any liability, including liability for infringement of any proprietary rights, regarding the use of this document or any information contained herein is disclaimed. No license, express or implied, by estoppel or otherwise, to any intellectual property rights is granted by or in connection with this document. This document is subject to change without notice. ASHVIN has been financed with support from the European Commission. This document reflects only the view of the author(s) and the European Commission cannot be held responsible for any use which may be made of the information contained.

## ACRONYMS & DEFINITIONS

AHN	<i>Actueel Hoogtebestand Nederland</i> (Up-to-date height model of the Netherlands)
BH	Borehole
BIM	Building Information Modelling
BOTDR	Brillouin Optical Time Domain Reflectometry
DC10	Demonstration Case #10
FBG	Fibre Bragg Grating
FEM	Finite Element Method
FOSMO	Fibre Optic Structural Monitoring
GIS	Geographical Information Systems
GUI	Graphical User Interface
IFC	Industry Foundation Class
IoT	Internet of Things
LiDAR	Light Detection & Ranging
NAP	<i>Normaal Amsterdams Peil</i> (Amsterdam Ordnance Datum)
SHM	Structural Health Monitoring
SOFO	<i>Surveillance d'Ouvrages par Fibres Optiques</i> (Structural monitoring using fibre optics)
SQL	Structured Query Language
WP	Work Package

## ASHVIN PROJECT

ASHVIN aims at enabling the European construction industry to significantly improve its productivity, while reducing cost and ensuring absolutely safe work conditions, by providing a proposal for a European wide digital twin standard, an open source digital twin platform integrating IoT and image technologies, and a set of tools and demonstrated procedures to apply the platform and the standard proven to guarantee specified productivity, cost, and safety improvements. The envisioned platform will provide a digital representation of the construction product at hand and allow to collect real-time digital data before, during, and after production of the product to continuously monitor changes in the environment and within the production process. Based on the platform, ASHVIN will develop and demonstrate applications that use the digital twin data. These applications will allow it to fully leverage the potential of the IoT based digital twin platform to reach the expected impacts (better scheduling forecast by 20%; better allocation of resources and optimization of equipment usage; reduced number of accidents; reduction of construction projects). The ASHVIN solutions will overcome worker protection and privacy issues that come with the tracking of construction activities, provide means to fuse video data and sensor data, integrate geo-monitoring data, provide multi-physics simulation methods for digital representing the behavior of a product (not only its shape), provide evidence based engineering methods to design for productivity and safety, provide 4D simulation and visualization methods of construction processes, and develop a lean planning process supported by real-time data. All innovations will be demonstrated on real-world construction projects across Europe. The ASHVIN consortium combines strong R&I players from 9 EU member states with strong expertise in construction and engineering management, digital twin technology, IoT, and data security / privacy.

## TABLE OF CONTENTS

TABLE OF CONTENTS .....	5
LIST OF FIGURES.....	8
LIST OF TABLES.....	11
<b>1. INTRODUCTION .....</b>	<b>12</b>
<b>1.1 Deliverable Objective.....</b>	<b>14</b>
<b>1.2 Deliverable Outline .....</b>	<b>14</b>
<b>2 GEO-MONITORING .....</b>	<b>15</b>
<b>2.1 Objective Definition .....</b>	<b>15</b>
<b>2.2 Ground Characterisation .....</b>	<b>16</b>
2.2.1 Desk study .....	17
2.2.2 Intrusive investigation .....	19
2.2.3 Non-intrusive investigation .....	20
2.2.4 Laboratory testing .....	21
2.2.5 Parameterisation .....	22
<b>2.3 Performance Monitoring.....</b>	<b>22</b>
2.3.1 Reference readings.....	23
2.3.2 Measurement frequency.....	24
2.3.3 Temperature compensation.....	24
2.3.4 Instrument calibration.....	26
2.3.5 Instrumentation resiliency .....	26
2.3.6 Site activity .....	28
<b>3 DIGITAL TWINS &amp; THE INCORPORATION OF GEO-MONITORING .....</b>	<b>30</b>
<b>3.1 Digital Twin Architecture.....</b>	<b>31</b>
<b>3.2 Connectivity Space.....</b>	<b>32</b>
3.2.1 Data acquisition layer .....	32
3.2.2 Data connectivity layer.....	32
3.2.3 Storage layer.....	34
<b>3.3 Digital Space .....</b>	<b>37</b>
3.3.1 Processing layer .....	38
3.3.2 Integration layer .....	39

3.3.3	Interpretation layer .....	40
3.3.4	User interface layer .....	41
4	DEMONSTRATION CASE #10: A QUAY WALL IN THE NETHERLANDS .....	43
4.1	Objective Definition .....	43
4.2	Desk Study.....	44
4.2.1	Site history .....	45
4.2.2	Geological overview .....	45
4.3	Intrusive Investigation .....	47
4.4	Non-Intrusive Investigation .....	48
4.4.1	Topography.....	48
4.4.2	Satellite data.....	49
4.4.3	Geophysical data .....	50
4.5	Quay Wall Geometry & Construction .....	51
4.5.1	Diaphragm wall.....	53
4.5.2	MV piles .....	54
4.5.3	Vibro piles.....	54
4.5.4	Superstructure & relieving platform .....	55
4.5.5	Non-geotechnical structures .....	55
4.6	Performance Monitoring.....	57
4.6.1	BOTDR: Strain & temperature .....	57
4.6.2	Monitoring wells: Water level .....	59
4.6.3	Seepage sensors .....	60
4.6.4	SOFO: Strain.....	60
4.7	Initial Digital Twin Development .....	61
4.8	Monitoring Results.....	63
4.8.1	Temperature compensation.....	63
4.8.2	Identifying fibre optic sections (BOTDR) .....	64
4.8.3	Outlier detection .....	65
4.8.4	BOTDR: piles .....	66
4.8.5	SOFO: piles.....	67
4.8.6	Monitoring well data .....	69
4.9	Discussion.....	71
5	CONCLUSION .....	73
	REFERENCES .....	74

APPENDIX A	QUAY WALLS AT THE PORT OF ROTTERDAM .....	81
APPENDIX B	CONE PENETRATION TEST DATA .....	84
<b>Appendix B1</b>	<b>Geotechnical Exchange Format (.gef) .....</b>	<b>84</b>
<b>Appendix B2</b>	<b>CPT Cross Section .....</b>	<b>85</b>
APPENDIX C	GEOMETRICAL DETAILS .....	86



## LIST OF FIGURES

Figure 1.1: ASHVIN work package (WP) structure .....	12
Figure 1.2: Some of the domains within geotechnical engineering (Eslami et al., 2020).....	13
Figure 2.1: Soil profile underlying Christchurch, New Zealand showing vertical and horizontal variability and a variety of soil layers (Canterbury Earthquakes Royal Commission, 2011) ...	17
Figure 2.2: Example of a CPT cone (left) and an example of a CPT cone resistance profile with borehole log (right) .....	19
Figure 2.3: (a) Electrical resistivity tomography (ERT) profile of a cross-section of a rail embankment (b) Interpretation of the soil layers in this cross-section based on the boreholes (BH) and the ERT profile (Donohue, Gavin and Tolooiyan, 2011) .....	20
Figure 2.4: InSAR measurements with (a) overview of settlement data points over the two years before the quay wall collapse (scale: -10mm in red to +10mm in blue). (b, d) Settlement point average of the zones on either side of the collapse in green rectangles in (a) and (c) settlement point average of the collapsed section in blue rectangle in (a); results from both ascending (yellow) and descending (blue) tracks are shown (from Korff, Hemel and Peters, 2022) .....	21
Figure 2.5: Driven precast piles lying on a site prior to installation so that a reference reading can be made. Following the initial reading, a second reading is made with the piles rotated 180° to compensate for bending effects between the two support beams .....	24
Figure 2.6: (a.) Temperature measurements from thermistor modules in the pile (b.) Strain readings in the pile, with varying degrees of temperature compensation (adapted from Duffy et al., 2022) .....	25
Figure 2.7: Two fibre optic cables used for strain monitoring with different types of reinforcing to improve resiliency and minimise damage to the optical fibre cores .....	27
Figure 2.8: Deep excavation during the construction of the New Zealand International Convention Centre (Grouting Services, 2017) .....	28
Figure 2.9: Impact of a seven-metre reduction in seabed level on the anchor measurements of a quay wall. The diurnal tidal cycles can also be seen in the measurements .....	29
Figure 3.1: Simplified digital twin architecture for a geo-monitoring programme .....	31
Figure 3.2: Digital twin connections and hierarchy among different levels (Lu et al., 2020) ...	32
Figure 3.3: timeline of storage formats over the course of 70 years (Franklin & Marshall College Library, 2022) .....	37
Figure 3.4: Measurements of a foundation pile during a load test, whereby the load was increased in steps and the corresponding force was measured using fibre optics .....	39
Figure 3.5: FEM model of a quay wall, indicating the degree of displacement in millimetres for each element of the mesh (amended from Schouten (2020)) .....	40
Figure 3.6: Example of the weather & tide dashboard at the port of Rotterdam (Port of Rotterdam Authority, 2022) .....	42
Figure 4.1: Areas of the port of Rotterdam. The DC10 quay wall is located on the Maasvlakte in the west (de Gijt et al., 2010) .....	43
Figure 4.2: Some possible failure modes of a quay wall (Roubos, 2019) .....	44
Figure 4.3: Overlay of a map by (Colom, 1750) on top of a current map of the Maasvlakte peninsula (Utrecht University, 2022). The mouth of the estuary is shown along with ship passageways around the Honde Plaet .....	45

Figure 4.4: Geological cross-section along DC10 (DINOloket, 2022). Names within brackets are Members within a Formation .....	46
Figure 4.5: CPT data available (i.e. the brown inverted triangles) across the port of Rotterdam in the DINOloket Dutch National Key Registry of the Subsurface (DINOloket, 2022) .....	48
Figure 4.6: Selected CPTs across the length of the quay wall.....	48
Figure 4.7: LiDAR flyover of the Maasvlakte in December 2016 (Actueel Hoogtebestand Nederland, 2016). The green areas are roughly five metres above sea level .....	49
Figure 4.8: Datapoints collected from the Sentinel satellites of a quay wall in the Maasvlakte, reported in bodemdalingskaart.nl. The extents of the quay wall structure itself are also indicated, showing the filtered out datapoints .....	50
Figure 4.9: Seismic surveys performed in the Yangtzekanaal (Vos et al., 2015) .....	51
Figure 4.10: Cross-section of quay wall (adapted from Kuster (2007)).....	51
Figure 4.11: BIM model of a quay wall section, developed by Digital Twin Technology.....	52
Figure 4.12: Overview of the construction process at DC10: 1. Creation of the Maasvlakte, 2. Installation of diaphragm wall, 3. Installation of vibro piles, 4. Installation of MV-piles, 5. Installation of above-ground constructions 6. Dredging of the quay 7. Quay wall completion (Port of Rotterdam, 2021) .....	52
Figure 4.13: Landside picture of the quay wall. The installation of the MV piles is shown in the foreground, with casting of the individual superstructure segments occurring in the background .....	53
Figure 4.14: Typical reinforcing configuration of a diaphragm wall panel. Note that this configuration can change depending on the quay wall position (De Vries, 2007). Stortkoker = tremie pipe .....	53
Figure 4.15: Picture of the widened tip at the base of an MV pile (Westerbeke, 2021) .....	54
Figure 4.16: Theoretical maximum (left) and minimum (right) cross-section sizes for the MV piles (Srigopal, 2018).....	54
Figure 4.17: Vibro pile installation procedure .....	55
Figure 4.18: Isometric drawing of a section of the quay wall superstructure (Scheel, 2007) ..	55
Figure 4.19: Example of fenders (in orange/red) and bollards (in yellow) at a quay wall (Shibata Fender Team, 2016) .....	56
Figure 4.20: Overview of instrumented structures across DC10.....	57
Figure 4.21: DiTeSt SMARTprofile fibre optic cable.....	58
Figure 4.22: (a) Protective channel welded to the flange of the MV piles, within which the SMARTprofile cable is glued (b) Indication of where the SMARTprofile cable (in red) was placed on the vibro pile reinforcing .....	58
Figure 4.23: Reinforcing on the diaphragm wall, (left) indicating the two measurement lines in red and green and (right) the reinforcing placed within the diaphragm wall .....	59
Figure 4.24: FOS&S Pressure Sensor P-01 used in the monitoring wells (FOS&S, 2009) ....	60
Figure 4.25: Principle of the seepage sensors (adapted from van Dam (2008)) .....	60
Figure 4.26: SOFO sensor (Smartec, 2017) .....	61
Figure 4.27: User interface of the FOSMO GUI (in Dutch), presenting the status of the instrumentation along the quay wall. Displayed is the working status of the data loggers (Status	

Apparatuur) and the correction function of the sensors, in terms of last measurement made in hours (Achterstand Sensordata (uren)).....	62
Figure 4.28: Example of selected BOTDR increments from a temperature fibre within a vibro pile .....	63
Figure 4.29: Count of the number of strain and temperature measurements in one of the vibro piles within the database .....	64
Figure 4.30: Direct measurement from data logger, indicating the slicing paths. Further fine-tuning is needed to remove connection points at the top. #S1, #S2 etc. refers to different sensor IDs or measurement axes .....	65
Figure 4.31: Example of outliers within a BOTDR measurement at a single depth range for one of the MV piles .....	66
Figure 4.32: Measurements of four sensors within a vibro pile. The pile head and pile based have been indicated, along with the depth of the Pleistocene sand layer – the primary load bearing layer. ....	67
Figure 4.33: All SOFO measurements on the MV and vibro piles (bottom figure), compared to ambient air temperatures from the Hook of Holland weather station (KNMI, 2009) .....	68
Figure 4.34: Zooming into a zone of measurements, beginning 3 <sup>rd</sup> August 2009.....	69
Figure 4.35: Monitoring well measurements from a one-week period. The reference measurement has been set on the 10 <sup>th</sup> of November 2009 .....	70
Figure 4.36: Selected measurements along the entire length of the quay wall from Section 11 (western side of quay wall) to Section (eastern side of quay wall). The reference measurement was taken on the 1 <sup>st</sup> of January 2015.....	70
Figure 4.37: Drift in seaside measurements at DC10 compared to measurements from a monitoring well on waterinfo.rws.nl.....	71
Figure A.1: Examples of quay wall structures across the port of Rotterdam with the geotechnical elements listed (amended from de Gijt & Broeken (2013)) .....	81
Figure A.2: Age of quay walls across the Port of Rotterdam (Roubos, 2019) .....	82

## LIST OF TABLES

Table 2.1: Sources of prior knowledge (amended from Clayton et al. (1995)) .....	18
Table 2.2: Types of laboratory tests (Clayton, Matthews and Simons, 1995) .....	22
Table 2.3: Example of site monitoring quantities.....	23
Table 3.1: A rule-of-thumb for determining expected storage capacity required for a single sensor (Sparkes and Webb, 2020).....	34
Table 3.2: Common file types in geo-monitoring.....	36
Table 4.1: Publicly available data available for the desk study. ....	44
Table 4.2: Geological soil layers at DC10. Depths are with reference to the Dutch ordnance system (Normaal Amsterdams Peil NAP, approximately equal to mean sea level.....	47
Table 4.3: Summary of instrumentation used.....	57

## 1. INTRODUCTION

The 21<sup>st</sup> century has seen huge technological advances thanks to digitalisation and interconnectivity. Humans can now connect with one another in a matter of seconds and are exposed to a tremendous source of knowledge and ideas. These rapid advancements are also seen on an industrial level, a change that has been coined as the Fourth Industrial Revolution, or Industry 4.0. This era has led to an upheaval of traditional production and business practices, in favour of implementing more automated and optimised routines.

An expansive and rich digital world has developed from Industry 4.0, a world which is both integrated with, but divergent from the physical world to varying degrees. This digital world is idealised as a hyper-efficient environment: a place where machines communicate with one another and self-optimize based on inputs from sensors in real-time and incorporate technologies such as artificial intelligence, big data, Internet of Things or cloud computing (Newman *et al.*, 2020). Encapsulating the concept of this digital world is the *digital twin*: a virtual representation of a physical entity between which an active connection is present (Grieves, 2014).

Industry 4.0 lead to radical improvements in procedures, quality and productivity in sectors such as the automotive, manufacturing or aerospace sectors. Advancements in the construction sector would also be expected to be spurred on as part of Industry 4.0 but on the contrary, apathy towards new innovations and adherence to the status quo has stifled possible growth and improvement (Craveiro *et al.*, 2019). From a research perspective, integration of Industry 4.0 into the construction industry is also still a relatively conceptual level and there is substantial room for improvement in this area of study (Maskuriy *et al.*, 2019).

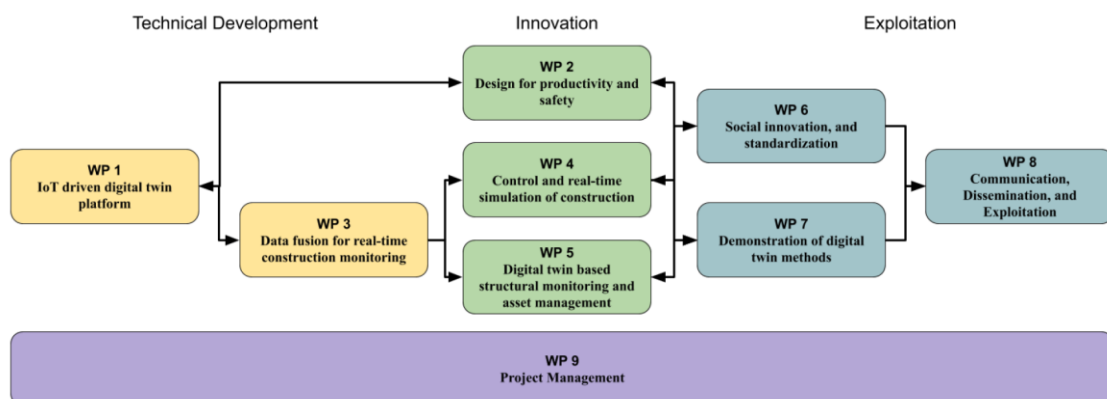


Figure 1.1: ASHVIN work package (WP) structure

In this regard, the ASHVIN project aims to enable the European construction industry to significantly improve its productivity while reducing cost and improving workplace safety by providing a proposal for a European wide digital twin standard and bringing the industry one step forward within Industry 4.0. A multi-faceted approach is being taken, allowing for the interaction of different disciplines at various stages of a research path (Figure 1.1).

Geo-monitoring forms a subset of this research plan within WP3 and is referred to as Task 3.3 with the associated Deliverable 3.2. It describes the measurement of physical phenomena associated with structures within the domain of geotechnical engineering

(Figure 1.2), referred to as *geo-structures* in this report. In other words, geo-structures can be considered as man-made structures which utilise the properties of subsurface materials to their benefit. As a result, both the material response of the structure and the soil itself is of great importance for a geotechnical engineer.

These geo-structures can be constructed from a range of different materials and are used in many ways. This can include load-bearing structures such as deep or shallow foundations, structures which retain a large amount of material such as levees, quay walls or dams or structures which facilitate the transport of a medium or transport such as tunnels or pipelines.

The discipline interlinks strongly with the discipline of Structural Health Monitoring, an area which has been discussed in ASHVIN WP5 (Casas, Stipanovic and Chacón, 2022). In contrast to Structural Health Monitoring, the geo-monitoring discipline deals with physical phenomena that generally cannot readily be seen, requiring some inferences and assumptions to determine the soil/structure. response and often involves dealing with materials that are non-homogeneous (i.e. naturally deposited), with considerable uncertainty as to the distribution of its material properties such as the soil strength and stiffness.

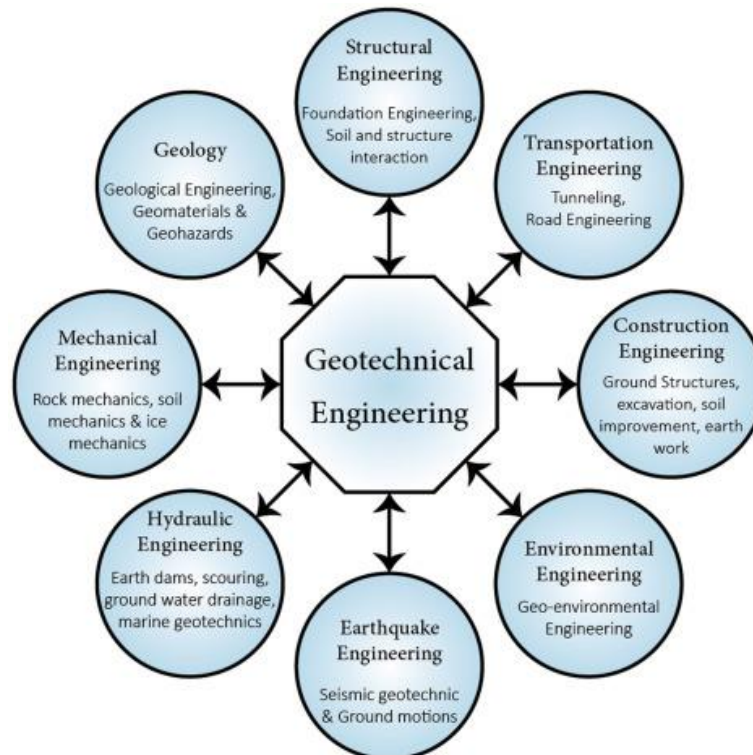


Figure 1.2: Some of the domains within geotechnical engineering (Eslami et al., 2020)

The implication of this means that there are certain requirements of geo-monitoring that need to be satisfied when developing a digital twin approach and likewise, there are requirements in digital twin development that need to be considered in the planning of a geo-monitoring program. Task 3.3 aims to delineate as many of these requirements as possible to help practitioners in developing accurate and reliable digital representations of their geotechnical assets.

### 1.1 Deliverable Objective

The deliverable targets the interface of two domains: geo-monitoring and digital twin development. In this regard, the deliverable does not aim to give a detailed overview of both domains, which are already well described in the literature (Dunnicliff, 1988; Jones *et al.*, 2020). Instead it targets practitioners in both domains to give them an easy-to-understand perspective as to how geo-monitoring and digital twins can be fused together effectively and efficiently, whilst providing an overview of the current state-of-the-art technologies and methods in both disciplines. Particular focus is given to the unique challenges of geo-monitoring and the needs and requirements of geotechnical engineers in the interpretation and analysis of geo-monitoring results.

The core of Deliverable 3.2 highlights a real-life example of a digital twin: *Demonstration Case #10: Quay Wall in the Netherlands* (DC10). Data from the quay wall was collected over a period from 2008 to 2016 and provides an excellent case study for a pre-existing digital twin from which lessons can be learnt in terms of digital twin development and insights into the geotechnical response of quay walls and its structural elements.

### 1.2 Deliverable Outline

To support this case study, a state-of-the-art review of data collection techniques in the geo-monitoring field will first be described. This will be followed by an in-depth look at how this data can be integrated into a digital twin in a structured and methodological fashion. The current state of the discipline with respect to digital twin based geo-monitoring will then be described, followed by a description of the demonstration case. Conclusions and lessons learned are also collated in the final chapter.



## 2 GEO-MONITORING

Geo-monitoring aims to estimate the performance and response of the subsurface and/or geo-structures based on the assessment of data collected by measurement tools. The focus of the report will be placed on the geo-structures which utilise soil, however, the discipline can also include the monitoring of geo-structures which utilise the properties of rock. However, this has not been discussed as part of this deliverable in the interest of brevity and to tie in with DC10.

Instrumentation for geo-monitoring can be subdivided into two different purposes: one purpose for estimating soil properties (*ground characterisation*, Section 2.2) and the other for monitoring individual elements of a geo-structure and/or the geo-structure as a whole (*performance monitoring*, Section 2.3). Both cases can be performed over the entire lifespan of a geo-structure, the timeline of which is as follows:

1. **Pre-construction:** Definition of the monitoring programme, ground characterisation, site assessment, instrumentation preparation, preliminary tests of structural elements
2. **Construction:** Instrumentation of the geo-structure, monitoring of the geo-structure and surrounding soil during construction processes (e.g. dredging, concrete casting), remedial measures
3. **Operation:** Monitoring of the geo-structure during routine operation, maintenance, upgrading, retrofitting and soil property re-assessment

This deliverable considers all phases of the project, including instrumentation used for assessing soil properties before and after construction, along with monitoring the response of the geo-structure during its construction and operational phases. Both facets are crucial in establishing an appropriate digital twin of a geotechnical asset and used in tandem with one another during the analysis of the results.

### 2.1 Objective Definition

An important first step to geo-monitoring is the establishment of the monitoring programme objective(s). Geo-monitoring can encapsulate different purposes that can be performed over both the short-term (defined as <1 year in this deliverable) and in the long-term (> 1 year). An example of some of these objectives could be (van Lysebetten *et al.*, 2022):

- Assessing the long-term performance of the geo-structure
- Extension of the design lifetime of a geo-structure based on the assessed structural reliability
- Optimisation of the inspection and maintenance strategy
- Establishment of an early warning system in the case of (impending) failure
- Verification of the geotechnical design and chosen soil parameters
- Assessing the impact of a proposed alteration to the geo-structure (e.g. proposed adjustment of external loading conditions)
- Optimising the design based on construction monitoring, referred to as the Observational Method (Peck, 1969)



- Ensure safety during construction and operation

Through a selection of these objectives, further investigation can be performed into the desired parameters and a prediction of the expected outcome can be made. This is then followed by selection and procurement of the required instrumentation and devising detailed instrumentation plans. A comprehensive overview of the planning and procurement phases of the geo-monitoring programme can be found in Dunnicliff (1988).

## 2.2 Ground Characterisation

In a geotechnical engineering sense, soil is considered as a three-phase material consisting of water, air and solids. The solid matter can be composed of a mixture of organic matter and minerals, ranging in size from microscopic particles such as clays to particles easily visible to the naked eye such as sands or gravels.

The properties of these soils are of particular importance to the design of geo-structures. Each soil type at each location has its own unique characteristics which need to be appropriately assessed. Some of these parameters are relatively straightforward to assess, such as soil type, unit weight or water content, whereas some other properties require more complex tests to determine them, such as the strength, and stiffness of the soil.

A site investigation is performed at the start of a project to characterise the ground properties. But this is not straightforward in itself: soil is a heterogeneous material which can vary in both the vertical and horizontal directions (Figure 2.1). Even within soil layers, as soil is a frictional material, parameters such as strength and stiffness vary with depth because of varying stress levels. Phoon, Ching & Shuku (2021) coined the acronym MUSIC-X to describe some of the difficulties of dealing with geotechnical-related data, outlined as follows:

- **Multivariate:** There are many variables associated with soil which can have a complex interdependency
- **Uncertain & Unique:** Soil properties can vary substantially from site-to-site (i.e. can be unique to a certain site) and uncertainty lies with measuring these properties appropriately
- **Sparse:** It is both economically and technically challenging to fully determine the soil properties at every single location across every single depth at a site. In other words, data sparsity is always an issue at each site
- **Incomplete:** Like data sparsity, soil data is not always present at certain intervals or locations due to the measurement method used
- **Corrupted (partially):** Bad or noisy data is always associated with whatever measurement procedure is chosen.
- **X – spatially variable:** Soil is spatially correlated in both the vertical and horizontal directions because of geological depositional processes

Therefore, each site that is considered has unique properties that need to be quantified as well as possible prior to construction. The design process should also account for an element of statistical and measurement uncertainty shall that is present when

characterising the soil, traditionally done by incorporating factors of safety within the design approach.

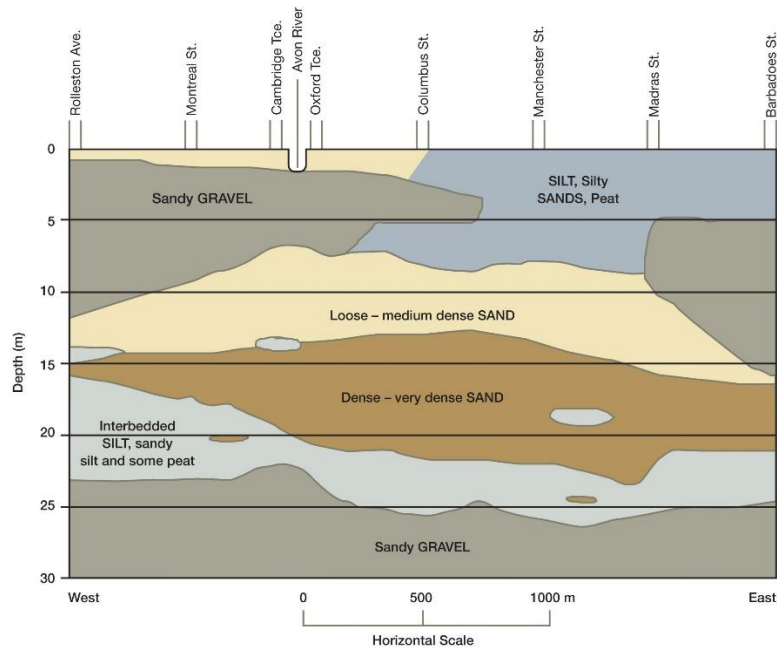


Figure 2.1: Soil profile underlying Christchurch, New Zealand showing vertical and horizontal variability and a variety of soil layers (Canterbury Earthquakes Royal Commission, 2011)

A robust site investigation approach utilises multiple different investigation methods. In this regard, most ground characterisation programmes consist of four core components:

1. Desk study
2. Intrusive investigation
3. Non-intrusive investigation
4. Laboratory testing

A brief outline of each component is given in this report. A site investigation can then conclude by summarising the findings of each component and determine the parameters to be used in the design process, referred to as parameterisation.

For further information on ground characterisation techniques, readers can refer to Clayton et al. (1995).

### 2.2.1 Desk study

A desk study is carried out to deliver preliminary information that is used to aid the planning of the site investigation and provide valuable information regarding the probable ground conditions. The desk study can also highlight potential problems associated with the site and establish the proposed type of construction given the present constraints.

The desk study for the most part is performed off-site and simple site walkovers can be performed to verify some of the information retrieved and identify potential issues associated with the intrusive investigation or construction. Multiple sources are available for a desk study and the sources available can vary substantially from region

to region. This report describes this process for a Dutch-specific context (Section 4) but readers can also refer to other examples such as Clayton et al. (1995) for the United Kingdom or Trautmann and Kulhawy (1983) for the United States.

Generic examples of information sources are given in Table 2.1. The broad range of information should be noted: some examples are easily readable qualitative data, such as topographical maps or meteorological records, whereas others are more implicit and subjective in form, such as the prior experience of the practitioner(s). Compiling this information and incorporating the information into a prior estimate of soil parameters is not a trivial task and can be highly dependent on the engineer(s) involved with the desk study.

Table 2.1: Sources of prior knowledge (amended from Clayton et al. (1995))

Aspect of investigation	Type of information
Site topography	Topographic maps Satellite data Aircraft fly-bys (e.g. LiDAR scanning)
Geology	Geological maps, models & records Geological publications Air photographs
Geotechnical problems and parameters	Academic journals Prior experience Previous ground investigation reports
Groundwater conditions	Topographical maps Air photographs Monitoring well records Previous ground investigation reports
Meteorological conditions	Meteorological records
Existing construction and service	Construction (as-built) drawings Topographical maps Plans held by utilities Construction press
Previous land use	Out-of-print topographical maps Out-of-print geological maps Air photographs Airborne remote sensing Archaeological society records

Estimates of soil parameters can also be made based on commonly cited ranges available in literature, both for a specific region (Netherlands Standardisation Institute, 2017, tbl. 2b) or in an international context (Cao, Wang and Li, 2016). This can give crucial insights into the site uniqueness and identify what uncertainties will need to be minimised during the intrusive investigation.

### 2.2.2 Intrusive investigation

Intrusive investigations (also known as in-situ tests) are one of the most direct ways of characterising the subsurface and obtaining soil parameters, albeit also one of the most expensive parts of a site investigation. On a simple level, trial pits can be performed whereby the first few metres below the surface are excavated out, providing a mostly qualitative description of the soil.

However, these trial pits provide no information on the soil beyond the first couple of metres. Boreholes allow for the retrieval of deeper soil samples from which the site stratigraphy can be directly identified. These samples are typically then used for both simple and advanced laboratory tests (Section 2.2.4), providing a relatively reliable way of obtaining soil parameters.

Nonetheless, extensive characterisation of a site using solely trial pits, boreholes and collected samples can be a costly and time-intensive procedure. In-situ testing is a branch of intrusive investigation techniques which obtain soil parameters from measurements made directly on site and are generally a quick, simple, and cost-effective way to evaluate the constitutive properties of the subsurface.

Worldwide, one of the most popular in-situ testing techniques is the Cone Penetration Test (CPT). The CPT is widely used thanks to its reproducibility, accuracy, and relatively low operational costs in comparison with other ground characterisation methods. During the test, the cone penetrometer (Figure 2.2) penetrates the ground at a constant rate, measuring the cone tip resistance  $q_c$  and the sleeve friction  $f_s$  as it does so. Other parameters can also be measured, such as the pore water pressure  $u_2$ . Empirical equations are then used to derive soil parameters used for design, a variety of which are provided in Lunne et al. (1997). CPT-based design methods are also common in the design of geotechnical structures such as that in Lehane et al. (2020) for the design of foundation piles.

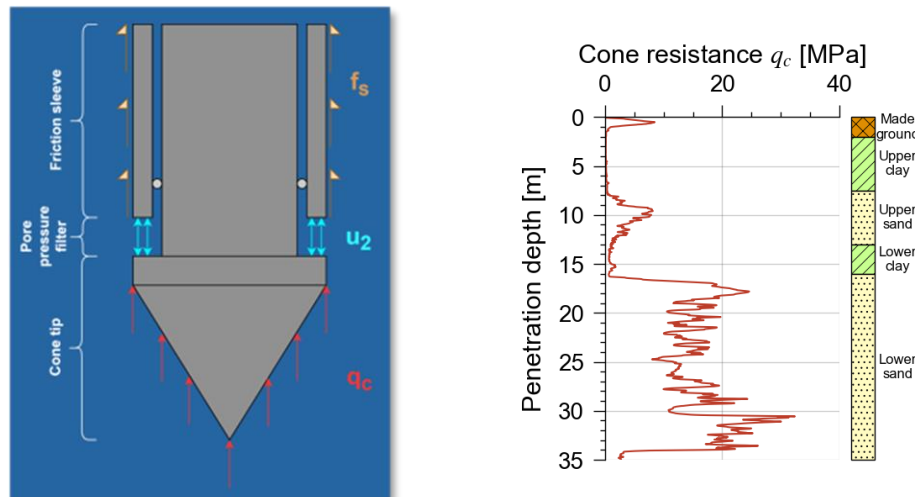


Figure 2.2: Example of a CPT cone (left) and an example of a CPT cone resistance profile with borehole log (right)

Other in-situ testing techniques are also possible, such as the standard penetration test (SPT), the field vane test (FVT) or the pressuremeter test (PMT). Selection of the appropriate in-situ technique is largely dependent on the findings of the desk study

(Section 2.2.1), the type of geo-structure and the local soil conditions. For further reference, readers can refer to Knappett and Craig (2012).

### 2.2.3 Non-intrusive investigation

Non-intrusive investigation techniques are those that do not involve significant alteration of the site or mechanical penetration of the subsurface.

Geophysical methods encompass a large amount of these non-intrusive techniques and can provide a significant amount of data of the subsurface. Geophysical techniques can measure, for example, the propagation of seismic waves in the ground or assess the electrical conductance of the ground (e.g. Figure 2.3), measurements which are strongly correlated to the soil type and its properties.

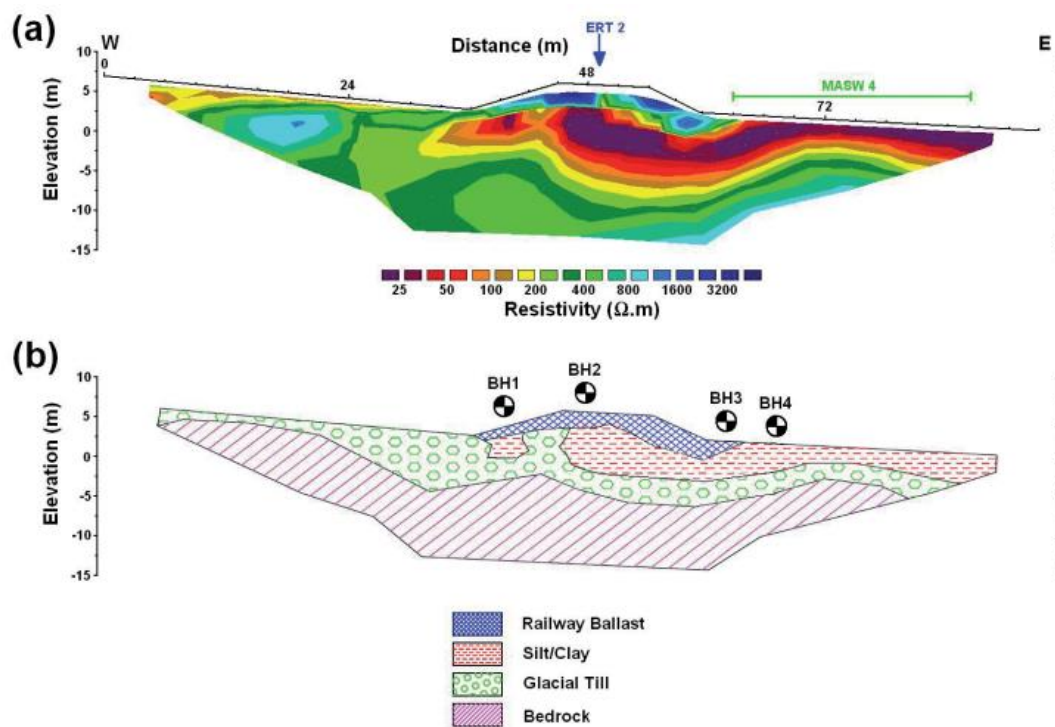


Figure 2.3: (a) Electrical resistivity tomography (ERT) profile of a cross-section of a rail embankment (b) Interpretation of the soil layers in this cross-section based on the boreholes (BH) and the ERT profile (Donohue, Gavin and Tolooiyan, 2011)

Remote sensing is also a rapidly growing area in this field and can be used for both ground characterisation and performance monitoring (Section 2.3). For instance, the Sentinel-1 satellite (Torres *et al.*, 2012) uses Interferometric Synthetic Aperture Radar (InSAR) to estimate relative ground movements using radar images from across Europe. This can then be used to provide early detection of, for example, quay wall failure (Korff, Hemel and Peters, 2022), as shown in Figure 2.4.



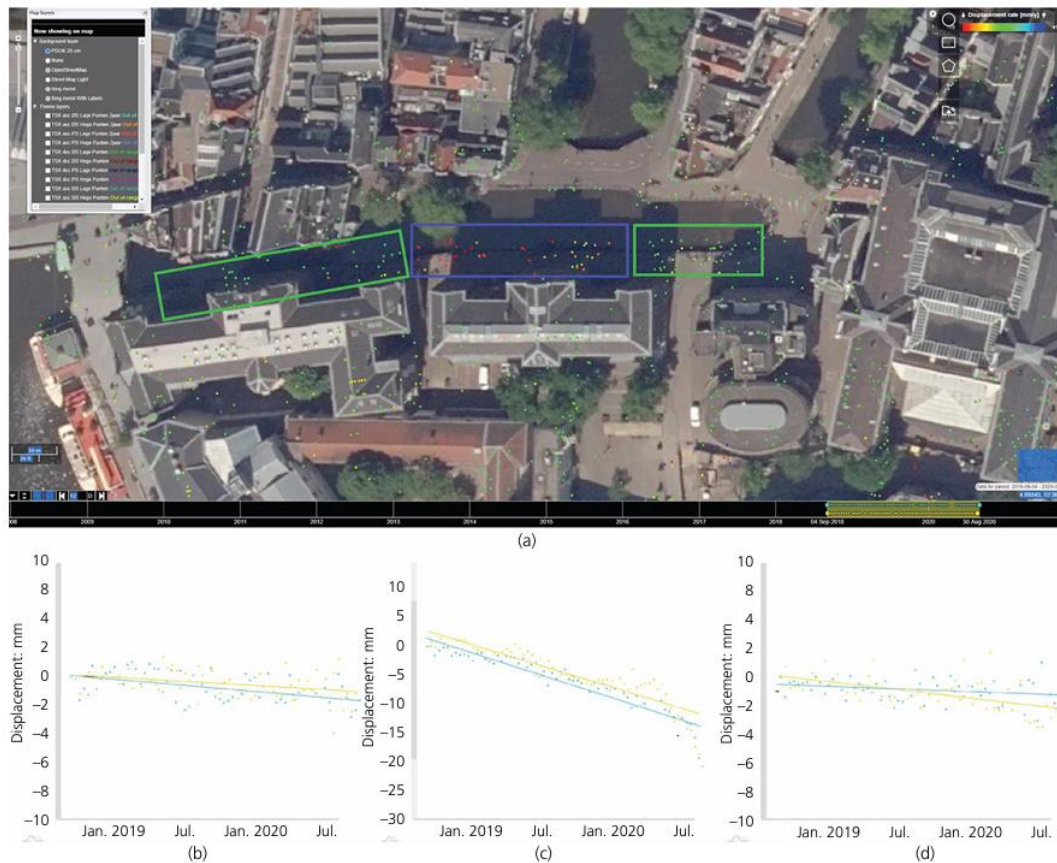


Figure 2.4: InSAR measurements with (a) overview of settlement data points over the two years before the quay wall collapse (scale:  $-10\text{mm}$  in red to  $+10\text{mm}$  in blue). (b, d) Settlement point average of the zones on either side of the collapse in green rectangles in (a) and (c) settlement point average of the collapsed section in blue rectangle in (a); results from both ascending (yellow) and descending (blue) tracks are shown (from Korff, Hemel and Peters, 2022)

## 2.2.4 Laboratory testing

A wide range of laboratory tests can be performed based on samples retrieved from site. These tests can loosely be classified into two groups: soil classification tests and tests for geotechnical parameters (Table 2.2), some of which are routine and simple, others which are more complex and costly. The procedure for these tests is typically guided by a national or international standard, such as the Eurocode or ISO (International Organisation for Standardisation) standards.

Results of the laboratory tests are used to enhance the existing understanding of the site subsurface, verify correlations such as those derived from the CPT and provide a robust and accurate system of deriving soil parameters for a site.

Table 2.2: Types of laboratory tests (Clayton, Matthews and Simons, 1995)

Soil classification tests	Tests for geotechnical parameters
Sample description	Strength tests
Particle size distribution tests	Stiffness tests
Plasticity tests	Consolidation tests
Compaction tests	Seepage and permeability test
Specific gravity tests	

### 2.2.5 Parameterisation

Parameterisation describes the selection of parameters values based on the results of the site investigation. The approach is largely dependent on the design philosophy: traditionally a “stochastic” design approach is taken whereby single parameter values are used to determine the geotechnical response. To come to a single input value, the mean of all values received during testing can be taken. Alternatively, a lower-bound characteristic value can also be taken, depending on the degree of conservatism desired in the design.

In recent decades, probabilistic design approaches have become more and more common. These calculation approaches consider the distribution of all received parameter values and incorporate them into the design through a probabilistic framework, for instance, through Bayesian statistical approaches.

## 2.3 Performance Monitoring

Performance monitoring involves instrumenting specific elements of the geo-structure and/or the surrounding soil to analyse its response to construction process and long-term changes during its operational phase. Planning of the monitoring programme can commence as soon as the first information on the site investigation and the design of the geo-structure itself is known, in addition to a well-defined objective (Section 2.1).

Based on this, expectations of how the geo-structure will respond should be outlined, allowing for the purpose of the instrumentation and the parameters to be monitoring to be identified (e.g. Table 2.3). From there, planning of the instrumentation process can be developed, focussing on the practicalities of the data collection and interpretation (Section 3). A thorough guide to the planning of monitoring programmes is provided in Dunnicliff (1988).

Table 2.3: Example of site monitoring quantities

Desired Parameter	Instruments
Load	Load cells
Strain	Vibrating wire gauges, resistivity gauges, fibre optics
Temperature	Thermocouples, thermistors, PT100 sensors, fibre optics
Settlements	Potentiometers, remote sensing, settlement beacons
Inclination	Fibre optics, inclinometers, Shape Accel Arrays (SAA), tilt sensors
(Ground)water level/pressure	Monitoring wells, piezometers, pore pressure sensors
Earth pressure	Earth pressure cell

Other important considerations are provided below and are important to consider and document as part of the planning and execution processes to provide transparency and clarity to the practitioner interpreting the monitoring data.

### 2.3.1 Reference readings

Many instruments require a reference reading (also known as a zero reading or initial reading). All subsequent measurements are then compared to the initial reading. Making this reading is not a trivial process and requires a comprehensive understanding of the state of the geo-structure at the time of the reference reading so that the end-user can fully interpret the result.

As an example, considering the case of foundation piles that are driven in place, stresses develop in the surrounding soil during installation (known as *residual stresses*). It is important to measure these as part of an evaluation of the overall pile response (Duffy, Gavin, De Lange, *et al.*, 2022). To achieve this, the piles are typically laid on site prior to installation and the strain gauges within the pile are zeroed at this point (Figure 2.5), accounting for any bending effects or temperature effects that may have developed during pile casting and transportation. Failure to account for these residual stresses during the structure's lifecycle will result in a miscalculation of the current state of the structure and can lead to significant misinterpretation of the load distribution within a pile.





*Figure 2.5: Driven precast piles lying on a site prior to installation so that a reference reading can be made. Following the initial reading, a second reading is made with the piles rotated 180° to compensate for bending effects between the two support beams*

If data loggers are changed or adjusted during the monitoring lifecycle, the state of the geo-structure at the time of replacement should also be considered, particularly in the event that the replacement leads to large data gaps whereby important structural changes may occur and yet are not recorded.

### 2.3.2 Measurement frequency

Determining the required measurement frequency needs to be considered during programme planning. This is largely dependent on the requirements of data interpretation (e.g. is the monitoring programme for rapid and dynamic events or more static situations) and how critical it is to capture specific important events (e.g. slope stability monitoring adjacent to a live railway may require detection to be almost instantaneous to stop the train).

In an ideal world, high frequency measurement allows for the practitioner to ensure all scenarios are covered and the data can be processed and/or reduced at a later stage. However, computational, network and storage requirements can prove costly and cumbersome to establish and maintain at high measurement frequencies and can impose a limitation on the desired measurement frequency as a result (Section 3.1).

### 2.3.3 Temperature compensation

Temperature monitoring is frequently performed in monitoring campaigns. Temperature can be set as a target parameter for design such as in the case of buried pipelines (Oswell, 2011), geothermal piles (Wang *et al.*, 2013) or embankments (Bersan, Koelewijn and Simonini, 2018). On top of this, the output of many measurement systems, including fibre optics or electrical-based sensors, are affected directly by temperature which can result in an “apparent” effect on the sensor and introduces a measurement error or bias to the outputted reading. Furthermore, temperature can also affect the structure being monitored through thermally induced strains and is something that may need to be described during the data analysis.

In some cases, temperature measurements can be performed at the exact same location as the measurement quantity being compensated for (e.g. a fibre optic cable being used simultaneously for distributed strain and distributed temperature sensing), minimising the influence of sensor positioning and uncertainty on the measurement. Yet systems such as those used in distributed temperature sensing can be expensive and generally a separate but cheaper temperature sensor is used. This can introduce challenges with respect to spatial and temporal interpolation, and not to mention increasing the cost and complexity of the monitoring programme.

Temperature compensation can be facilitated by directly measuring the temperature using instruments such as thermistors, PT100 sensors etc. Alternatively, the effect can also be inferred: for instance, for strain measurements a duplicate un-bonded strain gauge can be placed adjacent to the existing (bonded) strain gauge and the temperature effect on the strain readings can directly be assessed.

An example of temperature compensation being applied in a geo-monitoring context is given in Duffy et al. (2022) for monitoring residual strains in driven precast piles (Figure 2.6), whereby temperature compensation for the strain measurements was applied to accommodate for the temperature difference between two different points in time ( $T_{\text{residual}} - T_{\text{reference}}$ ). A large difference in the results was seen, with the initial uncorrected readings leading to an interpretation of the load that suggested the pile was in tension. Correcting for temperature effects resulted in a physically meaningful load distribution. In this case a large residual compression force exists at the pile base. From this point, the force reduces with distance from the pile tip to a zero load at the surface. In essence, the large locked-in base stress is balanced by negative shear stress mobilised along the pile shaft, resulting in an equilibrium of loads along the entire pile.

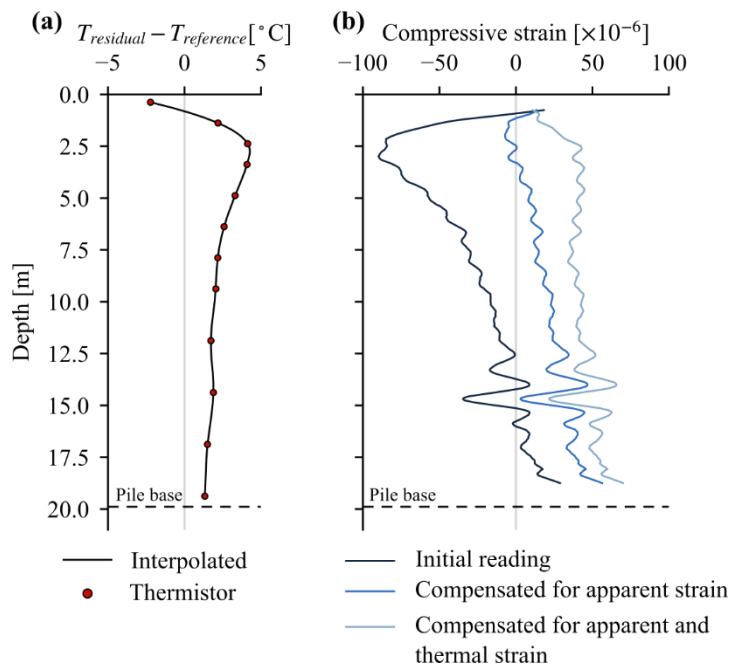


Figure 2.6: (a.) Temperature measurements from thermistor modules in the pile (b.) Strain readings in the pile, with varying degrees of temperature compensation (adapted from Duffy et al., 2022)

### 2.3.4 Instrument calibration

Calibration is a key step in determining and maintaining instrument accuracy. It can be performed at three different stages (Dunnicliff, 1988): prior to shipment of instruments to the user (*factory calibration*), when instruments are first received by the user (*acceptance test*) and during the operation of the geo-structure. Each stage offers a way of verifying that no defects occurred during manufacturing, transportation, instrumentation and operation.

The calibration procedure can vary substantially from instrument to instrument and can range from very simple procedures, for instance to verify the functioning of the instrument, to relatively complex ones, say to establish the absolute accuracy of the device particularly under complex loading schemes such as cyclical loading. Overall, it involves comparing the measurement from the instrument to a known reference measurement.

Furthermore, instruments often infer their target measurement property through other physical processes which are directly correlated to the measurement property. For instance, in Brillouin-based fibre optic sensing, the instrument measures the frequency shift in backscattered light within an optical fibre when compared to the input light-wave. This frequency shift  $\Delta v_b$  is directly proportional to the change in temperature ( $\Delta T$ ) and change in strain ( $\Delta \epsilon$ ) across the fibre. The relationship between which are guided by the calibration coefficients  $C_\epsilon$  and  $C_T$  (Horiguchi *et al.*, 1995). In the event Brillouin sensing is used for measuring strain in a structure, then temperature compensation is required to determine the true imposed strain (Section 2.3.1).

$$\Delta v_b = C_\epsilon \Delta \epsilon + C_T \Delta T$$

Errors in calibration can introduce complications for interpreting the long-term monitoring data. Hence, a clear and detailed outline of the calibration process and any calibration parameters used should be documented in the monitoring programme. This can give insights to future users of the monitoring data as to exactly how the measurements were obtained and understand the long-term resiliency and accuracy of the measurement devices.

### 2.3.5 Instrumentation resiliency

Resiliency of instrumentation is ever more important in geo-monitoring in comparison to the field of structural health monitoring given the fact that instrumentation is embedded (buried) in frequently harsh environments and that retrofitting geo-structures with instruments is difficult to achieve, whilst obtaining similar measurement quality.

Two categories of resiliency can be considered within the overall consideration of resiliency: short-term resiliency and long-term resiliency, both of which can also be intrinsically linked to one another. These are further explained below.

#### **Short term: Instrumentation & construction**

For geo-monitoring, instruments are often embedded within elements of the geo-structure, be it within concrete and/or in the soil itself. As retrofitting instrumentation after construction can be quite difficult, it is imperative that adequate planning is carried out in the pre-construction stage to ensure that instruments can be installed within the planning constraints of the construction project. If not, it needs to be investigated

whether adequate and accurate measurements can be obtained by installing instruments post-construction.

Data collection across all three stages is often characterised by the need to have high robustness of the measurement system not just during the structure's lifecycle but also during the instrumentation process and during the construction of the geotechnical structure. Where retrofitting is not possible, the monitoring system must be able to withstand the frequently harsh construction environment (e.g. large deformations, dynamic loads, extreme temperature environments, accessibility) and the establishment of the system must also align with tight construction schedules and planning. Not only should the actual region of measurement be well-protected, but also should the connecting cables, transmission devices etc., items which can frequently even be more exposed to construction traffic, large impacts or even arson compared to the region of measurement itself.

An example of some adaptations to instrumentation to accommodate for harsh environments is in the domain of fibre optic strain sensing whereby cables can have additional reinforcing and buffers/sheaths to provide extra resiliency both during the instrumentation process but also during the structure's lifecycle (e.g. Figure 2.7). Other considerations should be given towards instrumentation fixity to the structure itself during instrumentation, construction and operation, a procedure which may demand special welding procedures or the use of certain glues or grout mixes to ensure the instrument is fixed in the desired position and orientation. Appropriate documentation of these procedures also helps the end-user understand the effectivity of the instrumentation network and help identify and understand instrumentation failures if they occur.

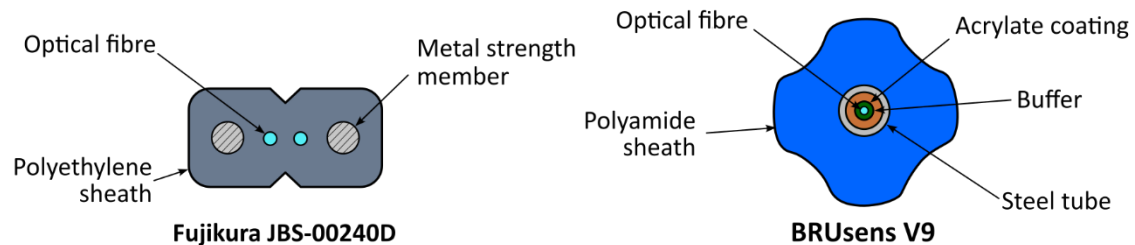


Figure 2.7: Two fibre optic cables used for strain monitoring with different types of reinforcing to improve resiliency and minimise damage to the optical fibre cores

### **Long-term: Network maintenance and sensor stability**

A continuously running measurement system is expected to (partially) fail at some point over the course of a few years and therefore upkeep is required to sustain the effectiveness of the measurement programme.

Such maintenance can involve the fixing or replacement of data loggers and/or sensors in response to, for example, power outages, deterioration of specific parts or loss of fixity. Consequently, experienced personnel may be required to go on-site and ideally, restore the monitoring system to its previous state. An upgrade or downgrade to the monitoring system may also be specified and as a result, interruption of existing systems may be incurred.

Whether maintenance or upgrading is prescribed, either process can induce data gaps in the measurements or cause adjustment to the reference readings or calibration of



the device. It is important that these periods of maintenance are appropriately described and accounted for if possible so that the end-user can fully understand any specific patterns that may arise in the data. In addition, (re)calibration of the devices should be performed as regularly as possible to verify that the prescribed accuracy and precision limits are still being attained.

### 2.3.6 Site activity

Tying in with the requirements of determining an appropriate time for reference readings, site activity should be well documented over the course of both construction and operation. Documentation can come of the form of construction timelines, photos and general reporting – all useful sources of information to assist with a data analysis.

Activity of importance will invariably include site activities which may cause changes in structural behaviour. However, assessing site activity is also important for assessing the cause of instrumentation damage or drifts in the measurements, something which may not be possible to explain without sufficient documentation. Invariably, adjustments to the construction procedure and design should also be well described, given the inability to re-evaluate these changes post-construction given that many geo-structures are underground and largely inaccessible.

An example of this can come in the form of a deep excavation (e.g. Figure 2.8) which are used to establish a stable foundation and basement of a building (depending on the ground conditions and the project scope). Retaining walls are constructed to hold back the large amount of soil during the preparation of the foundation, and it's critical that the deep excavation does not impose movements on adjacent buildings nor create an unsafe scenario on the site itself. Through monitoring of the retaining wall movements and observations of the local site activity (e.g. the excavation depth, placement of stabilising anchors or struts), engineers can try to understand the performance of the design and make adjustments where needed.



*Figure 2.8: Deep excavation during the construction of the New Zealand International Convention Centre (Grouting Services, 2017)*

Another example is also included in ASHVIN Task 4.4: Data driven Management (Deliverable 4.4) which uses measurements during quay wall construction (e.g. Figure 2.9) to validate the numerical design model. This process of validation is useful for evaluating potential adjustments to the quay wall design in the future, whilst confirming the input soil parameters. Throughout this process, not only were measurements

collected of movements and forces acting on the quay wall components, but bathymetric surveys of the seabed level adjacent to the quay wall were made so that correlations between the measurements and real site activities could be made.

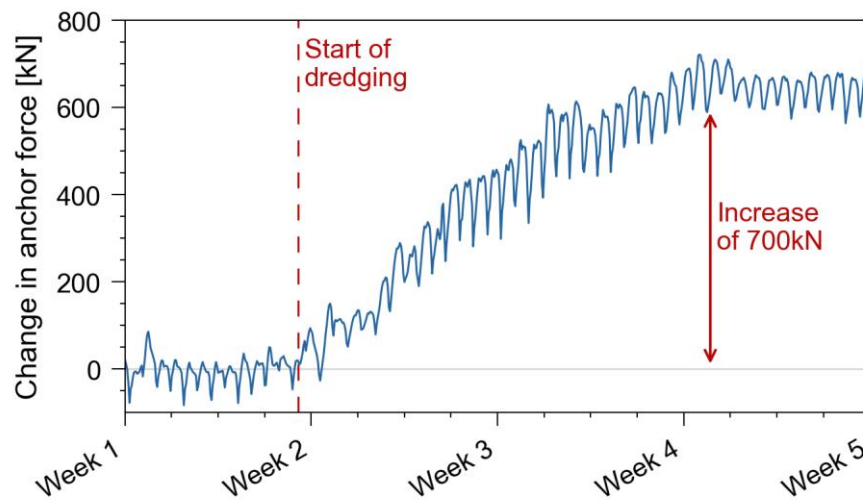


Figure 2.9: Impact of a seven-metre reduction in seabed level on the anchor measurements of a quay wall. The diurnal tidal cycles can also be seen in the measurements.

### 3 DIGITAL TWINS & THE INCORPORATION OF GEO-MONITORING

Monitoring equipment alone provides little value to asset managers or engineers. Instead, data from the monitoring network needs to be collected, visualised and interpreted so that insights can be developed into the performance of the geo-structure. By providing a continued and sustained data stream, the end-user can get real-time information regarding the geo-structure and actively make decisions on the maintenance of the structure or immediately react to impending failures. The real-time connection to the physical asset is what distinguishes a digital twin from other digital models (Bolton, Enzer and Schooling, 2018), such as Building Information Modelling (BIM). Consequently, the key component of a digital twin is the sustenance of a continuous connection between both the physical and digital assets so that a feedback loop is obtained.

In the field of geotechnical engineering, research on the topic of digital twins is relatively scarce (Wu *et al.*, 2022). Whilst developing a digital representation of a geo-structure is common practice in the field, the representation often does not facilitate a real-time connection between the physical structure and the digital representation (i.e. the digital twin).

Some specific examples of digital twin based geo-monitoring have been established in recent years: for instance, Wu *et al.* (2022) provides an explicit example of a digital twin being applied in geotechnical engineering, a model which represents a bored tunnel and the surrounding geological body and structural body, integrated together through BIM technology and the IFC standard.

Another example comes from that of Network Rail who manage most of the railway network assets in the United Kingdom and are heavily invested in monitoring systems of earthworks adjacent to rail lines. These systems respond to ground movement in real-time, providing early warning of (impending) slope failure and have already been instrumental in mitigating serious accidents along the rail network (Brightwell and Butcher, 2022).

Other examples (Song and Jang, 2018; De Gast *et al.*, 2022) involve collating existing site investigation data to assess liquefaction risk over large areas. These models are based on nationwide public databases and can be updated as more information is received in the database.

The domain of structural health monitoring can also offer some important learning points for digital twin based geo-monitoring (Davila Delgado and Oyedele, 2021; Casas, Stipanovic and Chacón, 2022). However, a high degree of spatio-temporal uncertainty is present in geotechnical engineering due to the high heterogeneity of soil properties and due to the embedded nature of most geo-structures, it can be challenging to separate structural behaviour from geotechnical behaviour.

This chapter collects some of the knowledge developed from these examples to present a generalised digital twin architecture for geo-monitoring programmes. Each component of this architecture is described in detail and thus, the chapter provides an overview of how geo-monitoring systems can be integrated into a digital twin platform and utilised to provide insights into the performance of a geo-structure.

### 3.1 Digital Twin Architecture

The architecture of a digital twin system describes the underlying algorithms behind the model and how all the model inputs are processed and integrated together. Most digital twin architectures vary in terms of the number of layers and their names, but in general, they consist of three main layers i.e. (i.) a data layer (ii.) a processing layer and (iii.) an interaction or user interface layer (Davila Delgado and Oyedele, 2021).

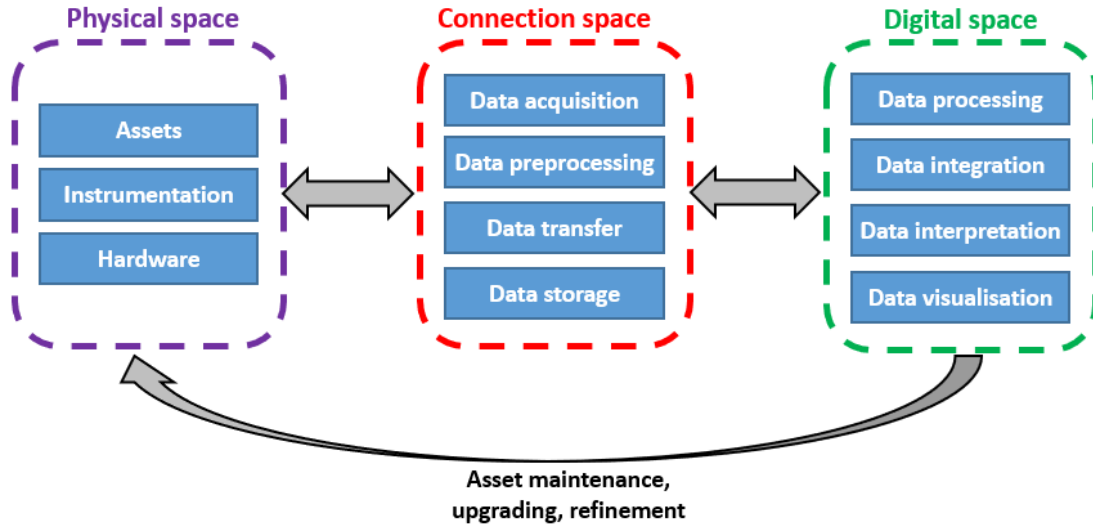


Figure 3.1: Simplified digital twin architecture for a geo-monitoring programme

A simple system architecture for geo-monitoring is shown in Figure 3.1. The schema consists of three different *spaces*, corresponding to the three core facets of the digital twin: the physical space, the digital space, and the connection in between. Within each space are different layers, within which are a cluster of different tasks, processes or items associated with that layer. By utilising the results of the digital twin, decisions can then be made to adjust the instrumented asset or inform future renovation programmes.

The schema shown can also be non-linear. For instance, a whittled down schema can be devised to prioritise rapid action to critical changes in the structure (such as sudden failure), by collecting only critical information and processing them swiftly so that alarms can be raised. In parallel, a more detailed schema can be executed which provides more detailed and accurate insights or trends regarding the long-term performance of the structure and compare observed with predicted behaviour.

Lastly, the site-specific digital twin should be considered within the overall hierarchy of digital twins in an organisation, particularly in terms of the degree of interaction expected between digital twins beyond just a site-specific response (Lu *et al.*, 2020). Through interconnectivity between digital twins, status updates on all the assets can be provided and allow for a seamless integration and management of maintenance programmes and improve the ability to develop long-term plans across an asset portfolio.



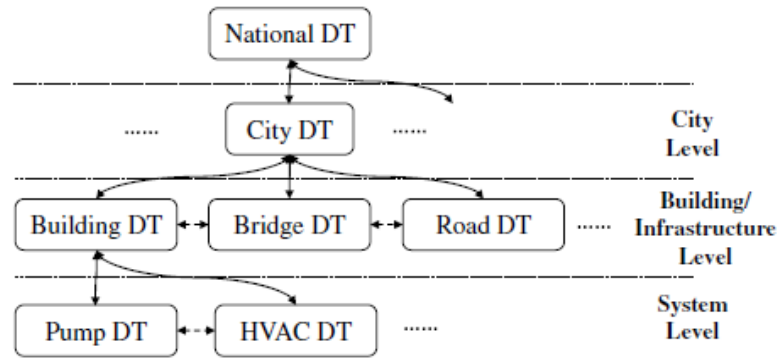


Figure 3.2: Digital twin connections and hierarchy among different levels (Lu et al., 2020)

The rest of this section shall consider each layer of the proposed digital twin architecture in more detail, explaining them in the context of geo-monitoring and highlighting important areas of emphasis for development.

### 3.2 Connectivity Space

The intermediary component of a digital twin, the connection between the physical and digital realms, is at the core of a digital twin model and distinguishes the digital twin from other digital models. Being at the physical/digital interface, the connectivity space is a blend of both physical and digital equipment, converting one from the other and transferring it to one or multiple hosting platforms (i.e. the digital space). For the most part, each layer within the connectivity space is performed sequentially.

#### 3.2.1 Data acquisition layer

The data acquisition layer is the fundamental starting block for any digital twin, in essence, capturing changes in states imposed on the instrumentation and transforming these to electrical (digital or analogue) data. Data acquisition is inherently dependent on the type of data collection methods used, discussed in Section 2.

A proportion of the data processing is generally done by data loggers which directly record the sensor outputs. For instance, data loggers can apply the appropriate calibration factors or convert the data to specific file types. The range of capabilities is highly dependent on the data logger used and it is important to consider the degree of data pre-processing carried out, particularly in the case where proprietary software is used to produce the desired measurements.

Within the data acquisition layer, the frequency of measurements can be set in line with the considerations outlined in Section 2.3.2. Some flexibility can be accounted for at this level: for instance, if impending failure is recognised by the digital twin, the frequency rate can be increased to ensure more real-time information is received over the impending failure. Conversely, at times of relative stability, the frequency rate can be kept low to minimise data processing and data transfer required.

#### 3.2.2 Data connectivity layer

The data connectivity layer aims at transmitting to the collected data towards other layers for processing and analysis. Its development is primarily driven by site constraints such as:

- **Connectivity:** Can a direct internet connection be established on site through Wi-Fi or cellular networks? How quickly does data need to be transferred? Is the bandwidth sufficient to transfer the data collected?
- **Power supply:** Is a continuous power supply (e.g. from mains) available? Can the energy used by the monitoring system be utilised more efficiently? Are there opportunities for energy harvesting (e.g. solar or wind power)? What redundancy measures are available in the event of a power outage?
- **Site Accessibility:** How accessible is the site? Is easy maintenance or data collection feasible? Is the site actively used when in normal operation and could this pose a threat to the monitoring system?

By examining these constraints, the type of connectivity to be used for the monitoring network can be established. Two types of networks can be considered: wireless sensor networks and wired sensor networks. Both network types can generally consist of the same sensors but in the case of the wireless system, a transmitter and receiver are used in lieu of connecting wires (electrical or fibre optic) for transferring data to the host(s). Coupled wired-wireless system can also be used, for instance, whereby sensors are connected to an on-site central server using a wired system and then the collected data is transferred wireless to an off-site server.

#### **Wired sensor networks**

Wired sensor networks have been more common traditionally due to their simplicity. It describes a sensor network that is physically connected to a central processing unit using typically electrical or fibre optic lines. While establishing and developing a wired sensor network can be difficult, the network can be quite robust and can be installed in the subsurface, mitigating the risk of accidental/deliberate damage or theft. The system can also easily be integrated with most commercially available data loggers and sensors and requires very little specialist expertise. The power demand of the system is usually integrated into the wired connections themselves and so the system generally works off mains power.

Wired networks can be greatly limited by their high cost and difficulty of installation and can be susceptible to disturbance in case where entire structures are instrumented (Abdulkarem *et al.*, 2020). Such direct-wired systems are also typically centralised, with sensors connected to a centralised processing unit via long connections, make the system vulnerable to single points of failure (Park *et al.*, 2008). Retrofitting is also considerably difficult, if not impossible in the case of embedded structure for geo-monitoring purposes, and so scalability can also be an issue.

Generally the system is used where specialist experience in wireless network is not available or to minimise the costs of having data loggers or processing nodes at every instrumentation location, particularly for instrumentation-dense projects.

#### **Wireless sensor networks**

Wireless sensor networks are facilitated by a range of devices varying from simple open-source platforms such as Arduino or ESP32/8266 microcontrollers to other commercially or academically developed hardware (for an overview, see Abdulkarem *et al.*, 2020). Wireless sensor networks are generally considered easier to install, to scale and maintain and are consequently more cost-effective in the long-run when compared to wired networks.

Wireless sensor networks are nonetheless limited by the amount of data they can transfer and the availability of power (Abdulkarem *et al.*, 2020). As a result, maximising data transfer across constrained bandwidth and battery sizes is crucial and can be performed through network optimisation. In the context of geo-monitoring, wireless sensor networks are also constrained by the position of the sensor, which is generally located below the surface and can often be permanently inaccessible following the construction of the geo-structure (e.g. a foundation pile).

The transfer of data within a wireless network is generally facilitated through short-range network technologies (e.g. WiFi, near-field communication (NFC)), wider-range technologies (e.g. 3G, 4G and 5G wireless broadband communication) or low-power wide-area networks (LP-WAN) (Lu *et al.*, 2020). If data security and privacy is a requirement of the digital twin, consideration should also be brought towards vulnerabilities within the chosen transmission technology, such as security issues associated with the unlicensed spectrum band of WiFi (Lehr and McKnight, 2003).

The density and topology of the sensor network is also important to consider in terms of network optimisation and data storage capabilities and the impact it may have on network scalability, performance and resiliency (Aygün and Cagri Gungor, 2011). A feedback loop within the digital twin itself can also optimise data transmission, for instance, by adjusting the sampling rate of the (certain) sensors depending on the likelihood of a critical event occurring and thus optimising the amount of bandwidth available (Brightwell and Butcher, 2022).

The greater flexibility of wireless sensor networks and their application towards large and remote sites means that practical implementation issues such as power supply are also key components in their efficient development. Through network optimisation, dynamic voltage management (Tuming, Sijia and Hailong, 2010; Chéour *et al.*, 2020) and dynamic power management (e.g. active, idle and sleep modes) the energy demands of a network can be minimised. Furthermore, harvesting energy from the surrounding environment through, for example, solar, wind or vibrational energies can offer an excellent way of developing a resilient network over the long-term (Park *et al.*, 2008), but nonetheless, they require specialist expertise and careful planning.

### 3.2.3 Storage layer

#### Data management

A range of storage options are available, ranging from a physical server to cloud-based solutions. In this regard, the amount of storage required needs to be accurately pre-defined. This varies greatly depending on the scale of the monitoring system in both physical scale and duration and the type of data obtained. A general rule-of-thumb can be found in Table 3.1 for estimating the memory required for a single sensor.

*Table 3.1: A rule-of-thumb for determining expected storage capacity required for a single sensor (Sparkes and Webb, 2020)*

Sampling rate	Rate per day	Rate per month	Rate per year
1 reading per hour	7 kB	0.21 MB	2.6 MB
1 Hz	25 MB	0.75 GB	9 GB
10 Hz	253 MB	7.5 GB	90.2 GB
100 Hz	2.47 GB	75.2 GB	902 GB

Decentralised computing architectures such as edge computing (Shi *et al.*, 2016; Buckley, Ghosh and Pakrashi, 2021) can help reduce the storage demand on the central server and connectivity networks by storing and processing (some of) the data close to the sensor node itself, in contrast to centralising all storage and computation on a singular server. This can be particularly useful in instances where rapid response to changing conditions is required by minimising the demand on the connectivity network. Nevertheless, the choice of system will alter the communication approach and pose certain advantages and disadvantages.

Redundancy in the event of failure of the data storage system should also be considered. Data contingency practices such as the RAID (Redundant Array of Independent Disks) architectures for hard disks or solid-state drives provide ways of developing a resilient data storage system which minimise the risk of complete data loss or corruption (Chen *et al.*, 1994).

### **Data formatting**

On a small-scale and short-term level with minimal users interacting and working with the data, simple data formats that are familiar to most people (e.g. .csv, .txt, .json) can prove to be optimal. However, data management beyond very small-scale monitoring programmes becomes prohibitive, particularly when scalability is desired. Furthermore, some data formats, such as .txt or .csv, require prior understanding of the structure of the data file (known as *non-associative* data types), which may risk the how future-proofed the dataset is due to the potential difficulty for future users to interpret the data file. Associative data formats such as .xml, .json or .yaml reduce the degree of interpretation required for the end-user when dealing directly with the raw data.

More robust systems can store data in more memory-efficient manner and tie in with good data management practices, particularly for very large datasets. These include SQL-based relational databases or tools developed specifically for big data such as the Hadoop open-source framework or NoSQL (Arcadius Tokognon *et al.*, 2017). In all cases, the interaction between the end-user and the dataset should be considered, particularly taking into consideration the capabilities of the average practitioner in more advanced database management systems.

Regardless of the database management system, a variety of file formats will be introduced over the course of construction and operation of a geo-structure from different contractors and sub-contractors and interoperability/interaction between these formats within the digital twin paradigm can be challenging. The format used is largely dependent on the measurement contractor, the country and/or the monitoring software used.

A list of some of the most common file formats is included in Table 3.2, some of which can contain near identical data, albeit in different formats. Inevitably, qualitative data or non-machine-readable formats are also likely to be introduced and how these are incorporated into the digital twin (or if they should) can be challenging. This can include reports or graphs nested within .pdf files and may require extensive processing to obtain the required information if the original electronic data is not available.

Table 3.2: Common file types in geo-monitoring

Category	File extensions	Description
Geotechnical	.ags, .gef, .dfn	Open-source human-readable formats for sharing site investigation data
	.px2d, .cae	Used for geotechnical numerical models (e.g. PLAXIS or ABAQUS)
Civil	.shp, .qgs	Storing geographical data (e.g. through ArcGIS or QGIS)
	.dwg, .dxf	Vector format for construction drawings (Autodesk AutoCAD)
	.dem, .flt, .tif	Storing digital elevation models
	.ifc, .rvt	Format for storing BIM data
Generic	.txt, .json, .xml	Text-based human-readable formats. Typically outputted by monitoring systems
	.csv, .xlsx	Microsoft Excel-based file systems
	.m, .py, .cpp	Computer programming scripts. Generally used for data processing and analysis
	.docx, .pdf	Files associated with word processing and reporting
	.png, .gif, .jpg	Image formats (maps, graphs, photos etc.)

Within Table 3.2, some formats specific to geotechnical data are listed and can be effective in storing the largest amount of relevant geotechnical data, including details such as instrument ID, calibration details, operator etc. Examples of such formats include the .ags format (Bland, Walthall and Toll, 2014) or the .gef format (Schaminée, den Adel and Bezuijen, 2006), an example of which is given in Appendix B1. Both formats are text-based human-readable formats that are typically interacted with using proprietary software or scripts.

Nonetheless, file types similar to the .ags and .gef formats can sometimes send sequential data files which contain a lot of duplicate information between each other, increasing network congestion and reducing storage efficiency. Data pre-processing can help minimise the amount of duplicate or unnecessary information sent, increasing the amount of available bandwidth and storage space.

### Future proofing

Regardless of the data management system, an important consideration for the end-user is the level of interaction they require with the data (e.g. solely for visualisation or directly working with and analysing the dataset). The typical lifetime of engineering structures ranges between 20-100 years, greatly exceeding the lifetime of most electronic components and it should be anticipated that with both planned and unplanned obsolescence, substantial changes can occur with respect to computer hardware and software during that time period (McNeill, 2009). For instance, over the lifespan of a structure built in the 1950's, a huge change in storage formats has occurred and multiple changes in the management system would have been anticipated for a hypothetical digital twin developed in that period (Figure 3.3).

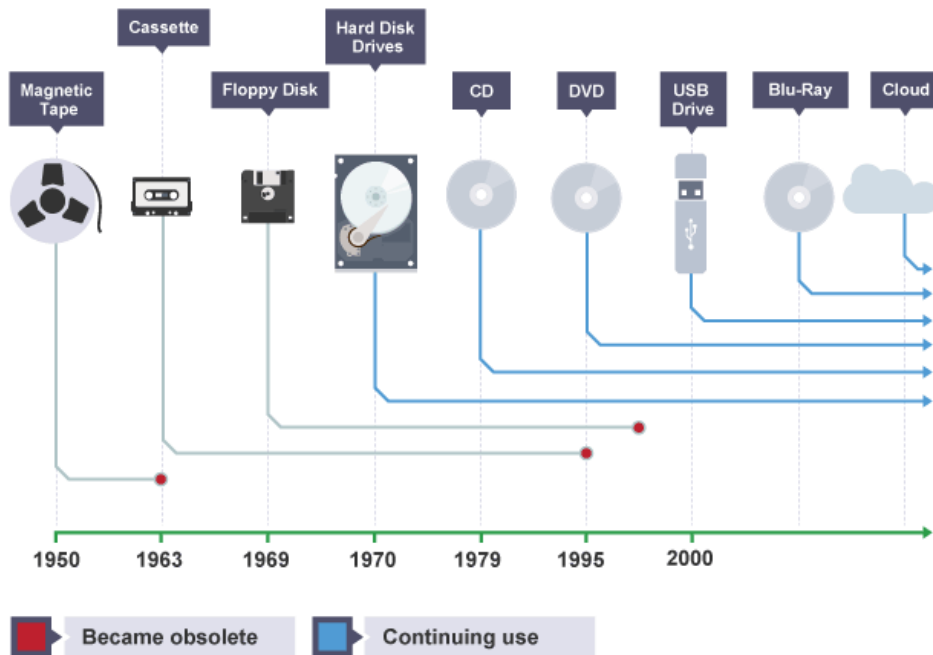


Figure 3.3: timeline of storage formats over the course of 70 years (Franklin & Marshall College Library, 2022)

Consequently, digital twins should be designed in a way such that there is flexibility with regards to how data is accessed or is performed through future-proof methods, or at least the data structures utilised are well documented and ideally open-source. In the case of online storage, data may also need to be transferred to new newer systems as current equipment becomes obsolete and so redundancy should be ensured both in terms of equipment failure and failure to properly transfer all of the data (McNeill, 2009).

Long-term storage of data, typically referred to data archiving or data warehousing, is also an important factor, particularly if the digital twin becomes obsolete. Information gained from the digital twin can be extremely useful for future practitioners and as a result, storing the data in a way that promotes accessibility and efficiency in terms of storage space should be considered. This includes appropriate descriptions of the dataset for future users, for instance, through summary statistics and description of the database structure itself. Archiving may also entail reducing the size of the raw measurements to both minimise storage costs and improve data readability and conciseness.

### 3.3 Digital Space

The digital space focusses on taking the collected data and producing a tangible and meaningful result for the end-user. It involves directly working with the data, altering and adjusting it. As a result, the process opens the opportunity for insights to be gained, whilst also potentially creating opportunities where insights can be lost. A regimented and well-tested procedure needs to be created as a result, ensuring minimal data loss or misinterpretation during the process. These processes have become more and more automated, particularly in cases where instantaneous results are expected. However, the value of human input and judgement should not be underestimated (and similarly, overestimated)



A set of layers are presented below, comprising of data processing, data interpretation, data visualisation and data integration and while these processes are typically executed sequentially, some interaction or fusion between the different layers should be expected.

### 3.3.1 Processing layer

An initial screening of the data should be performed, ensuring the instruments are correctly functioning and are not sending critical warning functions. The signals can then be processed and converted to the desired parameter based on the calibration test results (Section 2.3.4).

#### Outlier removal

Outliers are unusual values in a dataset which may distort the data analysis and interpretation, particularly within the real-time updating of a digital twin. In this regard, two types of data can be removed:

- **Anomalous data:** behaviour that does not comply with expected patterns or trends in the data
- **Noisy data:** random variations in the sensor's output, typically within the range of how accurate the sensor is

Both data types are not always independent of one another, yet they can require different types of outlier removal. This can be carried out at a very simple level (e.g. setting thresholds based on the standard deviation of the received data, moving average windows) or at a more advanced level incorporating machine learning algorithms such as DBSCAN (Ma *et al.*, 2022), Extended Isolation Forest (Hariri, Kind and Brunner, 2021) or Kalman filter (Mu and Yuen, 2015).

Nonetheless, automated outlier removal should be considered very carefully, particularly with regards to the high dimensionality of many engineering parameters and furthermore, sensors shouldn't be considered completely in isolation as sometimes apparent noise can reflect something occurring on a larger scale or is indicative of more serious underlying problems associated with the dataset. In all cases, the extent at which outlier removal should be extensively documented and tested and if possible, the original, raw data should be made available.

Identifying what readings should be removed in a geotechnical engineering context can be challenging due to the combination of instrument effects, structural effects (e.g. element shape and concrete quality in the case of a pile foundation) and geotechnical effects. For instance, Figure 3.4 shows measurements of the force distribution in a pile measured incrementally during a load test. In the test, the axial load is increased in steps by means of a hydraulic jack connected to a load frame. The distribution of load along the pile gives information of the development of the separate soil resistance components (e.g. shaft and base resistance). Noisy data can be seen in the periodic fluctuations due to strains induced on the fibre optic cable itself during manufacturing along with anomalous changes with the sudden change in trend at a depth of approximately 20 m. By identifying these outliers, an appropriate and accurate interpretation of the shaft friction of the pile in each soil layer can be made based on the rate of decrease of force.

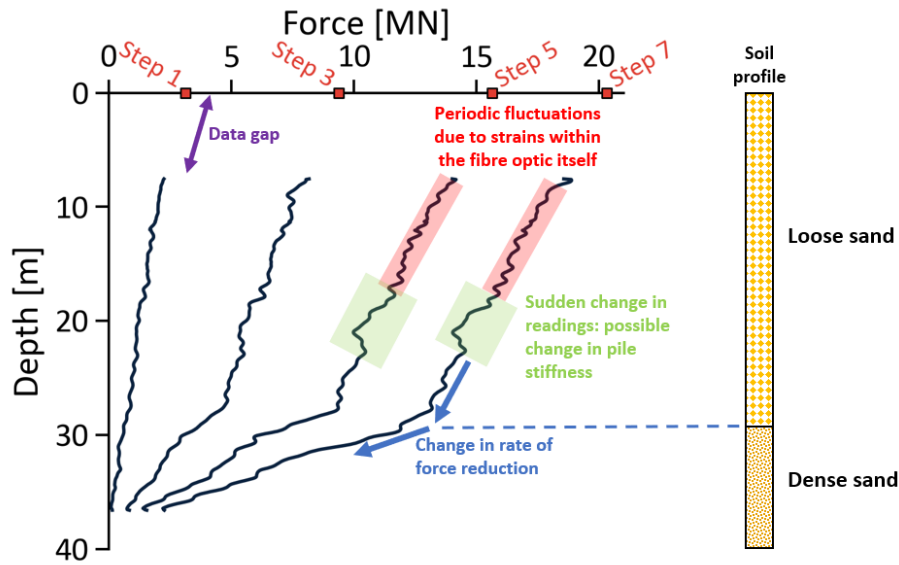


Figure 3.4: Measurements of a foundation pile during a load test, whereby the load was increased in steps and the corresponding force was measured using fibre optics

### Interpolation

In order to compare different measurement types with one another from different locations, interpolation in both the time and space domains is required. For instance, interpolation over time may be required for instruments for which temperature compensation is applied through a separate instrument measuring temperature (Section 2.3.3). This separate technique may record at different measurement frequencies, different measurement intervals, or even a certain distance away from the target measurement axis. Depending on the interpolation intervals, simple linear interpolation can be performed, the accuracy of which invariably depends on the size of the data gap.

Furthermore, monitoring data of a structural element may need to be correlated to soil data, and for this, the best estimate of the soil data at the given location may need to be calculated based on surrounding measurement points (such as data from a cone penetration test, see Section 2.2.2). As soil is correlated in the horizontal and vertical directions, specific interpolation techniques can also be used such as kriging (Rahman, Abu-Farsakh and Jafari, 2021) which accounts for the spatial correlation of soil properties. Using these interpolation techniques can assist with the development of a site-wide ground model whereby every part of the site is parameterised in terms of its soil properties.

Nonetheless, spatio-temporal interpolation will always introduce some uncertainty into the analysis and while literature takes sensor data capture and integration for granted, the delicate intricacies involved in this and interoperability with the rest of the digital twin components remains largely unexplored (Boje *et al.*, 2020).

### 3.3.2 Integration layer

Processed and interpreted monitoring data can also be coupled or fused with other data sources or analysis techniques to provide an intuitive and informative digital twin representation for the end-user.



For instance, design of geo-structures is frequently performed using advanced numerical models such as the finite element method (FEM). These models take inputs from the user and can predict the structural and geotechnical performance using underlying numerical approximations. In a geotechnical setting, this can be performed using software such as PLAXIS or ABAQUS which both provide outputs that can be paired with monitoring data. This can be incorporated by taking the mesh elements of the FEM software (e.g. Figure 3.5) and pairing them with a monitoring location.

Integration with Building Information Modelling (BIM) is also possible and can integrate well with the overall visualisation of the digital twin, outlined in Section 3.3.4. Further information and data fusion tools for real-time construction monitoring can be found in Deliverable 3.3 of the ASHVIN project (Imperiale, 2022).

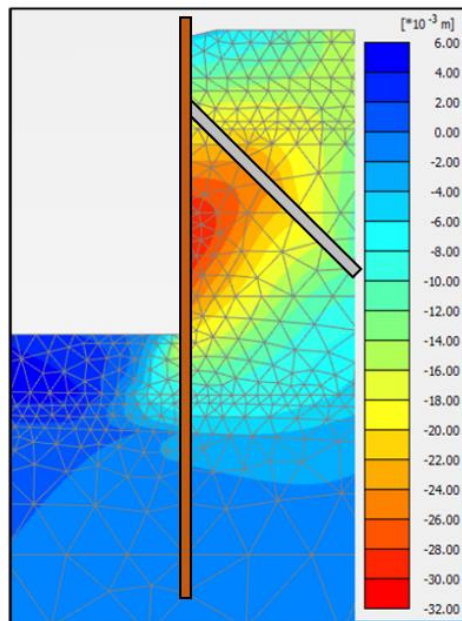


Figure 3.5: FEM model of a quay wall, indicating the degree of displacement in millimetres for each element of the mesh (amended from Schouten (2020))

### 3.3.3 Interpretation layer

Interpretation in the context of this report describes additional data processes that are required to get the desired output, be it through additional calculations and/or statistical analyses. In other words, the interpretation layer aims to bring reasoning to the generated data and to fulfil the objectives established at the beginning of the monitoring programme (Section 2.1). Data interpretation is oftentimes heavily dependent on the person working/interacting with the data and as a result, developing automated tools can either conceal some of the uncertainties behind the data or prevent the end-user from coming up with their own satisfactory conclusion and so care should be taken with regards to the interpretation and ensuring that any steps are clearly outlined.

Some of the interpretation is already nested with other layers within the digital space, such as spatial interpolation within the Processing Layer or the example given in Figure 3.4 of pile test interpretation.

### Alarms

Prescribing alarms or threshold for measurements parameters is frequently prescribed for digital twin so that rapid response measures can be developed in the event of (impending) structural failure. Thresholds can be set on the raw measurements directly from the data loggers or also on interpreted data although in both instances, defining the appropriate threshold involves anticipating the potential failure mechanisms of a geo-structure and anticipating the magnitude of the movements that may result. Whilst it is easy to err on the side of caution (i.e. minimise the number of false negatives), conversely, minimising the false positive rate is also critical in order to minimise the number of false positives which can reduce the swiftness of first responders in the event of a serious condition developing at the geo-structure.

### Model updating

Numerical representations of the digital twin (such as those developed by FEM, see Section 3.3.2) can be updated in different ways. One method of doing so is by directly measuring input parameters over time and re-configuring the input to numerical models to match these direct measurements. Alternatively, the model parameters can be updated through inferential methods such as Bayesian inference, maximum likelihood estimation or machine learning models (Bado *et al.*, 2022).

Achieving a balance between a sufficiently accurate and representative model with minimal manual input/analysis can be somewhat challenging and particularly in the early stages of digital twin development and operation, a lot of work is needed to ensure model reliability. This can have implications for the updating frequency of the model and so complex model updating pipelines for large geo-structures are generally not considered in real-time to ensure the accuracy and robustness of the model and are primarily utilised for informing asset maintenance or upgrading programmes.

#### 3.3.4 User interface layer

Data visualisation is inevitably, one of the primary means with which users interact with the digital twin, and as a result, a significant amount of the interpretation is made of data that has been thoroughly processed and integrated together, as discussed previously.

Typically, visualisation in the engineering sector comes in the form of plots and varies widely both within a project and between projects. Consequently, polling the end-users about the desired outputs can be hugely important as part of this process. Some of these plots can be relatively simple, such as plotting the received measurement data over time so that the end-user can readily recognise the data quality themselves. With increasing analysis and interpretation, comes increasing opportunities for graphical visualisations. Visualisations should also reveal the extent of uncertainty in the data by for instance, including a lower bound and upper bound of the measurements related to the measurement accuracy or interpolation schemes implemented.

A range of tools are available for data visualisation, ranging from low-level applications such as (pre-filled) Excel spreadsheets, to high-level applications such as dashboards (e.g. Figure 3.6) like Microsoft Power BI or Plotly Dash. Custom-built Graphical User Interfaces (GUIs) can also be developed, offering a high degree of flexibility compared to dashboards, albeit with increasing complexity in the background. This complexity

can be somewhat reduced using developmental toolkits such as Qt Designer, albeit a trade-off with flexibility.

The selection of these tools should then be based on the desired complexity and scalability of the system, in addition to the experience of the end-user and instrumentation/digital specialist.

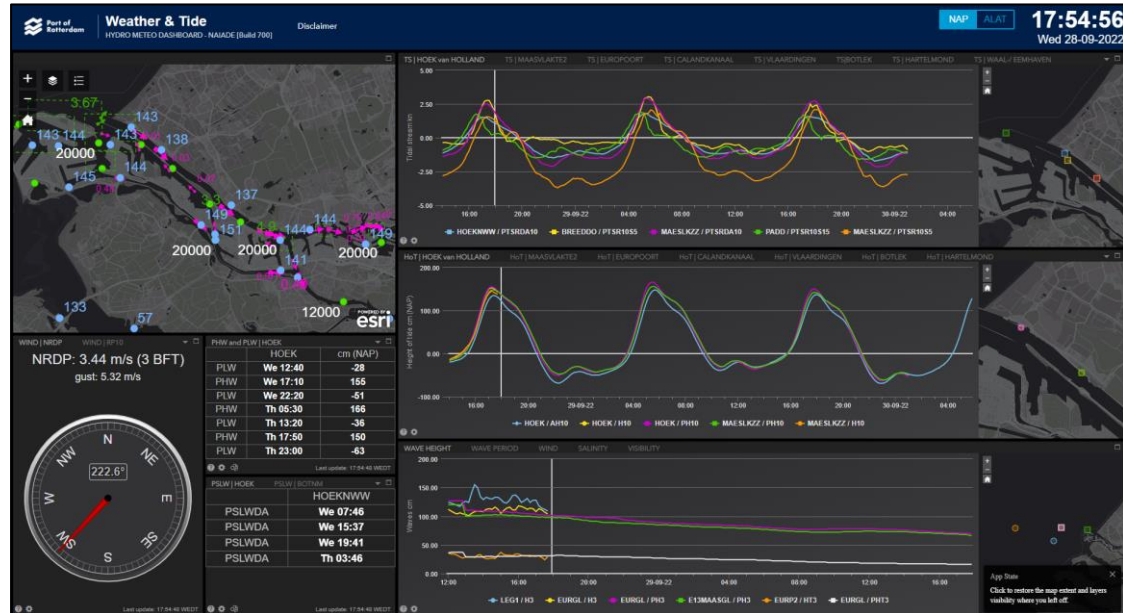


Figure 3.6: Example of the weather & tide dashboard at the port of Rotterdam (Port of Rotterdam Authority, 2022)

## 4 DEMONSTRATION CASE #10: A QUAY WALL IN THE NETHERLANDS

Demonstration Case 10 (DC10) is a quay wall located in the Maasvlakte (Figure 4.1) area of the port of Rotterdam. The container terminals around the Maasvlakte have direct access to the North Sea and are frequently visited by some of the largest cargo ships in the world. Nevertheless, ever-growing ship sizes have also increased the demands on the port and as a result, there are plans to extend the length of DC10 or increase the dredged depth of the quay to accommodate for larger and more ships.

Monitoring at DC10 has been performed since its construction in 2007 and an early version of a digital twin was developed. Since 2016, the responsibility of the monitoring programme changed hands and no further measurements were made at the quay wall, however, the monitoring system remains largely intact as of the time of writing. InGEO received the dataset in 2020 and no in-depth analysis of the data has been done to date.

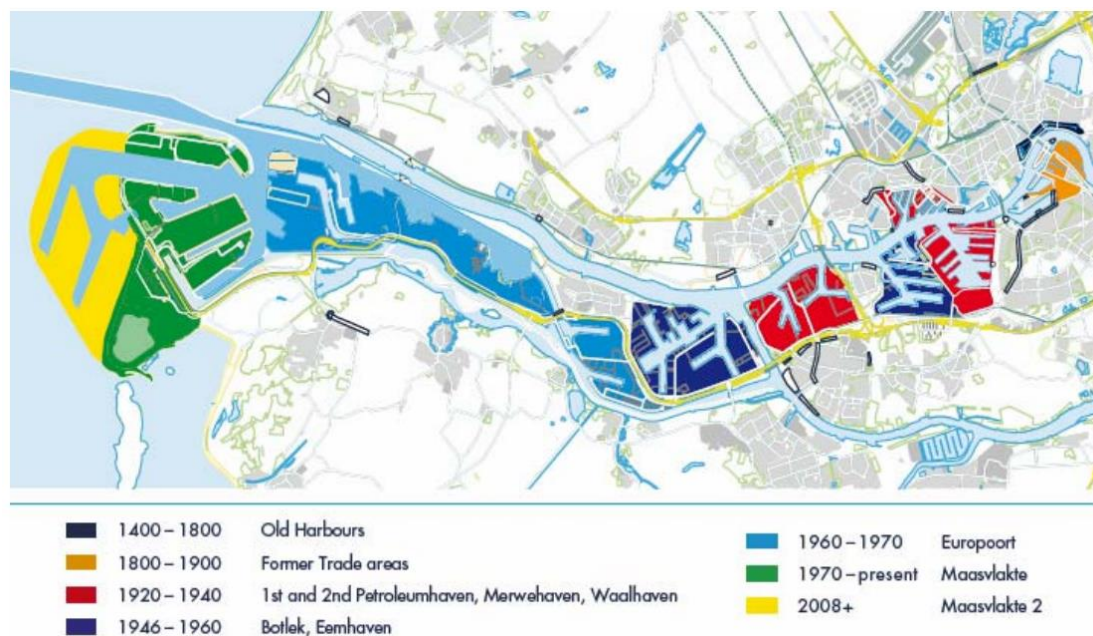


Figure 4.1: Areas of the port of Rotterdam. The DC10 quay wall is located on the Maasvlakte in the west (de Gijt et al., 2010)

DC10 forms part of a wider “smart quay wall” initiative by the Port of Rotterdam Authority to improve the understanding of their infrastructure, particularly with regards to asset maintenance and upgrading. Further details regarding the initiative and associated research are provided in Appendix A.

### 4.1 Objective Definition

The monitoring programme at DC10 was established to provide insights into the long-term reliability of the quay wall, enabling the asset owner and port engineers to make informed decisions on future quay wall rehabilitation programmes and make adjustments to the quay wall (e.g. seabed level, crane size) to accommodate for larger ships, if needed.

In addition, the monitoring programme was established to provide an early-warning system in the case of failure. Examples of quay wall failure mechanisms are included in Figure 4.2 and on this basis, the quay wall was specifically instrumented to help identify some of these failure mechanisms.

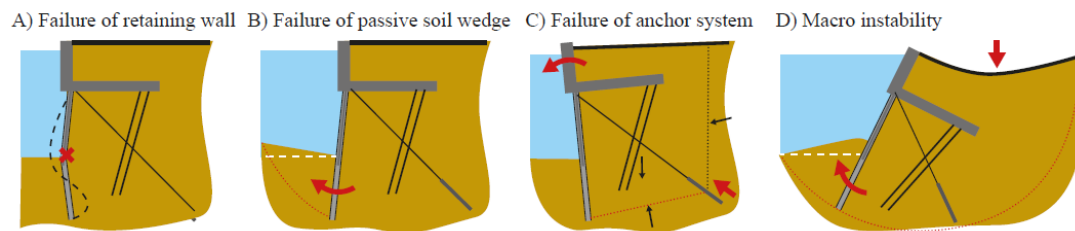


Figure 4.2: Some possible failure modes of a quay wall (Roubos, 2019)

## 4.2 Desk Study

Extensive development across the port, including the development of the Maasvlakte peninsula, has meant a wide range of data is already available and of a wide variety of types (Table 4.1). A lot of this data is freely available online and has been used as part of this deliverable.

Table 4.1: Publicly available data available for the desk study.

Category	Data source	Description	Data type
Geological/geotechnical	Dutch National Key Registry of the Subsurface ( <a href="https://basisregistratieondergrond.nl">basisregistratieondergrond.nl</a> )	Public-domain geological/geotechnical information (not available at construction)	Qualitative & quantitative
	Archaeological	Existing publications (e.g. Vos et al. (2015) archaeological survey of Yangtzekanaal)	Qualitative
Geotechnical	Existing projects	Existing quay wall projects, publications (e.g. de Gijt & Broeken (2013))	Qualitative
	Dutch National Key Registry of the Subsurface ( <a href="https://basisregistratieondergrond.nl">basisregistratieondergrond.nl</a> )	Public domain site investigation tests from existing and neighbouring locations	Quantitative
Meteorological conditions	Weather station	Daily weather reports from Hook of Holland weather station	Quantitative
	Waterinfo ( <a href="https://waterinfo.rws.nl">waterinfo.rws.nl</a> )	Daily tidal fluctuations, dredged depths, current strength, water temperature;	Quantitative
Existing/previous land use	Historical maps	<a href="https://kadastrelekaart.com">Kadastrelekaart.com</a> <a href="https://uu.georeferencer.com">uu.georeferencer.com</a>	Qualitative
	Satellite imagery	Google Earth; <a href="https://satellietdataportaal.nl">satellietdataportaal.nl</a>	Qualitative
Satellite data	Dutch Ground Motion Service <a href="https://bodemdalingskaart.nl">bodemdalingskaart.nl</a>	Nationwide InSAR settlement data	Quantitative
	Satellite imagery	Google Earth; <a href="https://satellietdataportaal.nl">satellietdataportaal.nl</a>	Qualitative
Site topography	Topographical map	<a href="https://www.ahn.nl">www.ahn.nl</a>	Quantitative



#### 4.2.1 Site history

A short overview of the history of the port of Rotterdam and Maasvlakte is provided in Hutter (2003). The port of Rotterdam has been a focal point for much of recent Dutch history. In the Netherlands' "Golden Age" in the 17<sup>th</sup> and 18<sup>th</sup> centuries, trade from the East India Company brought significant revenue from the port of Rotterdam. French occupation at the start of 19<sup>th</sup> century brought an end to this Golden Age and trade at the port of Rotterdam significantly decreased.

In the mid-19<sup>th</sup> century, plans were put in place to improve the position of the port, however, one of the main problems with this were the variety of obstructions and shallow areas in the Maas estuary between Rotterdam and the sea, such as the *Honde Plaet* (Figure 2.1). To combat this, a channel known as the *Nieuwe Waterweg* was dredged, improving the connection between the port and the sea.

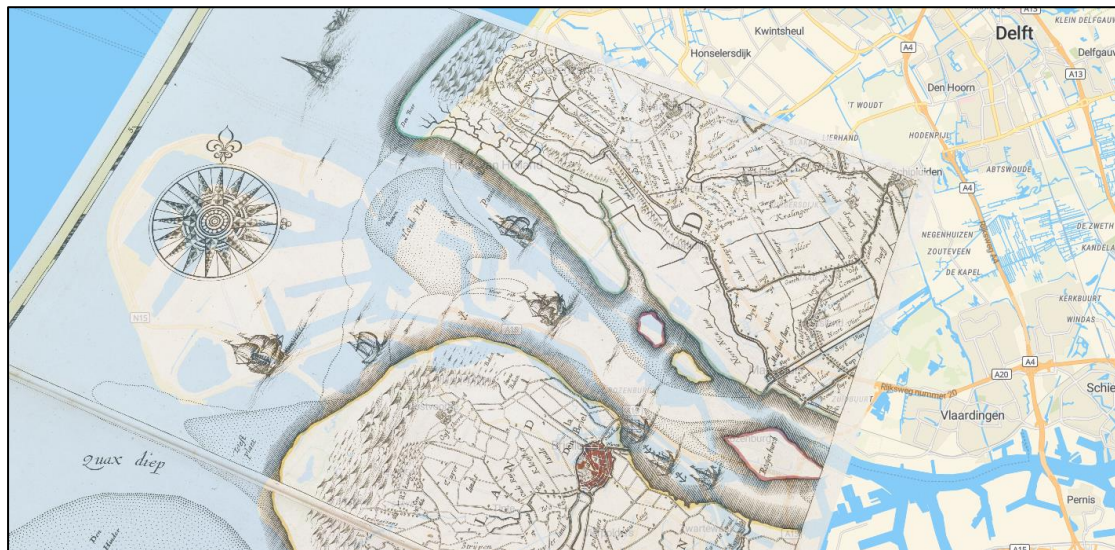


Figure 4.3: Overlay of a map by (Colom, 1750) on top of a current map of the Maasvlakte peninsula (Utrecht University, 2022). The mouth of the estuary is shown along with ship passageways around the Honde Plaet.

From thereon, Rotterdam port continued to expand westwards from the centre of Rotterdam and the first oil refineries began to open in the port. Nonetheless, the ever-increasing world trade system began to demand more and more of the port. To combat this, the Maasvlakte 1 peninsula was created in 1960s using soil extracted from dredged harbours and offshore locations immediately surrounding the Maasvlakte. DC10 is located on the Maasvlakte 1, although its construction came forty years after the construction of the peninsula, almost simultaneously with the second extension of the Maasvlakte peninsula, known as Maasvlakte 2.

In terms of the general ground characterisation, these old maps give indications as to the depositional conditions at the mouth of the port, potentially indicating high sedimentation rates across the port and giving some clues as to the geological conditions of the area.

#### 4.2.2 Geological overview

As shown in Figure 4.4, a simple geological cross-section can be developed from the GeoTOP model on DINOloket (Stafleu *et al.*, 2019), giving a preliminary understanding of the geological soil layers and their depths in the general area of the quay wall. Around the time of construction of the quay wall, an extensive geological survey was

carried out in the Yangtzekanaal as part of a wider archaeological survey (Vos *et al.*, 2015), providing extensive geological information and data.

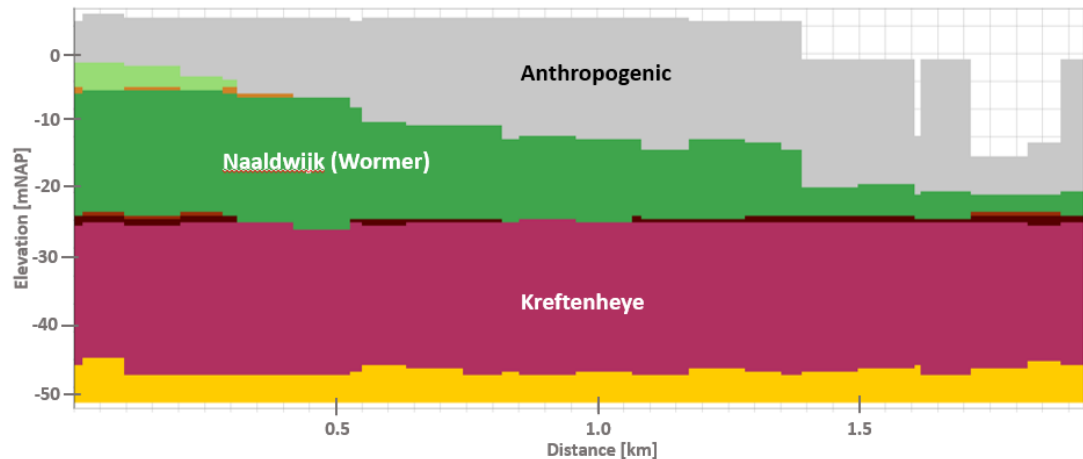


Figure 4.4: Geological cross-section along DC10 (DINOloket, 2022). Names within brackets are Members within a Formation

The Maasvlakte area overall has also been extensively studied due to its economic and archaeological significance and so there is a glut of geological and geotechnical information in the wider area (e.g. Hijma *et al.* (2012), Moree *et al.* (2015)).

To summarise the geological information available on the local subsurface, the geological history of the area has been strongly defined by the Rhine-Meuse river system which threads its way across the centre of Netherlands, reaching the sea at the Maasvlakte. In the Pleistocene geological epoch, the river deposited a layer of sand known as the Kreftenheye Formation (colloquially referred to as the “Pleistocene sand”). This layer is present across much of the Netherlands and its high density renders it a suitable load-bearing layer for foundations. As such it is a very significant geological formation for many structures across the Netherlands, including the quay walls in the port of Rotterdam.

Continued change in worldwide temperatures and retreat in glaciers marked the end of the Pleistocene epoch and the start of the Holocene epoch. This also led to rising sea levels and changing coastlines, causing a shift from fluvial depositional process to marine depositional processes during the Holocene epoch. Stagnant water (e.g. lagoons) in the area resulted in the deposition of organic-rich materials in some areas (such as the peat soils of the Naaldwijk Formation) along with very variable formations contain both clay and sand laminations, such as the Naaldwijk Formation.

The most recent marine depositions are primarily attributed to the Southern Bight Formation although it is likely that the presence of this formation is limited around the quay wall area due to human processes such as dredging and excavation which produces deposits known as anthropogenic deposits

A summary of these geological formations among others found at the DC10 site are provided in Table 4.2.



Table 4.2: Geological soil layers at DC10. Depths are with reference to the Dutch ordnance system (Normaal Amsterdams Peil NAP, approximately equal to mean sea level)

Layer Name	Code	Geological Origin	Primary Soil Type	Upper Level [mNAP]	Lower Level [mNAP]	Comments
Anthropogenic deposits	AAOP	Anthropogenic	Sand	+5 to	-17 to -19	Deposited during the formation of the Maasvlakte peninsula. With occasional clay lenses.
Southern Bight	SBBL	Marine	Very fine to moderately coarse sand	-17 to -18	-20 to -22	Much of SBBL was dredged away from construction of DC10.
Naaldwijk	NAWO	Tidal	Clay, strong silty and with few to many sand laminations	-18 to -20	-19 to -27	Channel deposit: occasionally incised into KR
Echteld		Fluvial	Silty clay	-18 to -21	-20 to -22	
Nieuwkoop	NIBA-EC	Lacustrine	Peat	-20 to -21	-20 to -21	Created from formation of MV1
Kreftenheye (Wijchen member)	KRWY	Fluvial	Stiff silty grey clay. Sand laminations at base	-19 to -21	-21 to -23	Found above BXDE. Can also be laminated with fine sand layers
Boxtel (Delwijnen Member)	BXDE	Aeolian	Well-sorted fine sand	-20 to -22	-21 to -23	Can be intermixed with upper part of KR
Kreftenheye (Wijchen member)	KRWY-2	Fluvial	Laminated grey loam, sandy clay and clayey sand	-22 to 23	-23 to -24	Found under BXDE, where present. Can be intermixed with upper part of KR
Kreftenheye	KR	Fluvial	Dense medium to coarse sand	-21 to -28	-40 to -50	

### 4.3 Intrusive Investigation

An extensive investigation was carried out at the site using cone penetration tests (CPT), giving a detailed picture of the soil conditions along the quay wall. This information is publicly available on DINOloket (Figure 4.5) as .gef files and an example of a transect is shown in Appendix B2. The results of the CPTs can be used to identify the subsurface stratigraphy, develop soil parameters used in numerical models and for design and analysis.

From the CPT profiles Figure 4.6, the high cone end resistance value,  $q_c$ , of the Kreftenheye Formation can be observed. These  $q_c$  values reach up to 65 MPa and suggest a dense to very dense sand. As a result, the foundations of the quay wall are designed in such a way to maximise the load-transfer capacity of this formation and are generally founded in this formation.

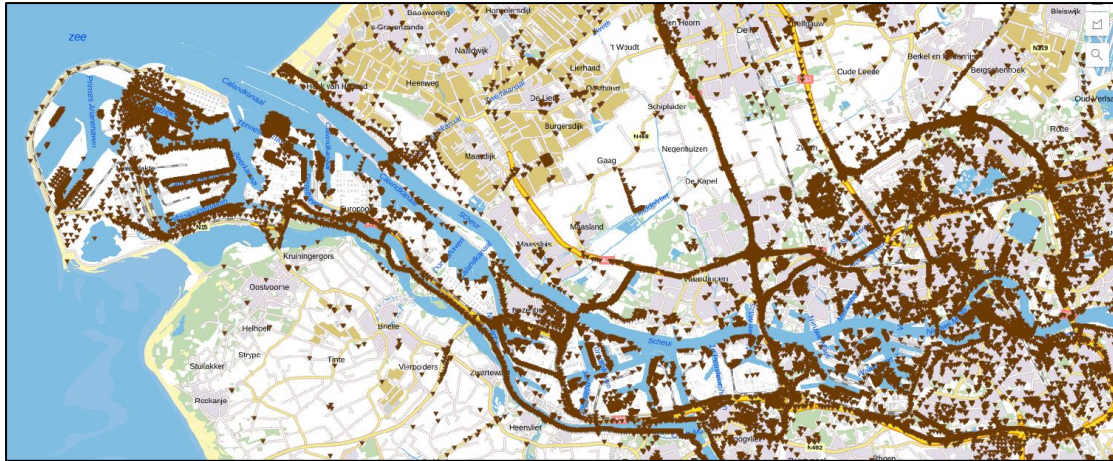


Figure 4.5: CPT data available (i.e. the brown inverted triangles) across the port of Rotterdam in the DINOloket Dutch National Key Registry of the Subsurface (DINOloket, 2022)

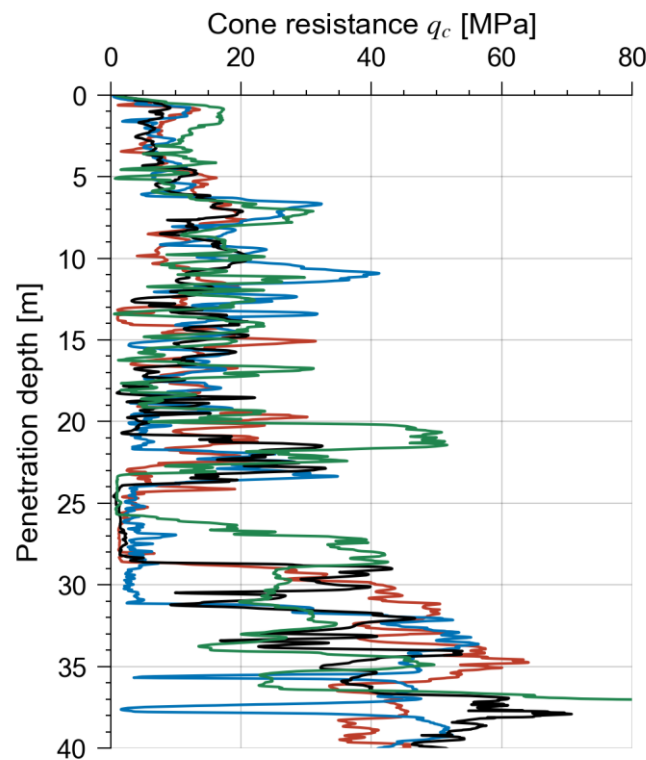


Figure 4.6: Selected CPTs across the length of the quay wall

## 4.4 Non-Intrusive Investigation

### 4.4.1 Topography

Topographical data of the site is an important factor in the design and construction of the quay wall and can also highlight impending failure depending on the resolution of the data. In the Netherlands, extensive topographical data is collected every few years using LiDAR (Light Detection and Ranging) and is available publicly and free of charge through the AHN (*Actueel Hoogtebestand Nederland*) online viewer (Actueel Hoogtebestand Nederland, 2016). The result is a point cloud of elevation data with a density of approximately one point every 16 m<sup>2</sup> and an accuracy threshold of no more than ±5 cm.

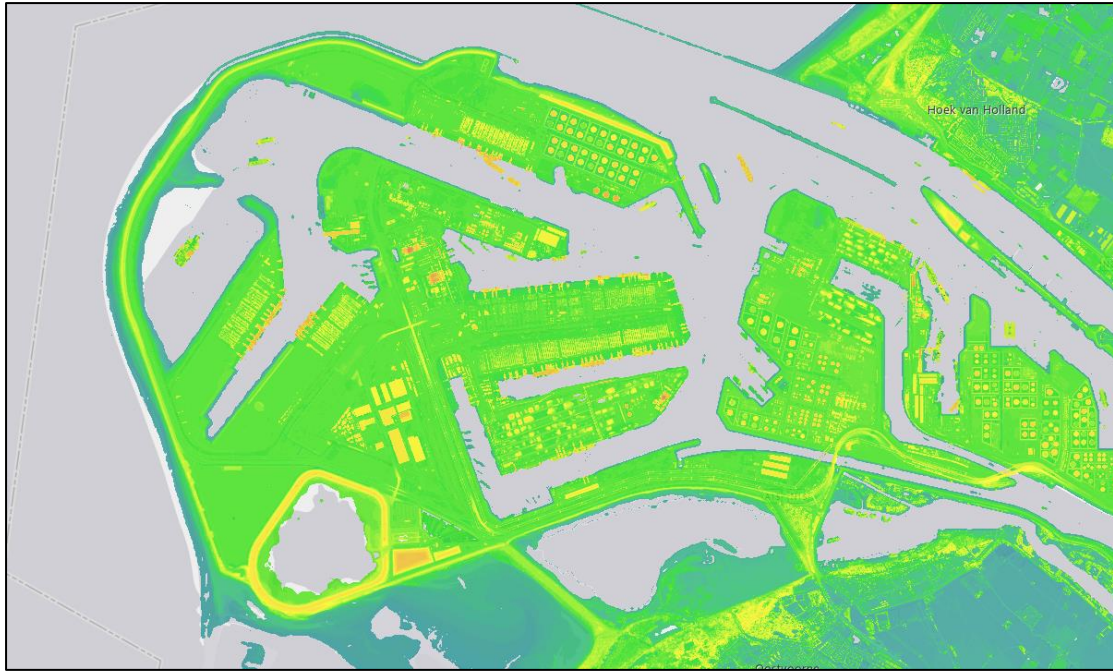


Figure 4.7: LiDAR flyover of the Maasvlakte in December 2016 (Actueel Hoogtebestand Nederland, 2016). The green areas are roughly five metres above sea level

In line with both current projects and past projects, a site-specific survey was also carried out before and after construction. Selected elevations across the site before quay wall construction are present in PDF format, with the (proposed) design elevations also indicated in these construction drawings.

#### 4.4.2 Satellite data

Data from the Sentinel-1 satellites provides settlement data using a technique known as interferometric synthetic-aperture radar (InSAR). In the Netherlands, this data is available in the public domain through [bodemdalingskaart.nl](https://bodemdalingskaart.nl), produced by the company SkyGeo. In comparison with the AHN dataset, the measurement frequency is much higher (approximately every six days), albeit with lower accuracy and resolution.

However, the InSAR dataset does not extend to the quay wall itself (Figure 4.8) as these points have been filtered out due to the amount of noise present (typically from ships or cranes blocking the satellite's signal). Specific data processing can be performed to consider these points but this has not been pursued further for this report.



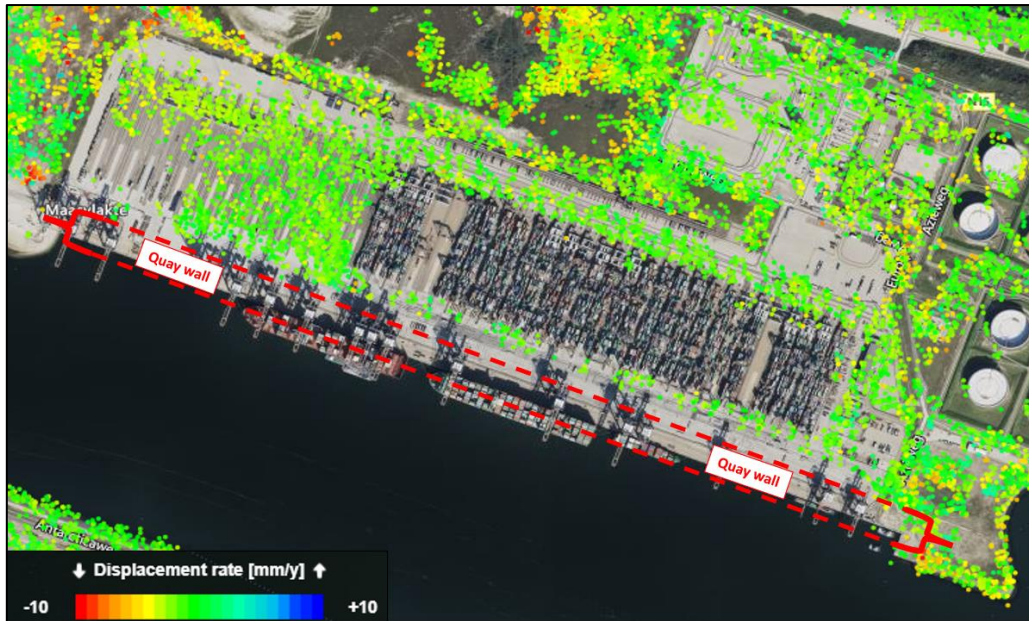


Figure 4.8: Datapoints collected from the Sentinel satellites of a quay wall in the Maasvlakte, reported in [bodemdalingkaart.nl](http://bodemdalingkaart.nl). The extents of the quay wall structure itself are also indicated, showing the filtered out datapoints

Satellite imagery is also provided by Google Earth and [satellitedataportaal.nl](http://satellitedataportaal.nl) (only accessible from within the Netherlands). This can be used to indicate various construction periods of the quay wall and changes in quay wall use over time.

#### 4.4.3 Geophysical data

No geophysical data has been collected explicitly for the purpose of deriving geotechnical parameters for Demonstration Case 10 quay wall.

Seismic surveys were conducted as part of the archaeological study of the Yangtzekanaal by Vos et al. (2015) who aimed at investigating the archaeological potential of the late-Pleistocene to early-Holocene soils such as the Kreftenheye Formation (see Table 4.2). This data was used in interpreting the geological stratification of DC10, however, no soil parameters were derived from the dataset.

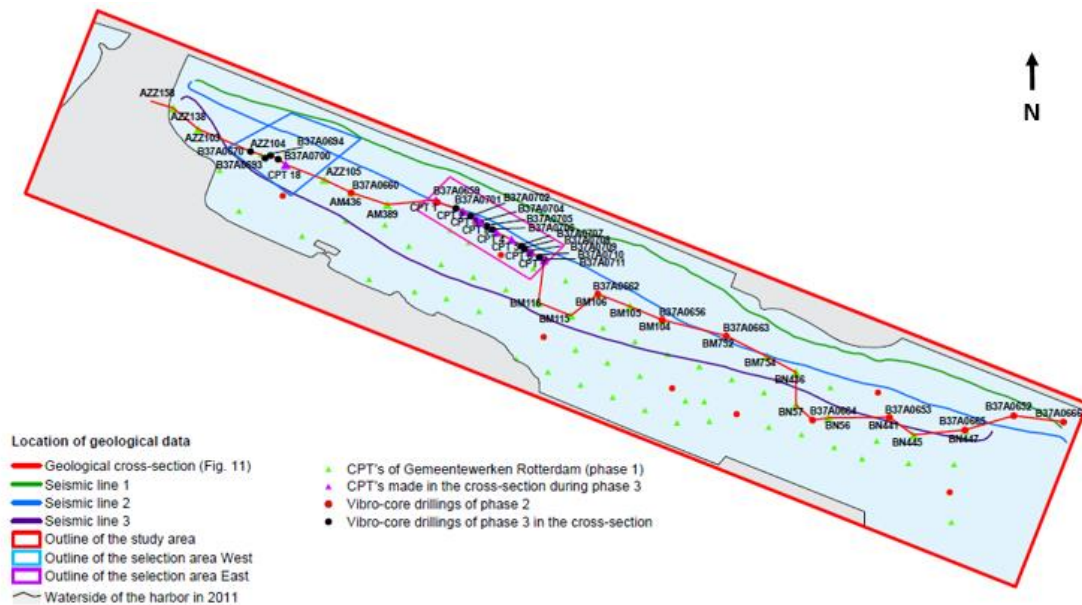


Figure 4.9: Seismic surveys performed in the Yangtzekanaal (Vos et al., 2015)

#### 4.5 Quay Wall Geometry & Construction

The quay wall consists of four primary geotechnical elements, shown in Figure 4.10:

- **Diaphragm wall:** used to retain the soil behind the quay wall
- **MV piles** (also known as MV anchors): reduces overturning moments in the diaphragm wall. Loaded in tension
- **Relieving platform:** Reduces the overturning moments acting on the diaphragm wall
- **Vibro piles:** transfers stress from the relieving platforms to deeper soil layers

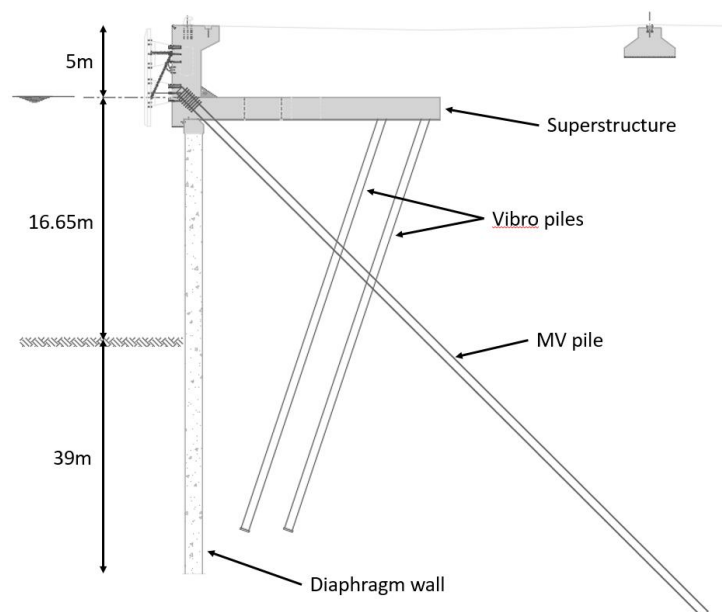


Figure 4.10: Cross-section of quay wall (adapted from Kuster (2007))

The three-dimensional representation of the quay wall (Figure 4.11) also illustrates the high density of foundation elements underneath the relieving platform, all of which can interact with each other when their capacity begins to be mobilised.

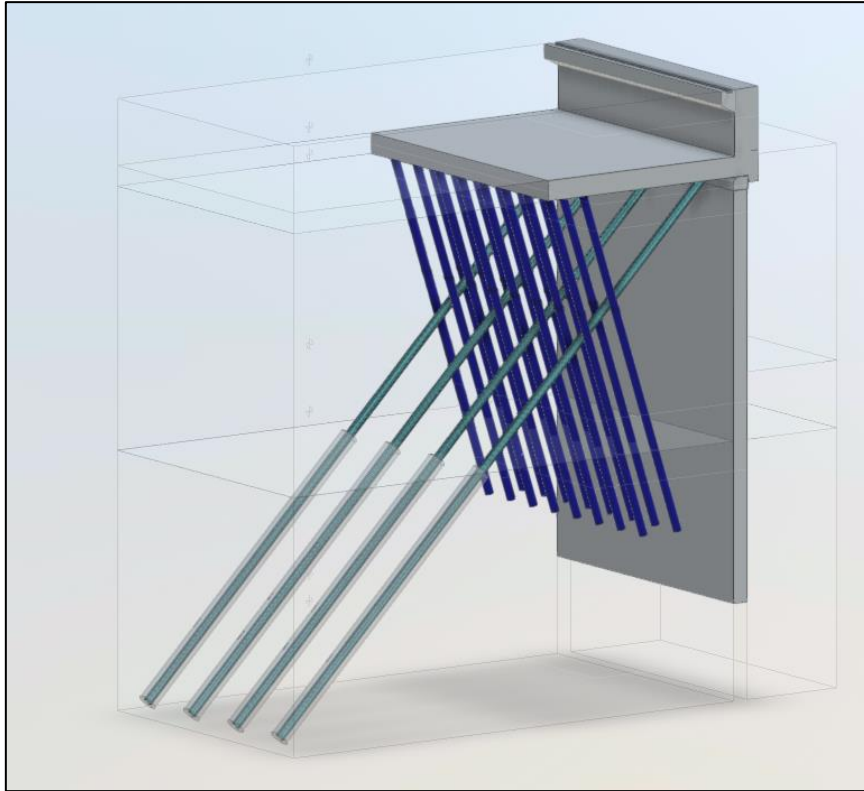


Figure 4.11: BIM model of a quay wall section, developed by Digital Twin Technology

The quay wall was constructed “in the dry”. Following the completion of the subsurface structure, the land in front of the quay wall was dredged to the prescribed contract depth of 16.65m below sea level.

An overview of the construction process is shown in Figure 4.12. The first 375m was handed over to the client (Port of Rotterdam Authority) in May 2006, with the total quay wall length of 1,975m being handed over in June 2007.

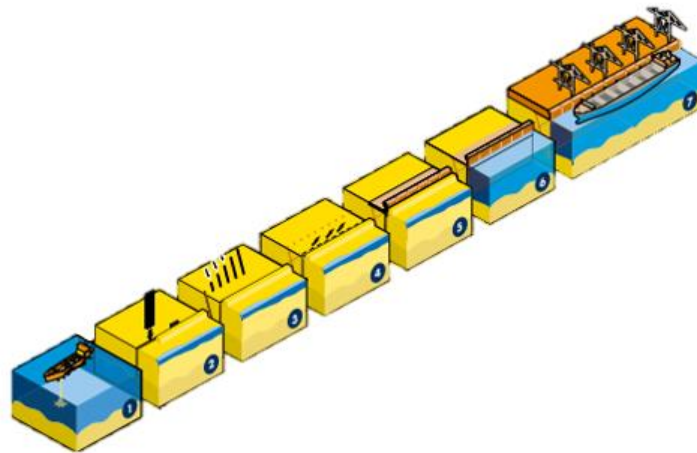


Figure 4.12: Overview of the construction process at DC10: 1. Creation of the Maasvlakte, 2. Installation of diaphragm wall, 3. Installation of vibro piles, 4. Installation of MV-piles, 5. Installation of above-ground constructions 6. Dredging of the quay 7. Quay wall completion (Port of Rotterdam, 2021)





Figure 4.13: Landside picture of the quay wall. The installation of the MV piles is shown in the foreground, with casting of the individual superstructure segments occurring in the background

Further details on each element and its construction are outlined hereunder, with more detailed information provided in Appendix B2.

#### 4.5.1 Diaphragm wall

The diaphragm wall is on average 31–32m deep, with a retaining height of approximately 21.65m and a thickness of 1.2m. The wall is constructed in a series of 7.5m long segments and within each segment, two reinforcing cages were placed (Figure 4.14). Rubber is placed in between each segment to prevent the seepage of soil from the landside to the sea.

The wall is constructed by bringing a tremie pipe to the bottom of the excavation and filling the trench with concrete. Spacers were used to ensure the position of the reinforcing cage and no shear reinforcing was used, further ensuring concrete flowability during concrete pouring.

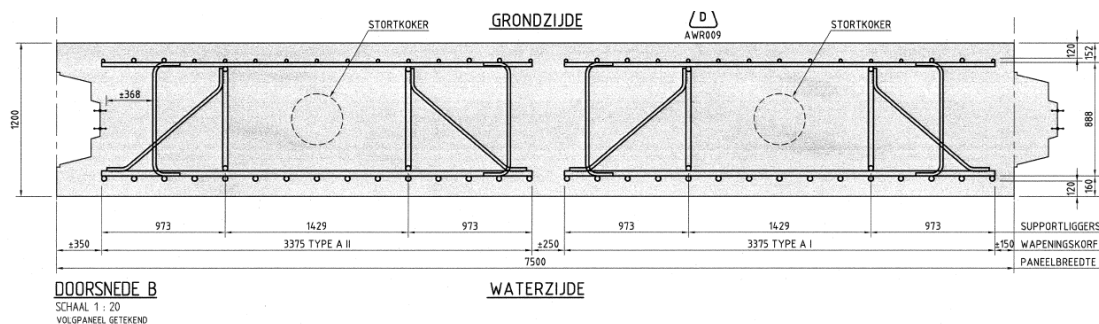


Figure 4.14: Typical reinforcing configuration of a diaphragm wall panel. Note that this configuration can change depending on the quay wall position (De Vries, 2007). Stortkoker = tremie pipe

Across the top of diaphragm wall there is a continuous reinforced concrete beam that bridges the joints between the panels, upon which the superstructure rests. As a result, the superstructure also imposes a vertical load on the diaphragm wall and (partially) restrains against horizontal movement in the upper part of the diaphragm wall.



#### 4.5.2 MV piles

MV piles (Müller Verpress piles, also known as MV anchors) are used to resist tensile loads imposed by the diaphragm wall. The core of the pile is a steel H-beam with a widened pile base (Figure 4.15). The pile is hammered into the ground, whilst a grout mixture is injected through a nozzle at the pile base. This grout mix reduces the friction between the steel and soil and creates a grout body around the pile, increasing its cross-sectional stiffness. This grout injection means the exact shape of the pile body is relatively uncertain if the piles are not extracted, however the theoretical minimum and maximum stiffness is given in Figure 4.16.

At DC10, the MV piles are 56m long and are embedded directly into the superstructure which rests on top of the diaphragm wall. The MV piles also underwent load tests prior to construction and the data is provided with the dataset.



Figure 4.15: Picture of the widened tip at the base of an MV pile (Westerbeke, 2021)



Figure 4.16: Theoretical maximum (left) and minimum (right) cross-section sizes for the MV piles (Srigopal, 2018)

#### 4.5.3 Vibro piles

Vibro piles (also known as driven cast-in-situ piles) are a type of pile installed by driving a steel auxiliary tube to a target depth using a diesel or hydraulic hammer (Figure 4.17). A sacrificial base plate, typically with an outer diameter typically greater than that of the auxiliary tube, is placed on the tube's end – creating a closed-ended tubular pile.

Once the target depth is reached, the tube is filled with concrete and a reinforcing cage is placed before or after concrete pouring. The tube is then withdrawn using either a reverse hammering or vibratory action whilst the base plate remains in the ground, resulting in it being colloquially named as a *vibro* pile in the Netherlands and Belgium.

The inner diameter of the auxiliary tube was 560mm, with the outer diameter of the base plate measuring 670 mm (for more geometrical details, see Appendix B2). The

piles were installed in pairs along the entire length of the quay wall and are used to resist compressive loads imposed by the relieving platform.

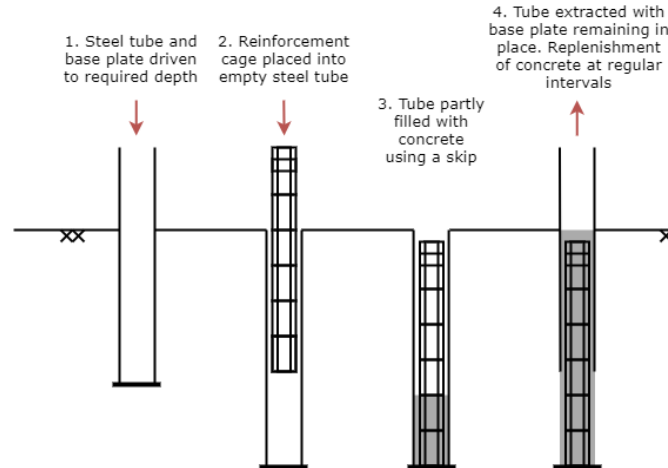


Figure 4.17: Vibro pile installation procedure

#### 4.5.4 Superstructure & relieving platform

The superstructure of the quay wall is a steel-reinforced concrete structure, divided into 85 different sections interlinked with one another using a simple interlocking system of mortises and tenons placed on the quay wall. Each section is approximately 22.5m in length and cast as one individual unit (Figure 4.18).

The relieving platform forms part of the superstructure extending 18.5 m back from the seaside and 1.5 m in thickness. The platform uses the weight of the overlying soil to reduce the bending moments induced on the upper part of the quay wall. Underneath the relieving platform a geotextile is placed to act as a suitable work floor and aid with the interaction between the relieving platform and the soil below.

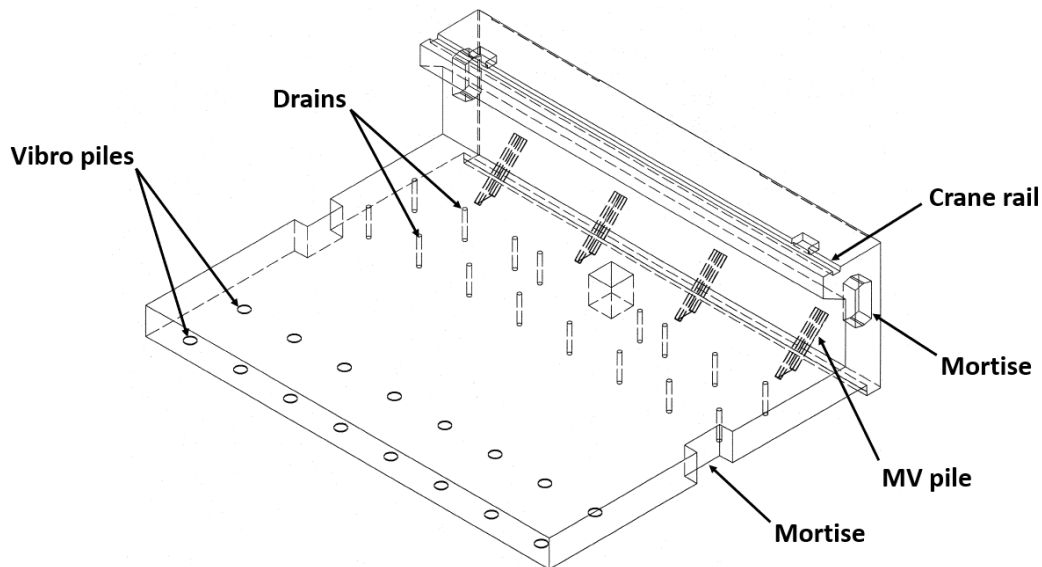


Figure 4.18: Isometric drawing of a section of the quay wall superstructure (Scheel, 2007)

#### 4.5.5 Non-geotechnical structures

The installation of fenders and bollards (e.g. Figure 4.19) were also included in the design and construction contract and are placed roughly every fifteen metres. The fenders are used to absorb the kinetic energy of a shipping vessel birthing against the

quay wall and to prevent damage to both the vessels and the quay wall superstructure. Bollards are fixed posts around which mooring lines of vessels are placed and ensure the safe berthing of ships at the quay. used to attach the mooring lines of shipping vessels.

Crane rails run the entire length of the quay wall and are used for both deep-sea container cranes and inland feeder/barge cranes. At DC10, the cranes can weigh up to 2,400 tonnes with a lifting capacity of 100 tonnes.



*Figure 4.19: Example of fenders (in orange/red) and bollards (in yellow) at a quay wall (Shibata Fender Team, 2016)*

## 4.6 Performance Monitoring

A total of 558 sensors across 78 different elements were instrumented on the DC10 quay wall (Figure 4.20). All structures were instrumented during the construction phase of the project by a subcontractor (voestalpine, formerly a division of Baas B.V.). The monitoring programme was active between 2008 and 2016 and while trial measurements were made during the construction period, no targeted and documented monitoring campaign were made during this period.

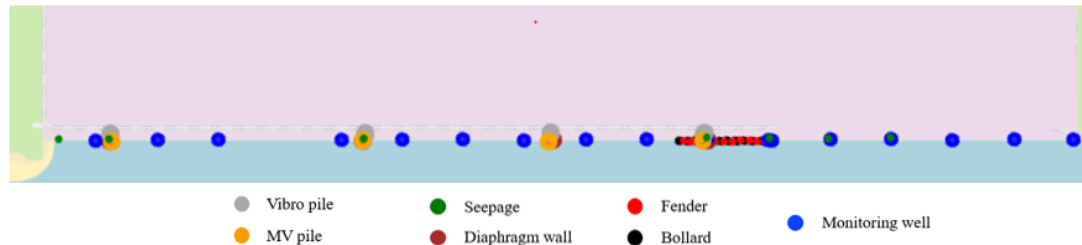


Figure 4.20: Overview of instrumented structures across DC10

The measurement systems are outlined in Table 4.3. All measurement systems use fibre optic-based measurement systems, technologies that would have been considered particularly innovative and new at that the time. Non-geotechnical structures (Section 4.5.5) have not been considered as part of this deliverable but are being incorporated into the ongoing analysis to correlate above-ground effects on the response of subsurface elements.

The quay wall was formally handed over to the client in 2008. As part of this, a site acceptance test was carried out and a tugboat was used to load the quay wall and check the corresponding measurements.

Table 4.3: Summary of instrumentation used

Measurement System	Data logger	Cable/sensor type	Quantity	Location(s)	No. of active sensors
BOTDR	Yokogawa AQ6803	SMARTprofile	Strain [-] and temperature [°C]	Vibro piles, MV piles, diaphragm wall, seepage	68
FBG	Micron Optics sm130	<i>Cable type not known</i>	Strain [-]	Bollards, fenders	294
		FOS&S Pressure Sensor P-01	Water level [m]	Monitoring wells	34
SOFO	SOFO Read-out unit	SOFO	Strain [-]	Vibro piles, MV piles	45

### 4.6.1 BOTDR: Strain & temperature

BOTDR (Brillouin Optical Time Domain Reflectometry) measurements were carried out using the Yokogawa AQ8603 data logger with a spatial resolution of one metre.

The system measures the Brillouin frequency shift in the optical fibre, described in Section 2.3.4, by injecting light down one end of the fibre optic cable and measuring the returning back scatter at the same end. To minimise the signal-to-noise ratio, the cable was terminated at the opposite end using a fibre optic connector whereby measurements could also be made down the same end.

The resulting measurement is a quasi-continuous profile of strain along the entire length of the fibre optic cable. A fibre optic cable fully embedded in a structure can therefore measure the deformation and temperature of the structure itself.

The cable used for the BOTDR measurements was the DiTeSt SMARTprofile cable. This contains two tight-buffered fibres for strain monitoring and two loose-buffered fibres for temperature monitoring. For the monitoring programme only one of each type of optical fibre was interrogated.

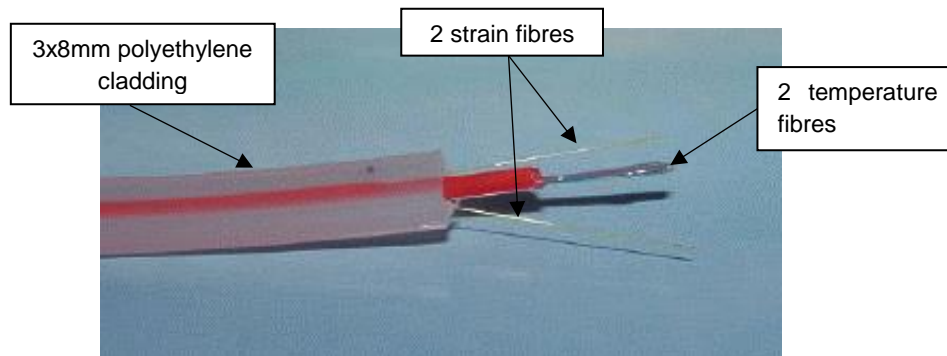


Figure 4.21: DiTeSt SMARTprofile fibre optic cable

Two vibro piles were instrumented with SMARTprofile cables attached to the reinforcing on four diametrically opposing points (Figure 4.22a). One MV pile was instrumented along its flanges, two on either side of the beam, by gluing the SMARTprofile cable within a groove welded to the surface (Figure 4.22b). In both cases, the cable looped around the bottom of the pile, forming one continuous measurement from the measurement cabin, across the container terminal, down the pile at all measurement axes and then back towards the measurement cabin. As a result, the region within the pile must be identified. This region is referred to as a “sensor” within the context of this deliverable.

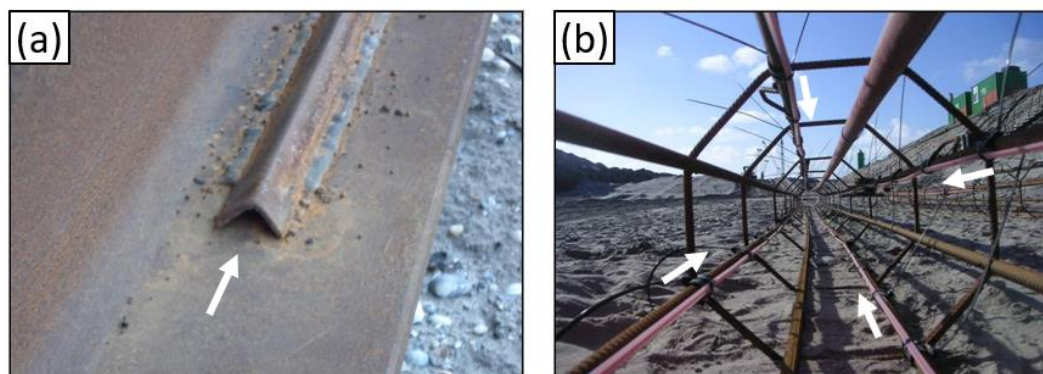


Figure 4.22: (a) Protective channel welded to the flange of the MV piles, within which the SMARTprofile cable is glued (b) Indication of where the SMARTprofile cable (in red) was placed on the vibro pile reinforcing



For each reinforcing segment of the diaphragm wall, two BOTDR loops have been placed, comprising of four “sensors”, as shown in Figure 4.23.

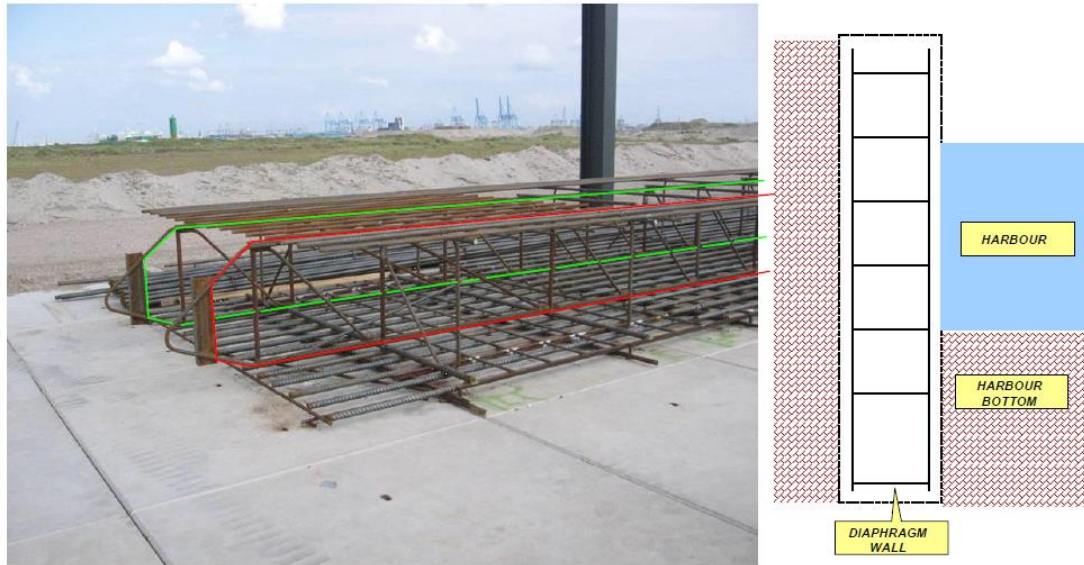


Figure 4.23: Reinforcing on the diaphragm wall, (left) indicating the two measurement lines in red and green and (right) the reinforcing placed within the diaphragm wall

#### 4.6.2 Monitoring wells: Water level

A total of seventeen monitoring wells were placed around the quay wall. These monitoring wells aim to provide a complete profile of the (ground)water profiles in front of and behind the quay wall and are critical to consider in relation to water pressures acting unfavourably on the quay wall and assess the potential of seepage or excessive water pressure differentials occurring.

Fourteen of the monitoring wells were placed on the landside, that is, behind the quay wall and under the relieving platform. Two monitoring wells were utilised as piezometers to measure the water pressure at depths at NAP -5m and NAP -15m respectively to give an indication of the porewater pressures behind the quay wall. One more monitoring well was placed on the seaside to measure seawater levels, expanding on the already extensive seawater monitoring dataset collected by the Port of Rotterdam Authority (Table 4.1).

All monitoring wells were measured using a pressure sensor (FOS&S Pressure Sensor P-01; see Figure 4.24) fitted with a porous tip, measuring change in strain of a diaphragm within the tip using Fibre Bragg Gratings (FBG) – a type of fibre optic sensing technique. This is then converted to a pressure across the diaphragm, which in turn can be converted to water level for hydrostatic conditions (i.e. on the seaside or within sand). A second unstrained FBG gauge is also placed within the sensor so that temperature compensation can be applied.



Figure 4.24: FOS&S Pressure Sensor P-01 used in the monitoring wells (FOS&S, 2009)

#### 4.6.3 Seepage sensors

Seepage sensors measure the flow of sand behind the quay wall, underneath the relieving platform. For this, a weight is tied to a fibre optic cable and exerts no force on the sensor when the weight rests on the soil. If there is a flow of soil from landside to seaside, the weight falls and exerts tension on the fibre optic cable and a qualitative assessment of any soil flow can be made (Figure 4.25). The fibre optic cable was interrogated using BOTDR sensing, similar to the deformation measurements within the piles.

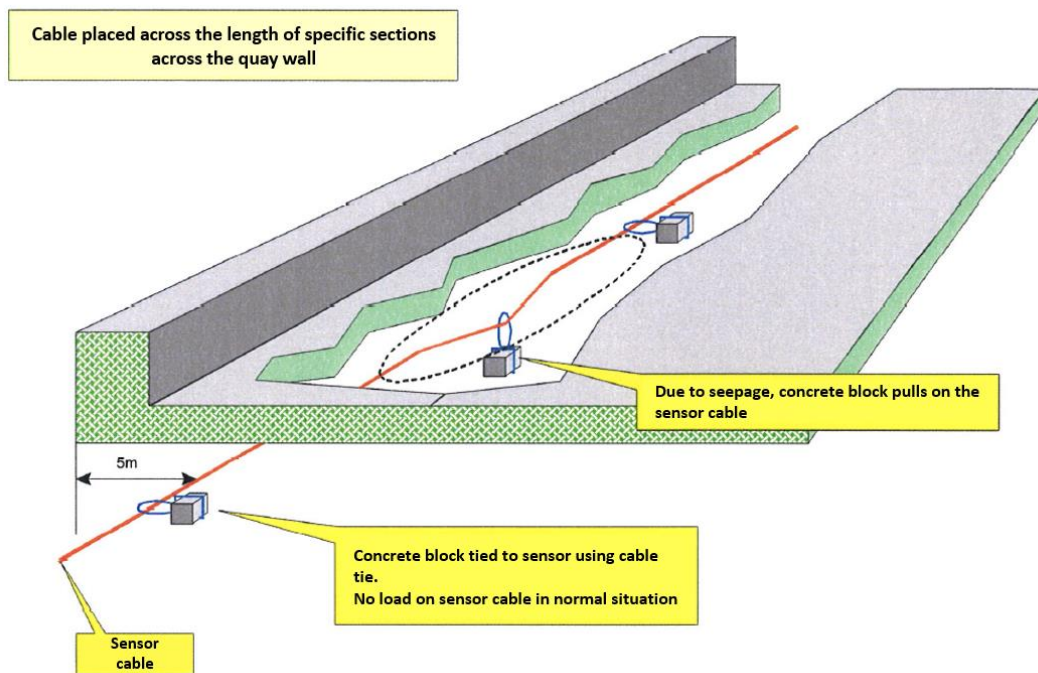


Figure 4.25: Principle of the seepage sensors (adapted from van Dam (2008))

#### 4.6.4 SOFO: Strain

SOFO (in French: *Surveillance d'Ouvrages par Fibres Optiques*) sensors measure the change in strain across their active zone (Figure 4.26; 50cm long) using a fibre optic sensing technique called low coherence interferometry. The temperature compensation of this sensor is performed using a reference fibre which is slack and as a result, is not affected by a change in length between the two anchors. A reading unit



accounts for the measurement of both fibres and outputs the temperature-compensated strain.

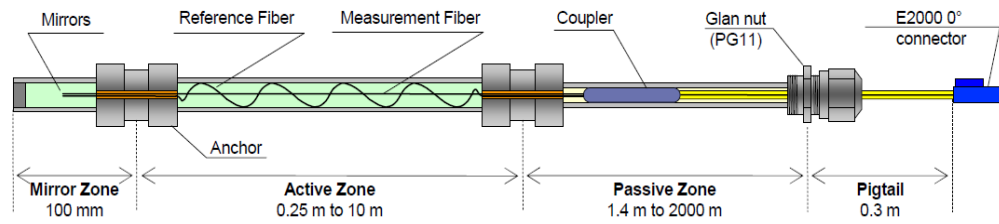


Figure 4.26: SOFO sensor (Smartec, 2017)

Ongoing problems with the readout unit for the SOFO sensors were observed within a year after construction and that there was a lack of support from the supplier to fix this. As a result, SOFO measurements were only performed between 2008 and 2009.

For both the vibro and MV piles, the SOFO gauges were attached to the head of the piles along the same measurement axes as the BOTDR readings (albeit on different piles). In the diaphragm wall, SOFO sensors were attached to the reinforcing on the landside, seaside and in the centre of the wall. These were placed twelve metres from the top of the diaphragm wall, close to point of maximum displacements. No structural elements were instrumented with both BOTDR and SOFO sensors.

#### 4.7 Initial Digital Twin Development

The DC10 quay wall, had a digital twin almost a decade before the surge of interest in digital twin development and documentation in the literature. Developed by Baas B.V. (now a division of voestalpine), the monitoring network was integrated into an online platform which displayed the status of the sensors and raised alarms when critical thresholds were reached. Minimal processing of the data was carried out, and so the data integration and interpretation layers (Section 3.3) were largely absent from the digital twin

As the entirety of the monitoring network is fibre-optic based, a fully-wired network was selected to minimise the cost of having multiple data loggers across different parts of the quay wall – one of the most expensive components of the monitoring system. Therefore, all instrumented elements were directly connected using fibre optic cables to a central on-site measurement cabin where the data loggers were stored. From the cabin, the entire length of the fibre optic cable running to each structural element was interrogated and then the data was processed and uploaded to an online server through a local area network (LAN) which could be accessed wirelessly. Data backups were made to a physical storage drive on-site, from where the current dataset was retrieved.

The database was run on a Microsoft SQL server, whereby readings from the data loggers were processed and sent to the server using scripts developed through the C++ programming language. A custom GUI to this server was developed known as FOSMO (Fibre Optic Structural Monitoring). All components within this GUI used ADO.NET architecture to access and manipulate data in the database. An overview of this GUI is provided in Figure 4.27 and could provide updates regarding the instrumentation status and direct measurements of the readings. Additional

geotechnical interpretation (Section 3.3.3) was not performed, except for alarm thresholds set on the measured parameters.

A weekly email report was sent to the client containing information of the measurements, along with automated emails sending alarms in the event prescribed thresholds were reached.



Figure 4.27: User interface of the FOSMO GUI (in Dutch), presenting the status of the instrumentation along the quay wall. Displayed is the working status of the data loggers (Status Apparatuur) and the correction function of the sensors, in terms of last measurement made in hours (Achterstand Sensordata (uren)).

Active evaluation and assessment of the monitoring programme and digital twin was not carried out during its operation for reasons unknown and extensive records of maintenance and or analysis have not been performed. In 2020, details of the digital twin and measurements up until 2016 were received by InGEO. Reassessment of the digital twin development and the value of the data has been performed as part of the ASHVIN programme, in tandem with other smart quay walls from across the port of Rotterdam.

## 4.8 Monitoring Results

As part of this, additions to the digital twin have been recommended and are continuing to be re-examined, with the aim to re-establish a real-time digital twin at the site and provide lessons learned for digital twin development across the port.

Part of this reanalysis includes an examination of the geotechnical effects at play and improving the data processing and interpretation elements of the digital twin. These are outlined below in a fashion similar to the digital twin architecture in Section 3.1.

### 4.8.1 Temperature compensation

Section 2.3.3 highlighted the importance of temperature compensation for piled foundations. In the case of the foundations at DC10, temperature compensation of the BOTDR readings can be applied using a loose-buffered (temperature sensing) fibre which is immediately adjacent to a tight-buffered (strain sensing) fibre and therefore, the impact of temperature on the tight-buffered fibre is expected to be like that of the loose-buffered fibre.

In reality, an overview of the temperature measurements (Figure 4.28) suggests this is not the case. Temperatures in the upper part of the pile are expected to fluctuate in tandem with daytime and seasonal temperatures, with the effect dampening out towards lower parts of the pile, where the temperatures are expected to be virtually constant. However, Figure 4.28 shows that selected points from the temperature profile appear to fluctuate at a virtually constant rate – suggesting extraneous influences other than temperature may be at play. Indeed, research (Duffy, Gavin, De Lange, *et al.*, 2022) into loose-buffered fibres embedded in piles that are interrogated using Brillouin sensing shows that these fibres can be impacted by mechanical stresses to the high constraining stresses that develop during pile pre-stressing and concrete curing.

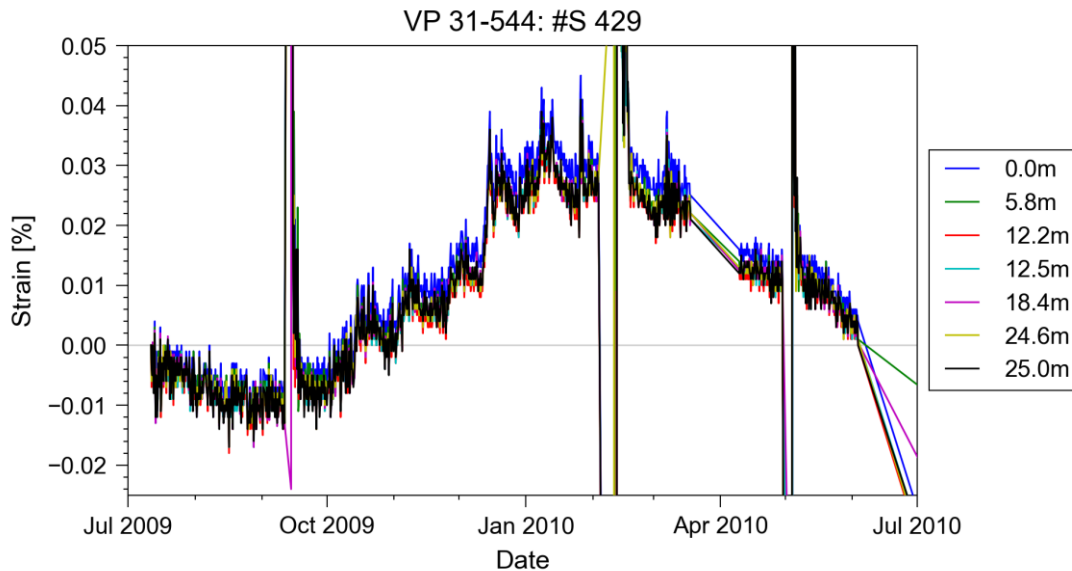


Figure 4.28: Example of selected BOTDR increments from a temperature fibre within a vibro pile

Furthermore, data gaps in the measurements (Figure 4.29) meant that temperature compensation could not be properly applied across all measurements. In the case of the vibro pile shown, when considering relative changes in strain/load, the impact of temperature is expected to be greatest at the surface i.e. closest to the high

fluctuations in ambient temperature. Nonetheless, consideration of the transfer of forces in the deeper load-bearing sand layers is generally most significant to consider for design purposes, particularly as it is less impacted by interaction effects with other quay wall elements which may confound the analysis. Being further away from the cyclical temperature effects at the surface, the fibre optic cable is unlikely to be substantially impacted by temperature when considering relative effects. As a result, temperature compensation has not been considered for further analysis.

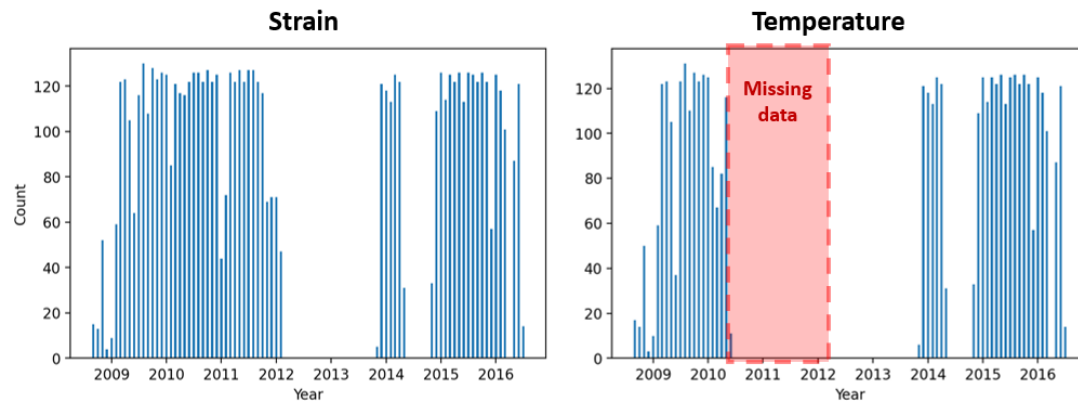


Figure 4.29: Count of the number of strain and temperature measurements in one of the vibro piles within the database

As a result, from a geo-monitoring point-of-view, accurately measuring temperatures for determining thermally induced stresses on instrumentation should be considered carefully. The digital twin developed with this should also not be agnostic to the fact that these measurements could potentially introduce problems with uncertainty and lead to improper conclusions by the end-user.

#### 4.8.2 Identifying fibre optic sections (BOTDR)

Interrogation of distributed fibre optics is generally carried out over the entire fibre optic length. For instance, measurements at DC10 are made of the cable connecting the instrumented structure to the measurement cabin or also of the transition from one side of the structure to the other (e.g. Figure 4.30).

Simple pressure tests are generally performed to assist in identifying the measurements that are made across the structure itself. Notwithstanding, fine tuning is often required and if the fibre optic network is adjusted (e.g. repair to the network, causing a shortening/lengthening of the fibre optic line), the allocation needs to be configured.

For DC10, the distances corresponding to the region of the pile was initially reported. However, an adjustment of the fibre optic network and a change to the internal interpolation parameter of the data logger meant that the appropriate sensor sections were not selected and a bias was introduced to attribution of depths to the readings. This has important implications for the measurement of the pile base stress, which requires the last fibre optic reading from the measurement axis to be as close as possible to the pile base to minimise uncertainties associated with extrapolating the data.

For this reason, it is imperative that documentation is meticulously kept of both the instrumentation process and operation and maintenance, whilst updating the digital twin's processing layer to account for adjustments in the monitoring systems.

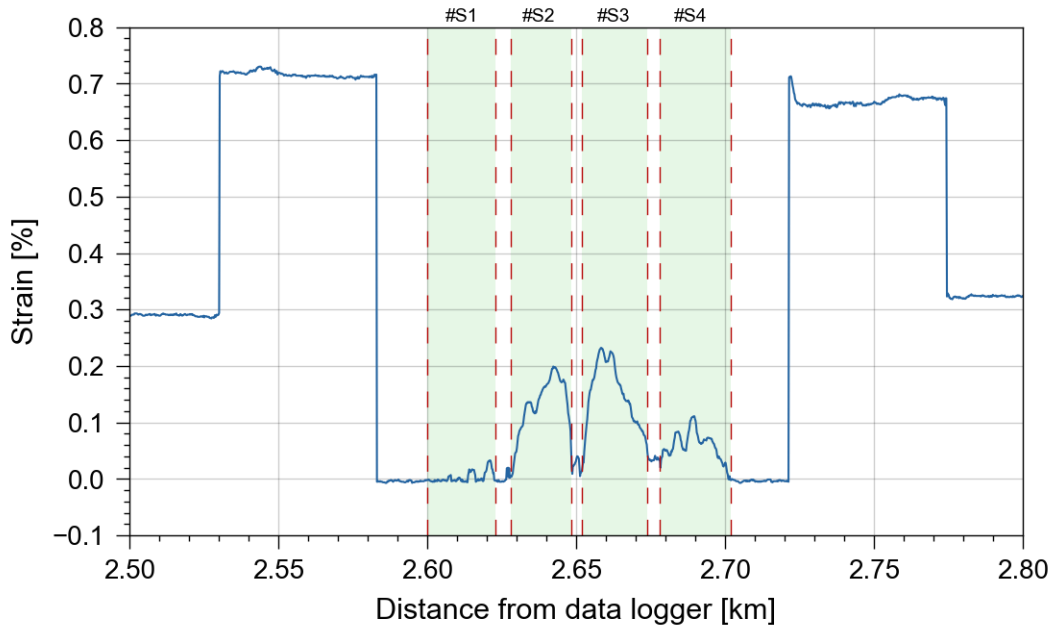


Figure 4.30: Direct measurement from data logger, indicating the slicing paths. Further fine-tuning is needed to remove connection points at the top. #S1, #S2 etc. refers to different sensor IDs or measurement axes

#### 4.8.3 Outlier detection

Algorithmic outlier detection provides a simple and swift means of assessing of analysing the database. However, ensuring that a robust and reliable system can be established is challenging and is evident by some the data from the quay wall (Figure 4.31). A review of the BOTDR data over time shows instances of measurement drift occurring. Across both piles, a change in strain of 0.1% corresponds to a change in load of the order of 10 MN ( $\approx 1000$  tonnes), a load beyond the capacity of the piles and would be likely to cause significant damage to the quay wall if this was realistically imposed. This drift is more likely to be as a result to internal effects within the BOTDR data logger itself or an adjustment in calibration parameters.

Accounting for drifts in measurements or general noise such as that present in Figure 4.31 can be done using be either removing the measurements or adjusting them correspondingly., e.g. by removing the measurement bias or adjusting the calibration parameters throughout.

Nonetheless, the implications of outlier removal just also be considered, particularly with regards to spatio-temporal interpolation. For instance, bending effects can play a quite significant role in how the data is interpreted across a foundation pile. To compensate for this, sensors in tension and compression zones of a structure are averaged together to give a generalised picture of the structural response. In the case of broken sensors, missing data, outliers etc. the process of averaging measurements should be considered appropriately,

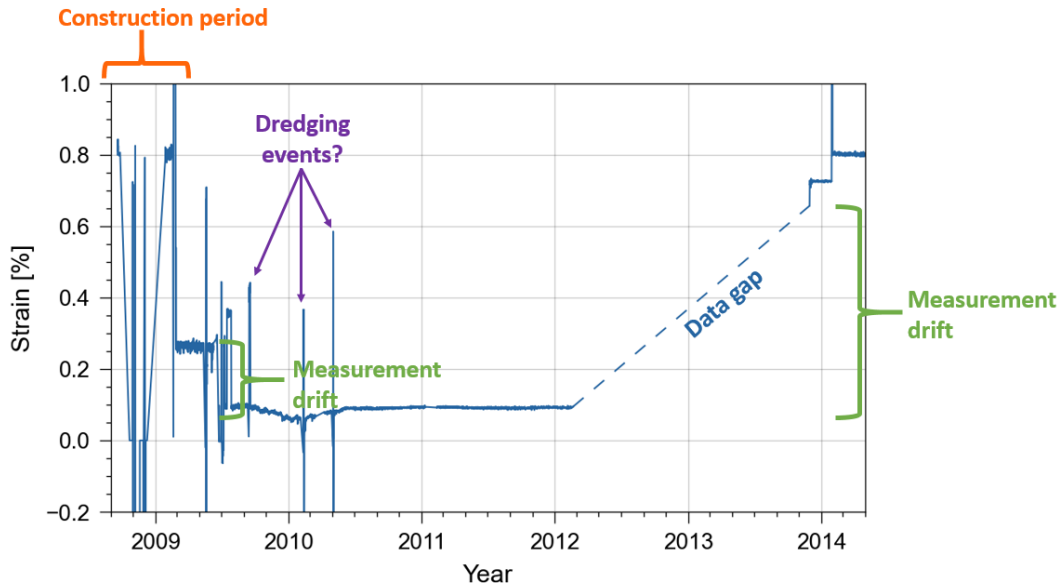


Figure 4.31: Example of outliers within a BOTDR measurement at a single depth range for one of the MV piles

As part of the further analysis, corrections have been applied to areas of measurement drift and areas that feature very noisy and anomalous measurements have not been considered.

#### 4.8.4 BOTDR: piles

To convert strain to a more useful quantity for geotechnical purposes, the strain measurements have been converted to normal force using the equation:

$$\varepsilon = \frac{\sigma}{E} = \frac{F}{EA}$$

Where  $\sigma$  = stress,  $E$  = Young's modulus,  $F$  = normal force in pile,  $A$  = cross-sectional area of pile.

The value assumed for  $EA$  (i.e. the cross-section stiffness) for the MV and vibro piles is provided in Appendix B2. Nonetheless, it should be noted that the pile stiffness is generally not a constant but is dependent on the stress-strain response of the material in question and the age of concrete for example. However, difficulties can arise in determining the stiffness of the pile. For prefabricated concrete piles where the concrete was poured in controlled conditions, this is somewhat easier. But for composite piles or piles cast-in-situ (such as MV piles), this is significantly trickier because of the uncertainties regarding the influence of the soil on the Young's modulus and cross-sectional area of the pile.

By measuring the load at the top of the pile and measuring the change in strain at the top of the pile across different loading conditions, a relatively reliable constitutive model can be developed e.g. Lam and Jefferis (2011). Yet even with this, uncertainties will persist with regards to the long-term performance of the pile body (e.g. with concrete degradation, corrosion of steel) and should be at least considered in a qualitative sense.

The lack of accurate load data at the pile heads of DC10 means that there are constraints with how the constitutive models for the piles can be obtained and so a constant value has been taken based on typical properties for materials within the piles.



An example of the force/depth readings for one of the vibro piles is presented in Figure 4.32. At a first glance, significant discrepancy between the four different measurement axes is evident. Two of the axes, South and East, display very different readings to that of the West and North axes, suggestive of problems associated with the instrumentation or concrete quality on the side of these axes.

The West and North axes display relatively similar patterns, with a build-up of normal force in the upper ten metres, most likely imposed by the soil/structure interaction effects underneath the relieving platform. This normal force then reduces with depth, suggesting a transfer of this normal force to the layers below. Small discrepancies are present between both axes, either a relic of the instrumentation process or suggestive of real physical effects within the pile, such as pile bending.

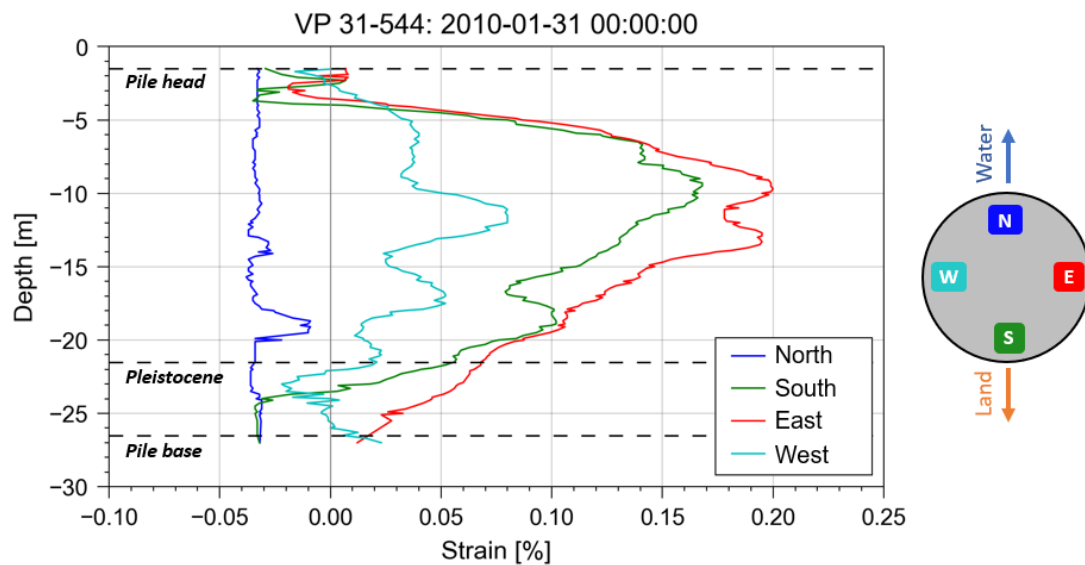


Figure 4.32: Measurements of four sensors within a vibro pile. The pile head and pile based have been indicated, along with the depth of the Pleistocene sand layer – the primary load bearing layer.

#### 4.8.5 SOFO: piles

Some of the SOFO measurements made during 2009 have given some interesting insights into the behaviour of the piles (Figure 4.33). Over the course of the year, the load in the piles undergo a cyclical change in roughly in correspondence with the seasonal change in temperature – albeit with a slight delay due to temperature storage effects of seawater.

The MV piles, which are designed to resist tension loads, experience the opposite change in loading conditions compared to the vibro piles, which are design to resist compressive loads. This cyclical nature is less distinct in the vibro piles, with the load remaining relatively constant after the summer period.

The change in load is a substantial percentage of the total design load and if this trend were to continue, this can substantially affect the long-term capacity of the structure, for instance, through phenomena such as friction fatigue (White and Lehane, 2004) whereby repeated cycling can degrade shaft friction in the structure and reduce its overall capacity.



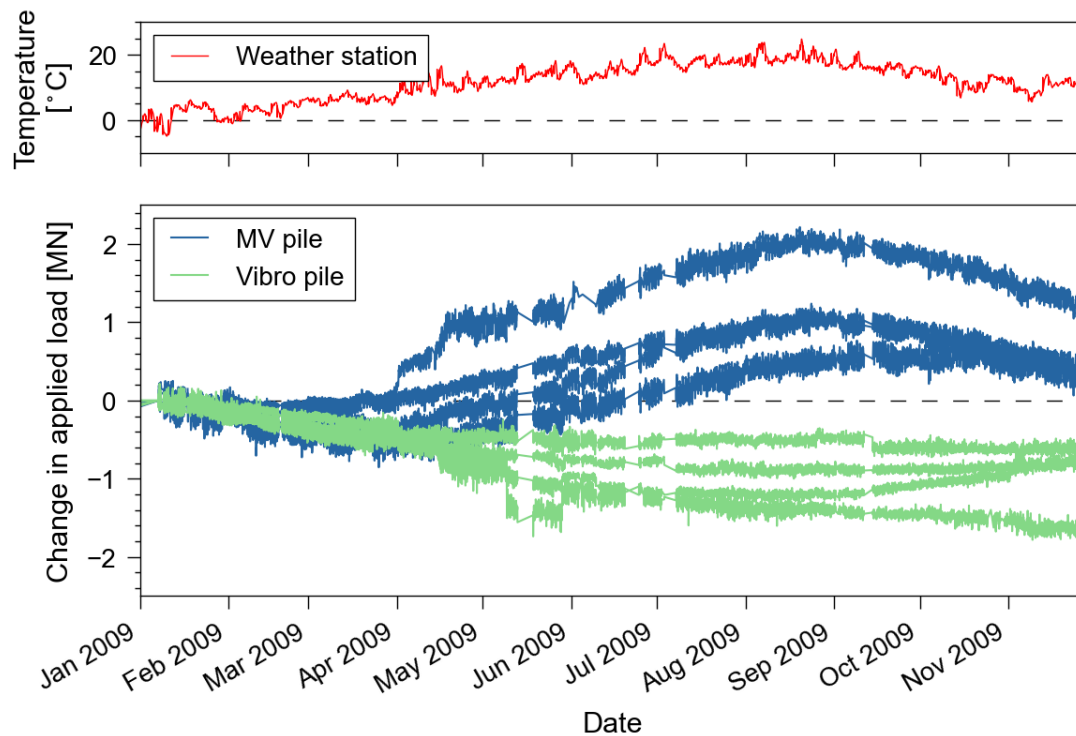


Figure 4.33: All SOFO measurements on the MV and vibro piles (bottom figure), compared to ambient air temperatures from the Hook of Holland weather station (KNMI, 2009)

Zooming into a one-week period in the results (Figure 4.34), the influence of tidal cycles can clearly be seen in the MV piles whereby a twice-daily cycle with an amplitude of approximately 3-5% of the design load can be seen. Conversely, this effect cannot be seen in the vibro piles, an effect most likely dampened out by the relieving platform.

The impact of the low frequency, large amplitude seasonal cycles, combined with the high frequency, low amplitude tidal cycles are being subject to further investigation through numerical modelling.

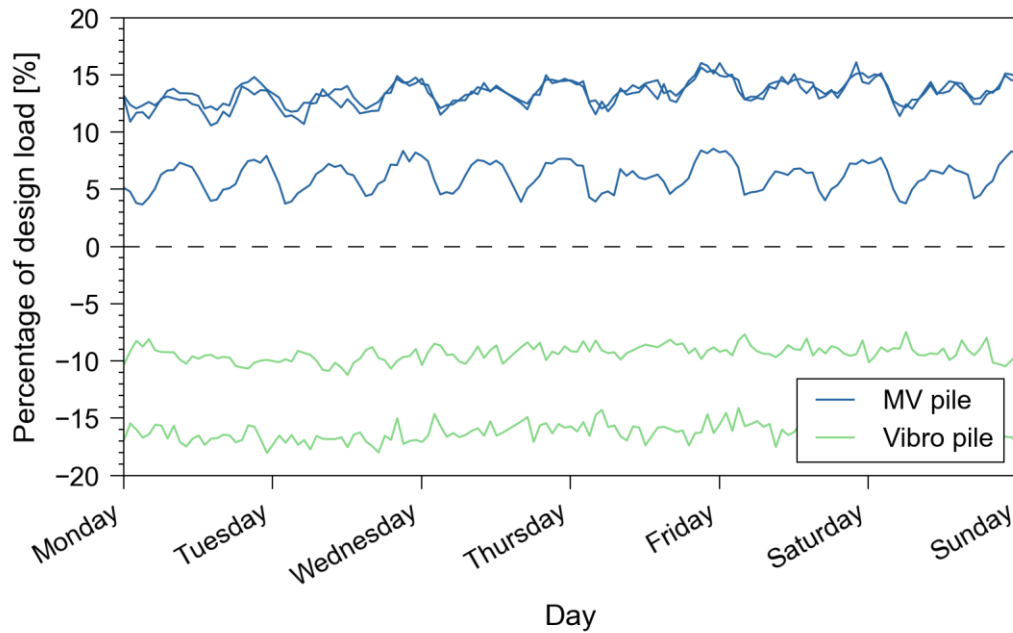


Figure 4.34: Zooming into a zone of measurements, beginning 3<sup>rd</sup> August 2009

#### 4.8.6 Monitoring well data

An analysis of the seaside monitoring well data from #S 358 indicates a semidiurnal tidal cycle, that is, with two high tides per day and two low tides per day with an amplitude of approximately 1.5m. The amplitude of these cycles is roughly in agreement with monitoring well data from other locations from around the Port of Rotterdam (Figure 4.37, [waterinfo.rws.nl](http://waterinfo.rws.nl)).

Focusing on the landside groundwater measurements (#S 360, in red), the cyclical deviation is less prominent and its trough of the cycle is smoothed out substantially. Peaks of up to 0.3m occur, in correspondence with the changing tides. In comparison, the piezometer which measures the hydraulic head at a depth of -15m exhibits less prominent deviations, with the cyclical effect less evident to see.

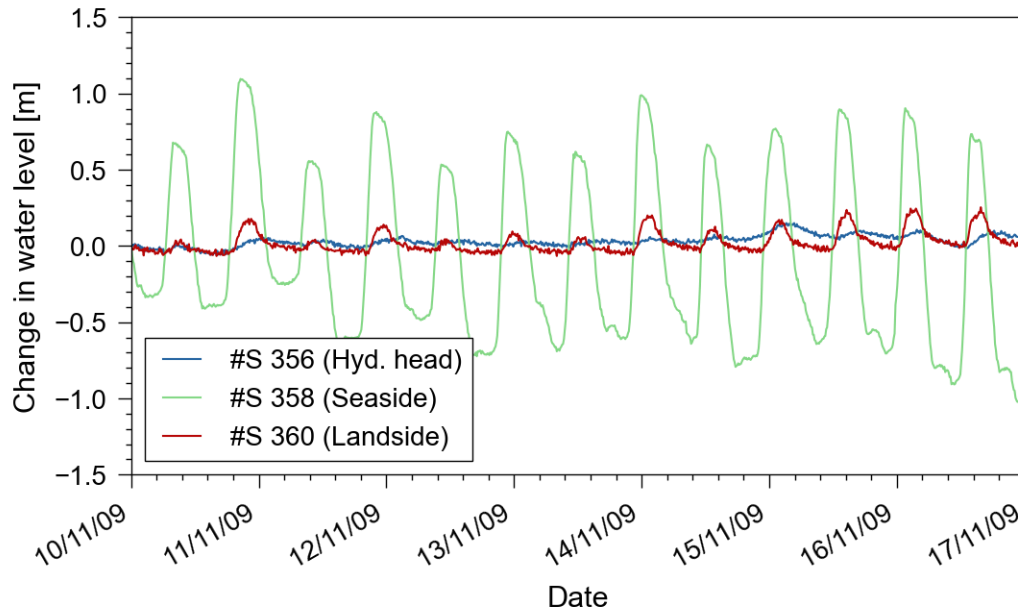


Figure 4.35: Monitoring well measurements from a one-week period. The reference measurement has been set on the 10<sup>th</sup> of November 2009

The data suggest a degree of groundwater flux across the diaphragm wall with every 1m change in tide corresponding to a 0.3m increase in groundwater level behind the quay wall. This is an important consideration for design with regards to the pressure exerted on the quay wall and a groundwater path analyses.

Delving into this further, measurements from monitoring wells along the entire length of the quay wall were taken and assessed over a one-year period (Figure 4.36). Across this period some deviation in the measurements is present. This may be indicative of an actual build-up of water pressure occurring behind the quay wall but may also be indicative of a faulty measurement system, such as a blockage within the filter of the pressure sensor.

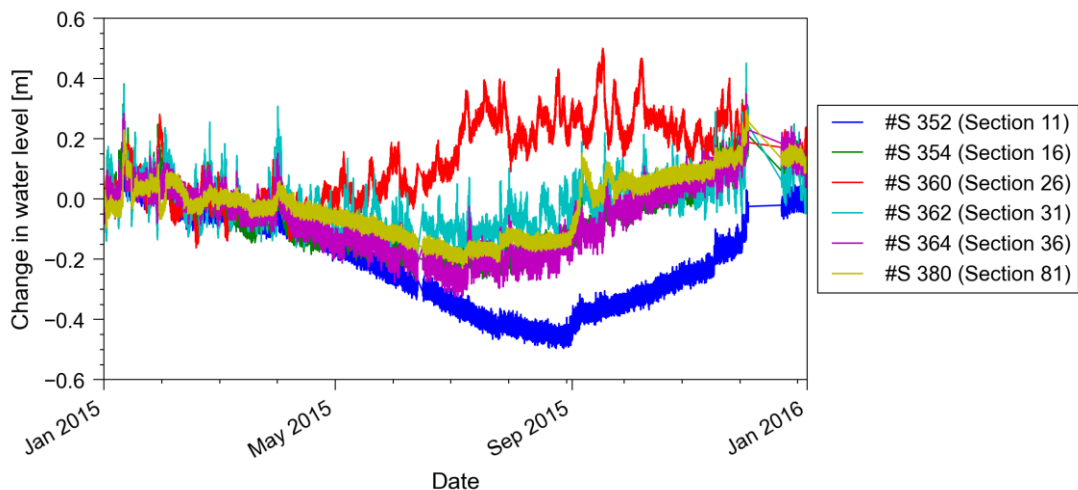


Figure 4.36: Selected measurements along the entire length of the quay wall from Section 11 (western side of quay wall) to Section (eastern side of quay wall). The reference measurement was taken on the 1<sup>st</sup> of January 2015

Further instability is evident in the monitoring well data when zooming in on the measurements made at the waterside, drifting of the measurement is present (Figure 4.37). Shortly after this point, a defect in the sensor was found and was not replaced. Fortunately measurements outside the quay wall can be supplemented by data from external sources (e.g. [waterinfo.rws.nl](https://waterinfo.rws.nl)) which allows for a reliable comparison of water levels outside the quay to the groundwater level behind the quay wall. Inevitably, it is imperative that an appropriate contingency plan is in place where redundancy measurements like this are not available.

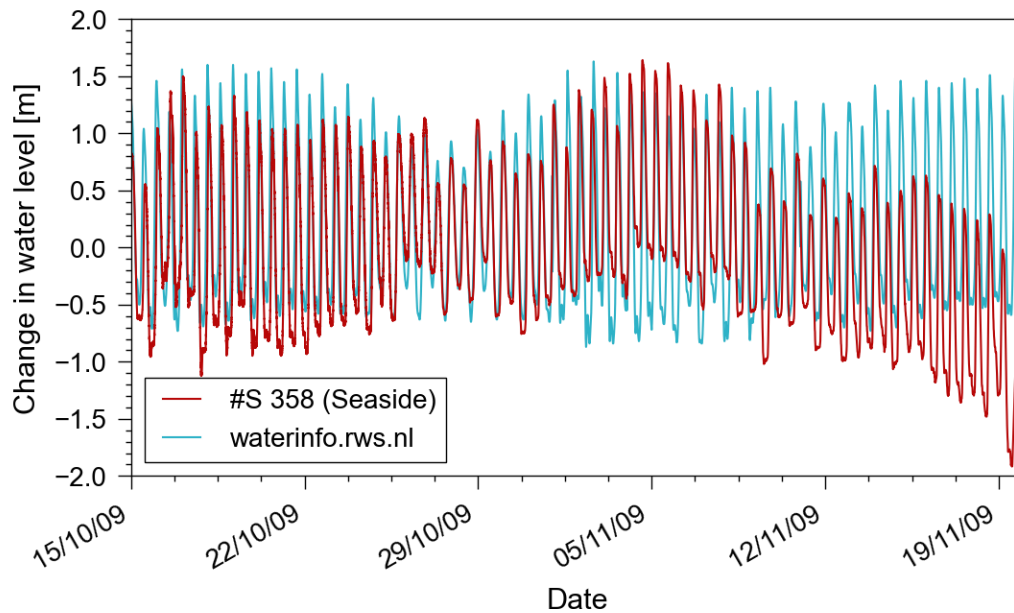


Figure 4.37: Drift in seaside measurements at DC10 compared to measurements from a monitoring well on [waterinfo.rws.nl](https://waterinfo.rws.nl)

Data of the monitoring wells has also been performed as part of ASHVIN Deliverable 3.3 (Imperiale, 2022) through the creation of a data processing pipeline. Weak correlation was found between the data collected at DC10 and data from external sources across the port based on different measures of statistical correlation. This is large in part due to the noise and drifting in the measurements and as a result, data processing pipelines will need to be able to identify instances of measurement drift and account for it appropriately.

## 4.9 Discussion

The dataset of Demonstration Case #10 is a large and expansive dataset, both in terms of the number of structural components instrumented and the timeframe across which these structural elements were measured. The initial digital twin was able to effectively manage the large network size, however, a back-analysis of the dataset has shown some of the complexity in developing a robust digital twin. For instance, instability in the fibre optic cables and/or data logger was evident, resulting in drifts in the measurement readings that were not accounted for as part of the original digital twin. Appropriately assessing this from the outset is critical in sustaining the robust operation of the digital twin, along with appropriate documentation of any instances of instrumentation failure.

The analysis has also brought some interesting insights and questions for the field of geo-monitoring. DC10 provides a unique example of the early use of distributed and discrete fibre optic sensing and its long-term implementation. The uniqueness of this dataset is highly valuable for improving the understanding of the performance of this type of monitoring system and the interpretation of existing programmes. A re-evaluation of the monitoring system is being developed at the time of writing, using modern data loggers and fibre optic integrity testing to accurately profile the resiliency of the network and illustrate some of the long-term effects acting directly on the instrumentation.

From a geotechnical point-of-view, a clear seasonal and tidal effect was evident from the measurements (Section 4.8.5), phenomena which can have implications for the geotechnical and structural response of the quay wall. Ongoing analysis of the monitoring data and that of other quay walls around the port of Rotterdam (Appendix A) aims to resolve to what extent these cyclic loading actions can affect the reliability of the quay wall.

Furthermore, interaction between the structural elements has had a clear impact on each of the structural elements. (e.g. Figure 4.32). Further work will involve fully delineating the effect across each of the structural elements and comparison to the numerical models of the quay wall, both to verify the phenomena measured and verify the numerical models themselves. In essence, this work is part of the development of the data interpretation layer discussed in Section 3.3.3 and aims to provide an update of the quay wall reliability and the potential for future design adjustments to the structure.

The geotechnical analyses that have been performed and those that are proposed are being done with the aim of bringing a resumption to the monitoring network, incorporating some of the findings regarding the data processing and interpretation and using the lessons learned as an input towards other quay wall digital twins across the port of Rotterdam.

## 5 CONCLUSION

This report has provided an overview of the domains of geo-monitoring and digital twin development highlighting the needs of both disciplines when it comes to a digital twin based geo-monitoring platform. Using an example of a quay wall in the Netherlands, some of the uniqueness of geo-monitoring has been highlighted:

- The need to have robust instrumentation that can survive instrumentation, installation and operational process
- Sensors are often embedded within structures and inaccessible during their lifetime
- Retrofitting of the geo-structure can be challenging, required detailed and timely planning
- A lot of interpretation needed to separate structural and geotechnical behaviour
- Many spatial and temporal uncertainties exist when extrapolating results between geotechnical tests and geo-structures or across time intervals

How these needs of geo-monitoring can be reflected in the digital twin development has been outlined in this deliverable by proposing a digital twin architecture and highlighting the key facets that should be targeted during the digital twin planning and development. This helps ensure proper interpretation of the results of the geo-structure and provide asset owners with accurate and reliable insights into their geo-structures' performances.

The deliverable has also shown that a wealth of knowledge has been developed from existing digital twins across the port of Rotterdam and has given a greater understanding of what impacts long-term quay wall response. Research is ongoing into these monitoring results to appropriately delineate the impacts on long-term quay wall reliability and further recommendations for digital twin models are being made.



## REFERENCES

Abdulkarem, M. *et al.* (2020) 'Wireless sensor network for structural health monitoring: A contemporary review of technologies, challenges, and future direction', *Structural Health Monitoring*, 19(3), pp. 693–735. Available at: <https://doi.org/10.1177/1475921719854528>.

den Abel, N. (2018) *Load testing of a quay wall: evaluating the use of load testing by an application of Bayesian updating*. MSc Thesis. TU Delft. Available at: <http://resolver.tudelft.nl/uuid:a46ff5e1-a949-4ba7-869a-0c7db3310470>.

Actueel Hoogtebestand Nederland (2016) *AHN Viewer*. Available at: <https://www.ahn.nl/ahn-viewer> (Accessed: 28 August 2022).

Arcadius Tokognon, C. *et al.* (2017) 'Structural health monitoring framework based on Internet of Things: A survey', *IEEE Internet of Things Journal*, 4(3), pp. 619–635. Available at: <https://doi.org/10.1109/JIOT.2017.2664072>.

Aygün, B. and Cagri Gungor, V. (2011) 'Wireless sensor networks for structure health monitoring: recent advances and future research directions', *Sensor Review*, 31(3), pp. 261–276. Available at: <https://doi.org/10.1108/02602281111140038>.

Bado, M.F. *et al.* (2022) 'Digital twin for civil engineering systems: An exploratory review for distributed sensing updating', *Sensors*, 22(3168). Available at: <https://doi.org/10.3390/s22093168>.

Bersan, S., Koelewijn, A.R. and Simonini, P. (2018) 'Effectiveness of distributed temperature measurements for early detection of piping in river embankments', *Hydrology and Earth System Sciences*, 22(2), pp. 1491–1508. Available at: <https://doi.org/10.5194/hess-22-1491-2018>.

Bland, J., Walthall, S. and Toll, D. (2014) 'The development and governance of the AGS format for geotechnical data', *Information Technology in Geo-Engineering*, 3, pp. 67–74. Available at: <https://doi.org/10.3233/978-1-61499-417-6-67>.

Boje, C. *et al.* (2020) 'Towards a semantic Construction Digital Twin: directions for future research', *Automation in Construction*, 114, p. 103179. Available at: <https://doi.org/10.1016/j.autcon.2020.103179>.

Bolton, A., Enzer, M. and Schooling, J. (2018) *The Gemini Principles: Guiding values for the national digital twin and information management framework*. Centre for Digital Built Britain, p. 28. Available at: <https://doi.org/10.17863/CAM.32260>.

Brightwell, S. and Butcher, D. (2022) 'Intelligent Monitoring Solution to manage slope risk on Network Rail earthworks: large scale deployment in Kent, Sussex and Wessex', in: *11th International Symposium on Field Monitoring in Geomechanics*, London, United Kingdom.

Buckley, T., Ghosh, B. and Pakrashi, V. (2021) 'Edge Structural Health Monitoring (E-SHM) using low-power wireless sensing', *Sensors*, 21(20), p. 6760. Available at: <https://doi.org/10.3390/s21206760>.

Canterbury Earthquakes Royal Commission (2011) *Canterbury Earthquakes Royal Commission Interim Report*. Wellington, New Zealand. Available at: <https://canterbury.royalcommission.govt.nz/Interim-Report>.

Cao, Z., Wang, Y. and Li, D. (2016) 'Quantification of prior knowledge in geotechnical site characterization', *Engineering Geology*, 203, pp. 107–116. Available at: <https://doi.org/10.1016/j.enggeo.2015.08.018>.

Casas, J.R., Stipanovic, I. and Chacón, R. (2022) *D5.1 SHM digital twin requirements for residential, industrial buildings and bridges*. D5.1, p. 106.

Chen, P.M. *et al.* (1994) 'RAID: high-performance, reliable secondary storage', *ACM Computing Surveys*, 26(2), pp. 145–185. Available at: <https://doi.org/10.1145/176979.176981>.

Chéour, R. *et al.* (2020) 'Accurate dynamic voltage and frequency scaling measurement for low-power microcontrollers in wireless sensor networks', *Microelectronics Journal*, 105, p. 104874. Available at: <https://doi.org/10.1016/j.mejo.2020.104874>.

Clayton, C.R., Matthews, M.C. and Simons, N.E. (1995) *Site Investigation*. 2nd edition. Oxford, United Kingdom: Wiley-Blackwell.

Colom, J.A. (1750) 'Carte nouvelle de la Comté de Hollande et de la Seigneurie d'Utrecht'. Covens et Mortier.

Craveiro, F. *et al.* (2019) 'Additive manufacturing as an enabling technology for digital construction: A perspective on Construction 4.0', *Automation in Construction*, 103, pp. 251–267. Available at: <https://doi.org/10.1016/j.autcon.2019.03.011>.

van Dam, M. (2008) *Factory Acceptance Test Protocol*. 0808.0185r.BV. Capelle aan den IJssel, Netherlands: Baas B.V.

Davila Delgado, J.M. and Oyedele, L. (2021) 'Digital Twins for the built environment: Learning from conceptual and process models in manufacturing', *Advanced Engineering Informatics*, 49, p. 101332. Available at: <https://doi.org/10.1016/j.aei.2021.101332>.

De Gast, T. *et al.* (2022) 'CPT based liquefaction potential of flood defences in the Netherlands', in: *Cone Penetration Testing 2022*, Bologna, Italy: Taylor & Francis, pp. 889–893.

De Vries, A.J. (2007) *Diepwand vorm en wapening: Paneeltype A*. Construction Drawings 005001 O-T-140. BAM Civiel.

DINOloket (2022) *Ondergrondmodellen* / *DINOloket*. Available at: <https://www.dinoloket.nl/ondergrondmodellen> (Accessed: 29 September 2022).

Donohue, S., Gavin, K. and Tolooiyan, A. (2011) 'Geophysical and geotechnical assessment of a railway embankment failure', *Near Surface Geophysics*, 9(1), pp. 33–44. Available at: <https://doi.org/10.3997/1873-0604.2010040>.

Duffy, K., Gavin, K., Askarinejad, A., *et al.* (2022) 'Field testing of axially loaded piles in dense sand', in: *Proceedings of the 20th International Conference on Soil Mechanics and Geotechnical Engineering*. 20th International Conference on Soil Mechanics and Geotechnical Engineering, Sydney, Australia.

Duffy, K., Gavin, K., De Lange, D.A., *et al.* (2022) 'Residual stress measurement of driven precast piles using distributed fibre optic sensors', in: *11th International Stress Wave Conference*, Rotterdam, The Netherlands.

Dunnicliff, J. (1988) *Geotechnical Instrumentation for Monitoring Field Performance*. New York, USA: Wiley. Available at: <https://www.wiley.com/en-ie/Geotechnical+Instrumentation+for+Monitoring+Field+Performance-p-9780471005469> (Accessed: 1 September 2022).

Eslami, A. *et al.* (2020) '1 - Geotechnical engineering', in A. Eslami *et al.* (eds) *Piezcone and Cone Penetration Test (CPTu and CPT) Applications in Foundation Engineering*. Butterworth-Heinemann, pp. 1–23. Available at: <https://doi.org/10.1016/B978-0-08-102766-0.00001-8>.

FOS&S (2009) *Pressure Sensor P-01 Specification Sheet*. Geel, Belgium. Available at: <https://www.ipac-sa.com.ar/catalogos/FOS-S/P-01%20-%20Pressure%20Sensor.pdf> (Accessed: 30 September 2022).

Franklin & Marshall College Library (2022) *Timeline of file storage media, Personal Archiving*. Available at: <https://library.fandm.edu/c.php?g=273502&p=1825686> (Accessed: 2 October 2022).

de Gijt, J. and Broeken, M.L. (2013) *Quay Walls*. 2nd Edition. Boca Raton, USA: CRC Press. Available at: <https://www.crcpress.com/Quay-Walls-Second-Edition/Gijt-Broeken/p/book/9781138000230> (Accessed: 17 July 2022).

de Gijt, J.G. (J G. deGijt@tudelft.nl) *et al.* (2010) 'Development of container handling in the Port of Rotterdam', in. *Port Infrastructure Seminar*, Delft, The Netherlands. Available at: <https://repository.tudelft.nl/islandora/object/uuid%3A0018e79d-ee56-44cb-a8c8-c35493888218> (Accessed: 6 October 2022).

Grieves, M. (2014) *Digital twin: Manufacturing excellence through virtual factory replication*.

Grouting Services (2017) *Deep Basement Construction*. Available at: <https://www.groutingservices.co.nz/grouting-news/deep-basement-construction/> (Accessed: 30 October 2022).

Hariri, S., Kind, M.C. and Brunner, R.J. (2021) 'Extended Isolation Forest', *IEEE Transactions on Knowledge and Data Engineering*, 33(4), pp. 1479–1489. Available at: <https://doi.org/10.1109/TKDE.2019.2947676>.

Hijma, M.P. *et al.* (2012) 'Pleistocene Rhine–Thames landscapes: geological background for hominin occupation of the southern North Sea region', *Journal of Quaternary Science*, 27(1), pp. 17–39. Available at: <https://doi.org/10.1002/jqs.1549>.

Horiguchi, T. *et al.* (1995) 'Development of a distributed sensing technique using Brillouin scattering', *Journal of Lightwave Technology*, 13(7), pp. 1296–1302. Available at: <https://doi.org/10.1109/50.400684>.

Hutter, R.A. (2003) *Maasvlakte 2, vanuit historisch perspectief: 'van Botlek tot Maasvlakte 2'*. MSc Thesis. TU Delft. Available at: <http://resolver.tudelft.nl/uuid:49b83c87-0da3-4cbe-9c9e-b43597721df5>.

Imperiale, M. (2022) *D3.3 Data fusion methods and digital twin based IoT data processing pipelines*. D3.3, p. 44.

Jones, D. *et al.* (2020) 'Characterising the digital twin: A systematic literature review', *CIRP Journal of Manufacturing Science and Technology*, 29, pp. 36–52. Available at: <https://doi.org/10.1016/j.cirpj.2020.02.002>.

Knappett, J. and Craig, R.F. (2012) *Craig's Soil Mechanics*. 8th edn. CRC Press.

KNMI (2009) *Daggegevens van het weer in Nederland*. Available at: <https://www.knmi.nl/nederland-nu/klimatologie/daggegevens> (Accessed: 27 July 2022).

Korff, M., Hemel, M.-J. and Peters, D.J. (2022) 'Collapse of the Grimborgwal, a historic quay in Amsterdam, the Netherlands', *Proceedings of the Institution of Civil Engineers - Forensic Engineering*, pp. 1–10. Available at: <https://doi.org/10.1680/jfoen.21.00018>.

Kuster, J.P.M. (2007) *Bovenbouw Moot Type A1 Vorm*. Construction Drawings 005001 O-T-004. BAM Civiel.

Lam, C. and Jefferis, S.A. (2011) 'Critical assessment of pile modulus determination methods', *Canadian Geotechnical Journal*, 48(10), pp. 1433–1448. Available at: <https://doi.org/10.1139/t11-050>.

Lehane, B. *et al.* (2020) 'A new "unified" CPT-based axial pile capacity design method for driven piles in sand: 4th International Symposium on Frontiers in Offshore Geotechnics', *Proceedings of the 4th International Symposium on Frontiers in Offshore Geotechnics*, pp. 463–477.

Lehr, W. and McKnight, L.W. (2003) 'Wireless Internet access: 3G vs. WiFi?', *Telecommunications Policy*, 27(5), pp. 351–370. Available at: [https://doi.org/10.1016/S0308-5961\(03\)00004-1](https://doi.org/10.1016/S0308-5961(03)00004-1).

Lu, Q. *et al.* (2020) 'Developing a digital twin at building and city levels: Case study of West Cambridge Campus', *Journal of Management in Engineering*, 36(3), p. 05020004. Available at: [https://doi.org/10.1061/\(ASCE\)ME.1943-5479.0000763](https://doi.org/10.1061/(ASCE)ME.1943-5479.0000763).

Lunne, T., Robertson, P.K. and Powell, J.J.M. (1997) *Cone Penetration Testing in Geotechnical Practice*, 1997. 1st edn. CRC Press.

van Lysebetten, G. *et al.* (2022) *Monitoring of structures and elements with fiber optics: State of the art*. Draft version 0.2. COOCK.

Ma, C. *et al.* (2022) 'Intelligent anomaly identification of uplift pressure monitoring data and structural diagnosis of concrete dam', *Applied Sciences*, 12(2), pp. 612–632. Available at: <https://doi.org/10.3390/app12020612>.

Maskuriy, R. *et al.* (2019) 'Industry 4.0 for the construction industry—how ready is the industry?', *Applied Sciences*, 9(14), pp. 2819–2845. Available at: <https://doi.org/10.3390/app9142819>.

Matic, I. *et al.* (2019) 'Full-scale load testing on long prefabricated concrete piles in the Port of Rotterdam', in *The XVII European Conference on Soil Mechanics and Geotechnical Engineering. Proceedings of the XVII ECSMGE-2019*, Reykjavik, Iceland: Icelandic Geotechnical Society (IGS), pp. 1–8.

McNeill, D.K. (2009) 'Data management and signal processing for structural health monitoring of civil infrastructure systems', in *Structural health monitoring of civil infrastructure systems*. 1st edn. Cambridge, United Kingdom: Woodhead Publishing, pp. 283–304.

Moree, J.M. *et al.* (2015) *Interdisciplinary archaeological research programme Maasvlakte 2, Rotterdam: Twenty meters deep! The mesolithic period at the Yangtze Harbour site - Rotterdam Maasvlakte, the Netherlands*. BOORapporten, volume 566. Gemeente Rotterdam. Available at: <https://dspace.library.uu.nl/handle/1874/309133> (Accessed: 29 September 2022).

Mu, H.-Q. and Yuen, K.-V. (2015) 'Novel outlier-resistant extended Kalman Filter for robust online structural identification', *Journal of Engineering Mechanics*, 141(1), p. 04014100. Available at: [https://doi.org/10.1061/\(ASCE\)EM.1943-7889.0000810](https://doi.org/10.1061/(ASCE)EM.1943-7889.0000810).

Netherlands Standardisation Institute (2017) *NEN 9997-1+C2:2017*. Delft, The Netherlands.

Newman, C. *et al.* (2020) 'Industry 4.0 deployment in the construction industry: a bibliometric literature review and UK-based case study', *Smart and Sustainable Built Environment*, 10(4), pp. 557–580. Available at: <https://doi.org/10.1108/SASBE-02-2020-0016>.

Oswell, J.M. (2011) 'Pipelines in permafrost: geotechnical issues and lessons 12010 R.M. Hardy Address, 63rd Canadian Geotechnical Conference.', *Canadian Geotechnical Journal*, 48(9), pp. 1412–1431. Available at: <https://doi.org/10.1139/t11-045>.

Park, G. *et al.* (2008) 'Energy harvesting for structural health monitoring sensor networks', *Journal of Infrastructure Systems*, 14(1), pp. 64–79. Available at: [https://doi.org/10.1061/\(ASCE\)1076-0342\(2008\)14:1\(64\)](https://doi.org/10.1061/(ASCE)1076-0342(2008)14:1(64)).

Peck, R.B. (1969) 'Advantages and limitations of the observational method in applied soil mechanics', *Géotechnique*, 19(2), pp. 171–187. Available at: <https://doi.org/10.1680/geot.1969.19.2.171>.

Port of Rotterdam (2021) 'Kadebouw: plaats voor containerreuzen'. Available at: <https://www.portofrotterdam.com/sites/default/files/2021-06/kadebouw-plaats-voor-containerreuzen-factsheet.pdf> (Accessed: 5 October 2022).

Port of Rotterdam Authority (2022) *Weather & Tide Dashboard, Weather & Tide*. Available at: <https://weather-tide.portofrotterdam.com/desktop/> (Accessed: 28 September 2022).

Rahman, M.H., Abu-Farsakh, M.Y. and Jafari, N. (2021) 'Generation and evaluation of synthetic cone penetration test (CPT) data using various spatial interpolation techniques', *Canadian Geotechnical Journal*, 58(2), pp. 224–237. Available at: <https://doi.org/10.1139/cgj-2019-0745>.

Roubos, A. (2019) *Enhancing reliability-based assessments of quay walls*. PhD Thesis. TU Delft. Available at: <https://doi.org/10.4233/uuid:40632b7a-970e-433d-9b4e-ff2d2249b156>.

Roubos, A., Blokland, T. and van der Plas, T. (2014) 'Field tests propellor scour along quay wall', in *PIANC World Congress*, San Francisco, CA, USA.

Roubos, A.A. *et al.* (2020) 'Time-dependent reliability analysis of service-proven quay walls subject to corrosion-induced degradation', *Reliability Engineering & System Safety*, 203, p. 107085. Available at: <https://doi.org/10.1016/j.res.2020.107085>.

Schaminée, P.E.L., den Adel, H. and Bezuijen, A. (2006) 'Geotechnical exchange format language a base for a physical modelling standard?', in *Physical Modelling in Geotechnics. 6th International Conference on Physical Modelling in Geotechnics*, Hong Kong: CRC Press, p. 1608.

Scheel, J. (2007) *Bovenbouw Moot Type A1 Vorm*. Construction Drawings 005001 O-T-200. BAM Civiel.

Schouten, O. (2020) *Optimising the functionality of smart quay walls using measurement data obtained during the construction process*. MSc Thesis. TU Delft. Available at: <http://resolver.tudelft.nl/uuid:1b827ff8-7b5f-4d6f-9c4f-b24f71203c98>.

Shi, W. *et al.* (2016) 'Edge computing: vision and challenges', *IEEE Internet of Things Journal*, 3(5), pp. 637–646. Available at: <https://doi.org/10.1109/JIOT.2016.2579198>.

Shibata Fender Team (2016) *SPC Cone Fender systems and bollards for Ghana*. Available at: <https://www.shibata-fender.team/en/news/news-detail/SPC-Cone-Fender-systems-and-bollards-for-Ghana.html> (Accessed: 30 September 2022).

Smartec (2017) *SOFO Deformation Sensor Datasheet*. SMA 10.1010. Manno, Switzerland. Available at: <https://smartec.ch/wp-content/uploads/2017/01/SOFO-Standard-Deformation-Sensor-E10-1010-SMA.pdf> (Accessed: 5 October 2022).

Song, S.-J. and Jang, Y.-G. (2018) 'Construction of digital twin geotechnical resistance model for liquefaction risk evaluation', in *Proceedings of the 2nd International Symposium on Computer Science and Intelligent Control*. New York, NY, USA: Association for Computing Machinery (ISCSIC '18), pp. 1–6. Available at: <https://doi.org/10.1145/3284557.3284739>.

Sparkes, P. and Webb, J. (2020) *Structural Health Monitoring in Civil Engineering*. CIRIA Report C788. London, United Kingdom: CIRIA.

Spruit, R. *et al.* (2022) 'Ultimate bearing capacity of MV piles derived from load tests, a suggested new design approach', in *11th International Stress Wave Conference 2022*, Rotterdam, The Netherlands.

Srigopal, J.D. (2018) *Comprehending the behaviour of a Muller Verpress pile under tensional loading*. MSc Thesis. TU Delft. Available at: <http://resolver.tudelft.nl/uuid:b001f9ae-99ee-40d6-b2b2-d1bfcf3f1b1f>.

Stafleu, J. *et al.* (2019) *Totstandkomingsrapport GeoTOP*. TNO 2019 R11655. Utrecht, The Netherlands: Nederlandse Organisatie voor Toegepast Natuurwetenschappelijk Onderzoek.

Torres, R. *et al.* (2012) 'GMES Sentinel-1 mission', *Remote Sensing of Environment*, 120, pp. 9–24. Available at: <https://doi.org/10.1016/j.rse.2011.05.028>.

Trautmann, C.H. and Kulhawy, F.H. (1983) 'Data sources for engineering geologic studies', *Environmental & Engineering Geoscience*, (4), pp. 439–454. Available at: <https://doi.org/10.2113/gseegeosci.xx.4.439>.



Tuming, W., Sijia, Y. and Hailong, W. (2010) 'A dynamic voltage scaling algorithm for wireless sensor networks', in. *2010 3rd International Conference on Advanced Computer Theory and Engineering (ICACTE)*, pp. V1-554-V1-557. Available at: <https://doi.org/10.1109/ICACTE.2010.5578956>.

United Nations Conference on Trade and Development (2018) *Review of Maritime Transport 2018*. New York, USA: United Nations, p. 76.

Utrecht University (2022) *Compare maps, Georeferencer: Compare maps*. Available at: <https://uu.georeferencer.com/compare#map/631781111740> (Accessed: 29 September 2022).

Voogt, H. (2022) 'Port facilities' asset management: Coping with aging infrastructure and constrained budgets in the long term', pp. 656–663. Available at: <https://doi.org/10.1061/9780784484401.065>.

Vos, P.C. *et al.* (2015) 'A staged geogenetic approach to underwater archaeological prospection in the Port of Rotterdam (Yangtzehaven, Maasvlakte, The Netherlands): A geological and palaeoenvironmental case study for local mapping of Mesolithic lowland landscapes', *Quaternary International*, 367, pp. 4–31. Available at: <https://doi.org/10.1016/j.quaint.2014.11.056>.

Wang, B. *et al.* (2013) 'Field investigation of a geothermal energy pile: Initial observations', in. *International Conference on Soil Mechanics and Geotechnical Engineering 2013*. Available at: <https://research.monash.edu/en/publications/field-investigation-of-a-geothermal-energy-pile-initial-observati> (Accessed: 26 August 2022).

Westerbeke, F.Y.H. (2021) *Geotechnical bearing capacity of MV piles*. MSc Thesis. TU Delft. Available at: <http://resolver.tudelft.nl/uuid:6f7bb64b-9dc2-4a30-85b8-8f47d1e698ea>.

White, D.J. and Lehane, B.M. (2004) 'Friction fatigue on displacement piles in sand', *Géotechnique*, 54(10), pp. 645–658. Available at: <https://doi.org/10.1680/geot.2004.54.10.645>.

Wu, J. *et al.* (2022) 'Theory and Technology of Digital Twin Model for Geotechnical Engineering', in G. Feng (ed.) *Proceedings of the 8th International Conference on Civil Engineering*. Singapore: Springer (Lecture Notes in Civil Engineering), pp. 403–411. Available at: [https://doi.org/10.1007/978-981-19-1260-3\\_37](https://doi.org/10.1007/978-981-19-1260-3_37).

## APPENDIX A QUAY WALLS AT THE PORT OF ROTTERDAM

Modern quay walls are large, complex systems comprising several structural elements working together to provide a safe and reliable asset. As vessel sizes have increased significantly in recent years, owners like the Port of Rotterdam are developing massive structures at the cutting-edge of design practice. As ports are competing in a global market over-design is not an option and port owners need to understand the current safety level of their quay walls. To do this, a variety of different designs can be implemented (e.g. Figure A.1), the choice and design of which is dependent on the requirements of the asset manager and the local site conditions. Common elements of almost all quay walls are the relieving walls and superstructures, after which piles, anchors or relieving platforms are added depending on the size of the quay wall and local site conditions.

Nonetheless, quay wall constructions are relatively complex due to the large variety of interacting geotechnical elements. Verifications can be carried out using simple analytical models but for the most part, deep-sea quay wall design is carried out using numerical models, such as the Finite Element Method (Section 3.3.2).

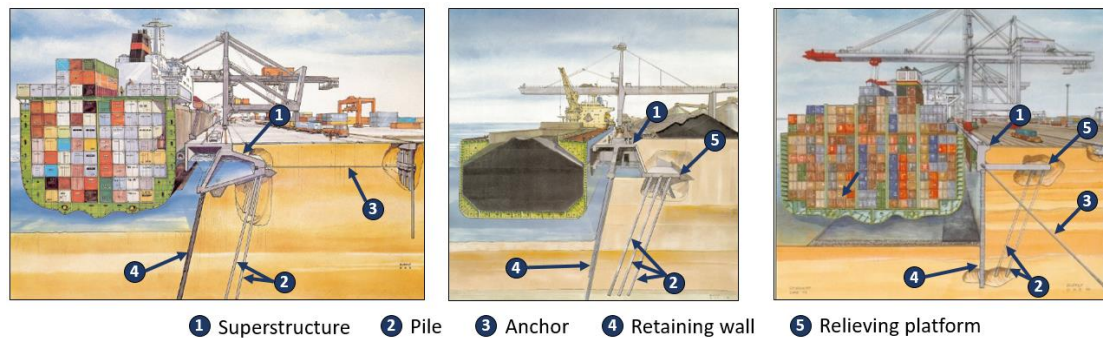


*Figure A.1: Examples of quay wall structures across the port of Rotterdam with the geotechnical elements listed (amended from de Gijt & Broeken (2013))*

As the tenth largest port in the world, and the largest in Europe in terms of cargo throughput (United Nations Conference on Trade and Development, 2018), the port of Rotterdam is heavily invested in efficient quay wall development and maintenance. The port has expanded greatly in the past century and new infrastructure is constantly being developed, although in recent years, the focus is shifting towards the maintenance, repair, rehabilitation and adaptation of existing structures in fully up-and-running terminals. Over half of the quay walls around the port of Rotterdam are reaching or have already reached the end of their design lifetime (Figure A.2). These quay walls have a combined value of approximately two billion euros. Despite exceeding their design life, many of the quay walls are still considered to be in good condition, within the realms of the data available (Roubos, 2019).

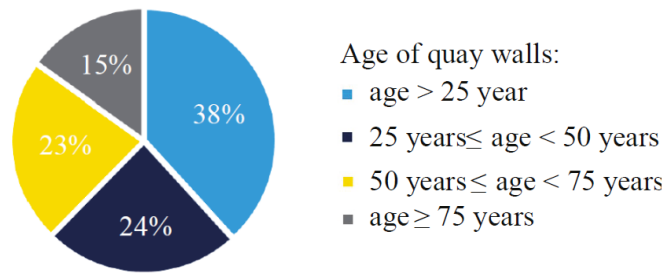


Figure A.2: Age of quay walls across the Port of Rotterdam (Roubos, 2019)

Nonetheless, the practicality of assessing the current condition of the quay walls from visual inspection is relatively difficult given that most of the quay wall is hidden below the subsurface. Monitoring at a surface level, such as surface settlement, can give some indication of what is happening underneath the surface, however, direct measurement of the subsurface elements is always optimal to provide reasoning and context to the above-ground observations. As a result, the Port of Rotterdam Authority (*Havenbedrijf Rotterdam*) have equipped several so-called “smart quay walls” with sensors which give real-time indications as to the quality of their existing assets (Voogt, 2022).

To date limited research has been performed on the available real-time monitoring data collected. Research by Schouten (2020) focussed on optimising the functionality of smart quay walls using monitoring data from the construction process. Data collected during quay wall construction is particularly useful due to the large deformations exhibited by the structures during, for example, excavation and dredging in front of the quay wall. The predictions of a numerical model can then be validated by comparing deformations in the retaining wall measured by inclinometers to the predictions of the model, ensuring confidence in the developed model and its inputs. This is particularly useful for assessing potential adjustments made to the quay wall over time, such as an adjustment of the dredged level or incorporation of time-dependent effects so that the capacity of the quay wall can be re-evaluated. This work is being extended as part of ASHVIN Task 4.4: Data driven Management (Deliverable 4.4).

Avenues can also be developed from this in terms of reviewing or updating the parameters based on the measurements. A theoretical example was taken by den Abel (2018) who used a real-life quay wall but devised fictitious measurements of a quay wall load test and developed a Bayesian updating paradigm to update the reliability of the quay wall, in other words, the current risk of failure of the quay wall. In a similar fashion, Roubos et al. (2020) also examined the potential effect of corrosion-induced degradation of the retaining wall on the overall reliability of quay walls.

While some of the previous examples involve dynamic updating, some other research has been performed on more static examples, such as field tests on instrumented quay walls and/or their structural elements. For instance, this could involve investigating the response of quay wall foundations and anchors (Matic *et al.*, 2019; Duffy, Gavin, Askarinejad, *et al.*, 2022; Spruit *et al.*, 2022) or assessing the impact of scour on quay wall stability (Roubos, Blokland and van der Plas, 2014). Where applicable, incorporation of the findings of these studies should be readily facilitated for in the

digital twin of the quay walls to ensure a realistic prognosis of the quay wall reliability can be made.

Patently, a wealth of data exists within the port of Rotterdam regarding the use of monitoring data and its impact on quay wall models. Nonetheless, the steps towards fusing this research within one or multiple digital twins is still being carried out. In doing so, accurate digital representations can be created which give a clear picture as to the current condition of quay walls across the port and provide indicators as to the degree of maintenance required or help inform planning and procedure for quay rehabilitation, reuse and upgrading.

## APPENDIX B CONE PENETRATION TEST DATA

### Appendix B1 Geotechnical Exchange Format (.gef)

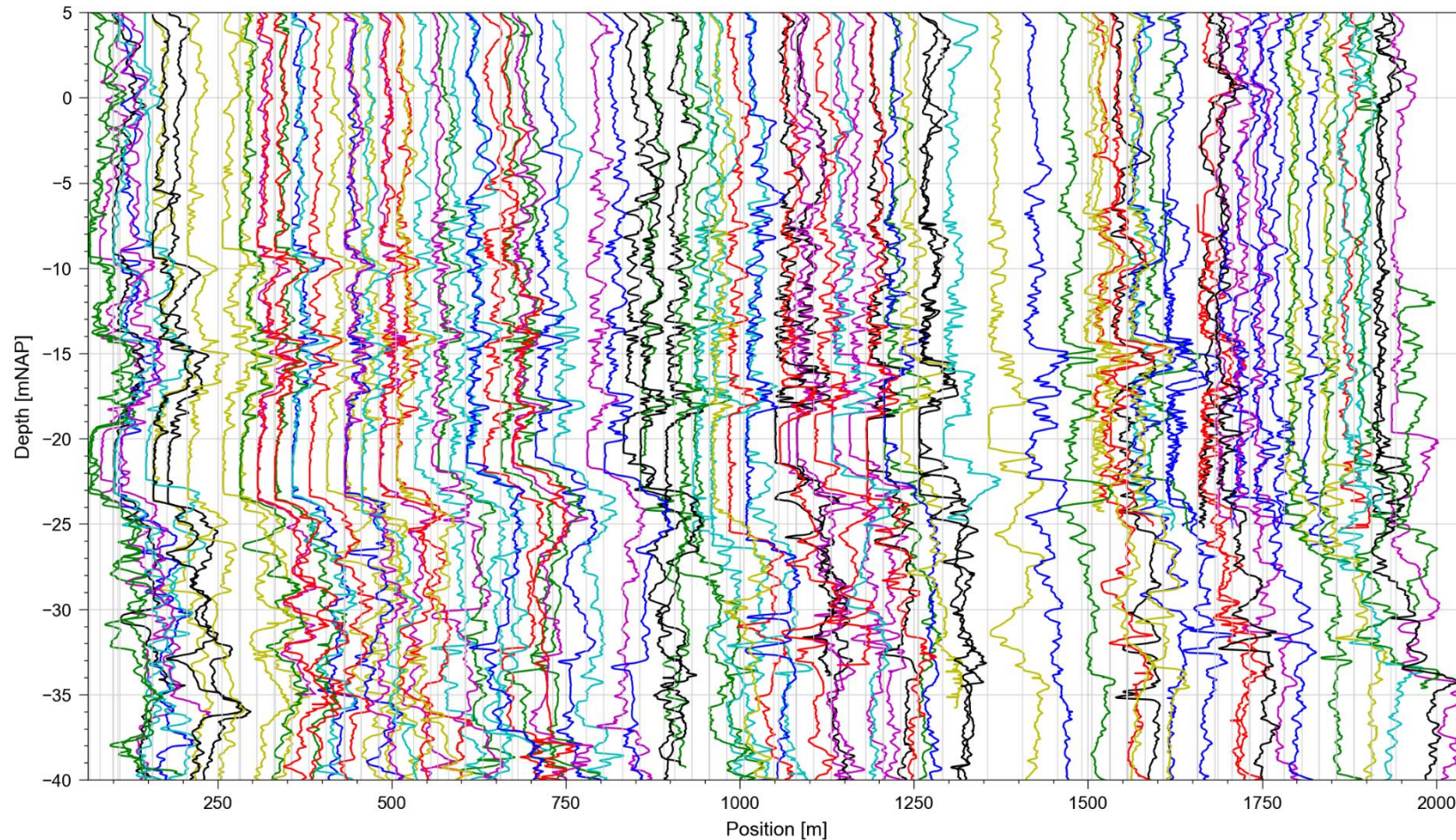
An example of the .gef file format is provided below for a cone penetration test. The example has been translated from Dutch to English and some information has been redacted to preserve confidentiality.

```
#FILEOWNER= DUFFY
#FILEDATE= 2019,01,01
#PROJECTID= CPT, 1234-01-01,
#COLUMNINFO= 1, m, Depth, 1
#COLUMNINFO= 2, MPa, Cone resistance qc, 2
#COLUMNINFO= 3, MPa, Friction sleeve resistance fs, 3
#COLUMNINFO= 4, %, Friction ratio Rf, 4
#COLUMNINFO= 5, inclination, X direction, 21
#COLUMNINFO= 6, inclination, Y direction, 22
#COLUMNINFO= 7, -, Classification zone Robertson 1990, 99
#COLUMNINFO= 8, m, Corrected depth, 11
#COLUMNINFO= 9, s, Time, 12
#COMPANYID= Fugro Geoservices B.V., NL0000XXXXXX, 31
#DATAFORMAT= ASCII
#DATATYPE= REAL8
#COLUMNVOID= 1-9, -99999.000
#XYID= 31000, 123456.7, 654321.0, 0.01, 0.01
#ZID= 31000, 1.23, 0.01
#MEASUREMENTTEXT= 1, -, opdrachtgever
#MEASUREMENTTEXT= 2, UCD Soil Investigation, project name
#MEASUREMENTTEXT= 3, Belfield, place name
#MEASUREMENTTEXT= 4, F7.5ABC1DE/ABC2DA/B 1234-56-8910-1234, cone type and serial number
#MEASUREMENTTEXT= 5, KDU/KSI/ML0, CPT operator
#MEASUREMENTTEXT= 6, NEN 5140 class 2, standard
#MEASUREMENTTEXT= 9, ground level, fixed horizontal
#MEASUREMENTTEXT= 44, -, orientation x-axis
#MEASUREMENTVAR= 1, 1500, mm2, cone tip area
#MEASUREMENTVAR= 2, 19956, mm2, friction sleeve area
#MEASUREMENTVAR= 5, 145, mm, Distance cone to middle friction sleeve
#MEASUREMENTVAR= 13, 0.00, m, pre-dug depth
#MEASUREMENTVAR= 16, 12.34, m, end-depth sounding
#MEASUREMENTVAR= 17, 0, -, Reason for stoppage : End depth reached
#MEASUREMENTVAR= 20, 0.357, MPa, Cone resistance before investigation
#MEASUREMENTVAR= 21, 0.354, MPa, Cone resistance after investigation
#MEASUREMENTVAR= 22, 0.010, MPa, Friction sleeve resistance before investigation
#MEASUREMENTVAR= 23, 0.012, MPa, Friction sleeve resistance after investigation
#MEASUREMENTVAR= 30, 8.5, degrees, inclination before investigation
#MEASUREMENTVAR= 31, -2.4, degrees, inclination after investigation
#TESTID= CPT01
#REPORTCODE= GEF-CPT-Report,1,1,0
#STARTDATE= 2019,05,01
#STARTTIME= 13,00,00
#OS= DOS
#EOH=
0.00      0.095 -99999.000 -99999.000      0.100      -0.100      0      0.00      50.0
0.02      0.123      0.004      0.010      0.200      -0.680      7      0.02      75.3
0.04      0.400      0.006      0.150      0.400      -0.900      7      0.04      64.1
0.06      0.662      0.008      0.400      0.580      -1.523      7      0.06      99.9
0.08      0.888      0.012      0.460      0.740      -1.592      2      0.08      78.1
```



## Appendix B2 CPT Cross Section

A cross-section of selected CPTs along the quay wall has been given below. Some patterns can be seen in the data: for instance, the stiff clay of the Wijchen Member which delineates the boundary between the Kreftenheye and Naaldwijk Formations (Section 4.3) can be seen between NAP -20m and NAP -23m.





## APPENDIX C GEOMETRICAL DETAILS

### *MV piles*

Steel Quality	S355
HP-profile	360x174 mm
Stiffness ( $EA$ )*	9.58 GN
Avg. driving depth below ground surface	36.00m
Average length	53.00m
Angle of installation	45°
Centre-to-centre distance	5.6m

\* Stiffness has been calculated based on the minimum theoretical stiffness (i.e. without grout)

### *Vibro piles*

Concrete Quality	B35
Reinforcement Steel	FeB500
Diameter	560/670mm
Stiffness ( $EA$ )*	13.52 GN
Average driving depth	28.50m
Average length	30.00m
Angle	3:1
Centre to centre	2.8m (two rows)

\* Stiffness has been calculated by assuming the pile diameter is equal to that of the base plate diameter